DEVELOPMENT OF REACTIVE CHROMATOGRAPHY SYSTEM FOR EQUILIBRIUM-LIMITED REACTIONS

A Thesis
Presented to
The Academic Faculty

by

Jungmin Oh

In Partial Fulfillment
of the Requirements for the Degree
Doctor of Philosophy in the
School of Chemical and Biomolecular Engineering

Georgia Institute of Technology
December 2016

DEVELPMENT OF REACTIVE CHROMATOGRAPHY SYSTEM FOR EQUILIBRIUM-LIMITED REACTIONS

Approved by:

Dr. Yoshiaki Kawajiri, Advisor
School of Chemical and Biomolecular Engineering
Georgia Institute of Technology

Dr. Krista S. Walton
School of Chemical and Biomolecular Engineering
Georgia Institute of Technology

Dr. Andreas S. Bommarius
School of Chemical and Biomolecular Engineering
Georgia Institute of Technology

Dr. Megan E. Donaldson
Engineering & Process Science Laboratory
The Dow Chemical Company

Dr. William J. Koros
School of Chemical and Biomolecular Engineering
Georgia Institute of Technology

Date Approved: October 25, 2016

ACKNOWLEDGEMENTS

There are many people I would like to thank who have helped me along the way to complete this research thesis. First, I would like to thank my advisors, Dr. Yoshiaki Kawajiri, and Dr. Andreas Bommarius, who are the consistent source of wisdom, direction and encouragement throughout graduate school. I learned much about numerical optimization, chromatographic reactor, and simulated moving bed chromatography from them. I am honored to be their student.

I am grateful to my thesis committee who reviewed and approved my thesis. They gave me many insightful comments from their expertise, and reviewed my proposals as well as my forth year review to check my progress to say on the course.

I am grateful to my colleagues, Dr. Balamurali Sreedhar, Dr. Gaurav Agrawal, Dr. Pakkapol Kanchanalai, Shan Tie, and Siwei Guo who have helped me in various ways, and we also had many fruitful discussions about this research. I'm also thankful to all of Dr. Kawajiri's and Dr. Bommarius' group members for being friendly coworkers as well as helping me to prepare several academic presentations. I am also thankful to the ChBE 2011 entering class who have been wonderful friends to me in graduate school.

I am thankful to my undergraduate research assistance, Leo Espinosa, who helped me in laboratory works and also gave me opportunity to practice leadership skill.

The financial support from The Dow Chemical Company are also gratefully acknowledged.

TABLE OF CONTENTS

	Page
ACKNOWLEDGEMENTS	iii
LIST OF TABLES	vii
LIST OF FIGURES	ix
SUMMARY	xv
CHAPTER	
1 INTRODUCTION	1
1.1 DOWANOL PMA	3
1.2 Principle of Reactive Chromatography	4
1.3 Simulated Moving Bed Reactor	6
2 SCOPE OF STUDY	13
3 EXPERIMENT METHODS	17
3.1 Well-stirred Batch Reactor	17
3.2 Single Chromatographic Reactor	18
3.3 Porosity Measurement	20
3.4 Analysis	20
4 MODELING AND OPTIMIZATION	22
4.1 Adsorption Isotherm	22
4.2 Single Column Model	23
4.2.1 Heterogeneously Catalyzed System	23
4.2.2. Homogeneously catalyzed system	25
4.2.3. Reaction Equilibrium	25

4.2.4. Activation Energy 26

4.2.5 Selectivity 26

4.3 Inverse method 27

4.3.1. Inverse method for well-stirred batch reactor 27

4.3.2. Inverse method for chromatographic reactor 27

4.4 SMBR 28

4.5 Optimization Strategy 30

5 ESTERIFICAITON FOR THE PRODUCTION OF DOWANOL PMA 33

5.1 Motivation 35

5.2. Materials and Methods 35

5.2.1. Materials 35

5.2.2 Methods 36

5.3. Results and discussion 38

5.4 Conclusion 59

6 TRANSESTERIFICATION FOR THE PRODUCTION OF PMA 61

6.1. Motivation 61

6.2. Materials and Methods 63

6.3 Results and discussions 65

6.4. Conclusion 83

7 HOMOGENEOUS TRANSESTERIFICATION FOR PMA PRODUCTION 85

7.1 Motivation 85

7.2 Materials and methods 88

7.3 Results and discussion 88

7.4 Modeling result and discussions 97

7.5 Conclusion and future work 104
8 HETEROGENEOUS TRANSESTERIFICATION WITH TYPE II RESIN 107
8.1Motivation 107
8.2 Materials and Methods 109
8.3 Results and Discussion 111
8.4 Conclusion 119
9 CONCLUSIONS AND FUTURE WORK 121
9.1 Conclusion 121
9.2 Future Work 125
REFERENCES 131

LIST OF TABLES

Page

Table 1. Physical and chemical properties of cation exchange resin, AMBERLYST™15[51] 35

Table 2 Batch experiment conditions 36

Table 3 Equilibrium constant at different temperature, and heat of reaction 42

Table 4 Reaction rate constants and adsorption constants and their 95% confidence intervals obtained by fitting Equation 13 to Figure 8 43

Table 5 Values of Hi and, km obtained from fitting adsorption data to linear isotherm model 47

Table 6 Influence of flow rate and injection volume on conversion at 110 °C 51

Table 7 Conversion of acetic acid calculated based on chromatogram from Figure 18. Compared batch conversions are the result from Figure 14. Values are the average of two replicated experiments. 53

Table 8 Parameters estimated from reactive chromatography experiment at 110°C 57

Table 9 SMBR system details 58

Table 10 Optimal operating conditions of SMBR from the multi-objective optimization analysis for maximizing PMA production rate and acetic acid conversion [60]. 59

Table 11 Properties of ion-exchange resins that are used in experiments 64

Table 12 Conversion of transesterification reaction at 40°C inside well-stirred batch reactor using four different catalysts 68

Table 13. Estimated parameters of PMA and EtOH by fitting linear isotherm to the injection experiment from Figure 26 74

Table 14 Estimated parameters from model fitting shown in Figure 31 80

Table 15 Adsorption parameters obtained by fitting Equation (1),(2) and (3) to Figure 38 91

Table 16 Model parameters obtained by fitting the model to the two reactive chromatography experiments in Figure 44. The lower and upper bounds of the parameters that were imposed in the fmincon function are also listed..... 99

Table 17 SMBR system details..... 100

Table 18 Optimal operating conditions for SMBR from the multi-objective optimization analysis for maximizing PMA production rate and ethyl acetate conversion. 102

Table 19 selectivity Coefficients of Various Anions (Compared with the Hydroxyl Ion) on Functionalized Styrene-Divinylbenzene Anion Exchange Resins of Different Base Strength [95] 110

Table 20 Properties of anion exchange resins that are used in Chapter 8..... 110

Table 21 Conversion and retention time of PMA and EtOH of transesterification experiments with different catalysts. Injection of 100% 1ml EtAc at 40°C while PM flows at 0.5ml/min. 118

LIST OF FIGURES

Page

Figure 1 Esterification of acetic acid and PM that produces PMA and water 3

Figure 2 Transesterification of ethyl acetate and PM that produces PMA and ethanol 4

Figure 3 Conventional methods for the production of PMA 4

Figure 4 Principle of reactive chromatography 5

Figure 5 Schematic of Simulated Moving Bed Reactor unit for the production of component C through the reaction of A and B (A+B□ C+D) 7

Figure 6 Schematic of Simulated moving bed reactor process with the internal concentration profile at cyclic steady state for reversible reaction of A+B<-> C+D (a) Step 1 (b) the internal concentration profiles at the beginning of Step 1 (c) Step 2 (d) the internal concentration profile at the beginning of Step 2. 9

Figure 7 Well-stirred batch reactor setup 18

Figure 8 Chromatographic reactor setup for obtaining (a) internal concentration profile (b) overall conversion of limiting reactant 20

Figure 9 Well-stirred batch experiment at stirring speeds of 270rpm and 400rpm. Temperature 90°C, Initial reactant molar ratio 1.8:1, catalyst loading 0.1g/mL (Run #1 and 2 in Table 2) 40

Figure 10 Well-stirred batch experiment with different size of catalyst particle. Temperature 90°C, Initial reactant molar ratio 1.8:1, Catalyst loading 0.1g/mL (Run #3 and 13 in Table 2) 40

Figure 11 Well-stirred batch experiment with different catalyst loadings. Temperature 90°C, Initial reactant molar ratio 1.8:1 (Run #3 and 11 in Table 2) 40

Figure 12 Well-stirred batch experiment with different initial reactant molar ratio. Temperature 90°C, Catalyst loading 0.1g/mL (Run #3,7,8, and 9 in Table 2) 40
Figure 13 Well-stirred batch experiment at different temperatures. Initial reactant molar ratio is 1.8:1, Catalyst loading 0.1g/mL, (Run #3,4,5,6 in Table 2)..... 41
Figure 14 Comparison of experimental data from Figure 8 to model fitting of equation 13 (a) 50°C (b) 60°C (c) 70°C (d) 90°C..... 44
Figure 15 Injection of single component into chromatographic column (a) Injection of 1.0mL water at 85°C flow rate 1.0mL/min (b) Injection of 1.0mL PMA at 85°C flow rate 1.0ml/min, measured by RID (c) Injection of acetic acid at 25°C with two different volumes, 200µL, 500µL flow rate 2.0ml/min. 47
Figure 16 Injection of 100% acetic acid and 50% acetic acid into chromatographic reactor. Temperature 85°C, flow rate 0.5ml/min..... 49
Figure 17 Schematic diagram of acetic acid injection at different concentration (a) Injection of 100% acetic acid, forming two reaction zones (b) 50% 50
Figure 18 Injection of 50 vol% acetic acid into chromatographic reactor at different temperatures. (a) 70 °C, (b) 85 °C, and (c) 110 °C. Flow rate is 0.5ml/min. 52
Figure 19 Model fitting results: comparison of the elution profiles predicted by the model and the experimental chromatograms obtained by injecting a pulse of acetic acid and PM at 110°C, 5ml injection and at 0.5ml/min flow rate.[9]..... 56
Figure 20 Pareto plot of the multi-objective SMBR optimization problem: PMA produced through the raffinate outlet in g/hr against the percentage conversion of acetic acid [9]..... 59
Figure 21 Reaction equation for the formation of sodium alkoxide..... 64

Figure 22 Conversion of transesterification reaction inside well-stirred batch reactor with four different catalysts 68
Figure 23 Conversion of transesterification reaction using NaOH as a homogeneous catalyst while varying water concentrations inside the well-stirred batch reactor 69
Figure 24 Normalized resin bed volumes saturated in different solvents. The volume of resins beds in PM is 1.0. 71
Figure 25 Conversions of EtAc when 1 ml of 100% EtAc was injected into chromatographic reactors filled with each resin. The experiment was performed at 40°C, 0.5 ml/min flow rate of desorbent, PM. 72
Figure 26. Adsorption experiment of two products, PMA and EtOH. Both products are separately injected at 40°C, at the PM flow rate of 0.5 ml/min. 73
Figure 27 Injection of 1 ml of EtAc into the reactor at 40°C while PM flows at 0.5ml/min. (a) 50% EtAc/PM (b) 100% EtAc..... 75
Figure 28 Injection of 1ml of 50% EtAc/PM into the system at different temperatures at the PM flow rate of 0.5ml/min (a) 40°C (b) 60°C..... 76
Figure 29 The effect of temperature on the esterification and the transesterification applied to the reactive chromatography. (a) The esterification reaction conducted with AMBERLYSTTM 15 resin by injecting 1 ml of 50% acetic acid at the PM flow rate of 0.5 ml/min[14] (b) The transesterification reaction conducted with IRA904 OH- by injecting 1 ml of 50% EtAc at the PM flow rate of 0.5 ml/min 77
Figure 30 The effect of feed concentrations to the esterification and the transesterification by reactive chromatography (a) The esterification reaction conducted with AMBERLYSTTM 15 resin at 85°C by injecting 1ml of acetic acid at the PM flow

rate of 0.5ml/min[14] (b) The transesterification reaction conducted with IRA904 OH- at 40°C by injection 1ml of EtAC at the PM flow rate of 0.5ml/min 78

Figure 31 The result of fitting the model to the experimental data. Experiments are conducted at 40°C by injecting 1 ml of EtAc of different concentrations while PM flows at 0.5 ml/min (a) 50% EtAc/PM (b) 100% EtAc 79

Figure 32. Setup for catalyst deactivation test with AMBERLITETM IRA904 OH- 81

Figure 33. Reactant conversion at the outlet of the column vs. the retention time for deactivation test. Flow rates of PM and ethyl acetate are both 0.3ml/min, and temperature is at 40°C 81

Figure 34 Deactivation mechanism of AMBERLITETM IRA904 OH- which is initiated by small amount of water present in PM 82

Figure 35 Schematic of a SMBR operation 87

Figure 36 Effect of the amount of catalyst, 1.7g/L,2.4g/L, and 3.4g/L at 40°C. The initial molar ratio of EtAc/PM=1 89

Figure 37 Effect of temperature, 40°C,50°C and 60°C on the conversion of EtAc, at 3.4 g/L of catalyst concentration and initial molar ratio of EtAc/PM = 1 90

Figure 38 Elution profiles of (a) PMA and (b) EtOH at different flow rates and various injection concentrations (Cinj = 10vol%, 30vol% and 100vol%). PM was used as a mobile phase 91

Figure 39 Influence of catalyst concentration on the transesterification reactions at 40°C. (a) Ccat =1.7 g/L (b) Ccat = 3.4 g/L (PM flow rate = 0.5 ml/min, feed concentration = 100%, injection volume = 1 ml, column length 25 cm) 93

Figure 40 Influence of temperature on the transesterification reactions (a) 40°C (b) 60°C (Catalyst concentration 3.4g/L, PM flow rate = 0.5 ml/min, feed concentration = 100% EtAc, injection volume = 1 ml, column length 25 cm) 94

Figure 41 Influence of flow rate on the transesterification reactions. (a) 0.5ml/min (b) 1ml/min (c) 2ml/min (feed concentration 100 vol%, temperature 333.15 K, injection volume 1 ml, column length 25 cm, catalyst concentration 1.7 g/L). 95

Figure 42 Elution profile of transesterification reaction at higher reactor column length, 50 cm (feed concentration 100vol%, temperature 333.15K, injection volume 1 ml, flow rate 0.5 ml/min). 96

Figure 43 Influence of residence time on the conversion of ethyl acetate (feed concentration 100vol%, temperature 40°C, injection volume 1 ml). 96

Figure 44 Model fitting results: comparison of the elution profiles predicted by the model and the experimental chromatograms obtained by injecting a pulse of ethyl acetate at 40°C and 1.7g/L catalyst concentration. (a) Flow rate: 0.5ml/min and (b) flow rate: 1ml/min..... 99

Figure 45 Comparison of the elution profiles predicted by the model and the experimental chromatogram obtained by injecting a pulse of 100% EtAc at 40°C, 1ml injection at 0.5ml/min flow rate, 1.7g/L catalyst concentration, using 50cm length column reactor. 100

Figure 46 Pareto plot of the multi-objective SMBR optimization problem: PMA produced through the raffinate outlet in g/hr against the percentage conversion of ethyl acetate 102

Figure 47 Plot of operating conditions against conversion..... 103

Figure 48 Internal concentration profiles inside the SMBR slightly after the beginning of the step (t/tstep=0.086), for 95% conversion of ethyl acetate. (a) Concentration profile of PM, EtAc, PMA, and EtOH (b) Value of Equation 19 104
Figure 49 Chemical structures of anion exchange resins..... 108
Figure 50 Deactivation test result of IRA904 OH- (Type I), Dowex 22(Type II) and PA 418 (Type II). PM and EtAc are injected into each column at a same flow rate, and PMA concentration at the outlet of the column is plotted. 112
Figure 51 Elution profiles for various injection concentrations of EtOH and PMA (flow rate = 0.5ml/min, injection volume = 100 □L). 113
Figure 52 Elution profiles for injection of 1ml 100% EtAc into a column packed with Dowex 22 at 40°C while varying the flow rates and column length..... 114
Figure 53: Conversion of EtAc from experiments performed at different column lengths (25 cm, 50 cm) and flow rates (0.5 ml/min, 1 ml/min) 115
Figure 54: Elution profile of EtAc injection into a column with 25 cm length while PM flows at 0.5 ml/min at 40°C at different feed volume and concentration..... 116
Figure 55 Injection of 100% 1ml EtAc at 40°C while PM flows at 0.5ml/min into columns packed with different adsorbent and catalyst (a) IRA 904OH- (b) Sodium alkoxide (c) Dowex 22 118
Figure 56 Variation of the inlet feed concentration [9] (1) constant feed concentration strategy (dotted) (2) ModiCon strategy (solid)..... 127

SUMMARY

Reactive chromatography is an integrated process that combines reaction and separation in a single unit that leads to a higher productivity. This process is especially advantageous when the reaction is equilibrium limited where in-situ separation of product shifts the equilibrium in the direction of conversion increase. A continuous reactive separation process, simulated moving bed reactor (SMBR), is an extension of this reactive chromatography process that performs in a continuous and counter-current fashion. The SMBR unit consists of multiple chromatographic columns that are interconnected in a cyclic configuration, which columns are packed with a resin that functions both as a catalyst and an adsorbent. Such process enables high throughput and low desorbent consumption compared to conventional chromatography.

In the present work, an application of reactive chromatography and SMBR using ion exchange resin as a catalyst and adsorbent will be studied, which will be a new platform for production of industrial esters. Among numerous esters, this study focuses on the production of propylene glycol methyl ether acetate (DOWANOL™ PMA glycol ether acetate), one of the most commonly used esters with a high industrial demand. DOWANOL™ PMA glycol ether acetate is the second-most used propylene glycol ether with nearly 90% of its use in surface coatings.

The first objective of the study is to apply esterification reaction for the production of PMA through SMBR. The first approach for PMA production employs ester formation from acid and alcohol with a cation exchange resin as a catalyst and adsorbent. However, the reaction kinetics for the esterification of PMA synthesis has not been previously reported in the literature. Therefore, experiments are first performed with well-stirred batch reactor at different conditions to study reaction kinetics. Then, the application to reactive chromatography is presented, where batch reactive chromatographic experiments are performed at different conditions and reaction parameters are obtained by the inverse

method. Reactive chromatography experiments demonstrate the advantage of the system over well-stirred batch reactors, by achieving high conversion of 80% and collecting the two products at high purity. Using parameters obtained from the experiments, the SMBR is designed and optimized considering multiple objectives. The SMBR optimization successfully shows operating conditions for 95% conversion while satisfying purity constraints.

The second objective of the study is to demonstrate the applicability of transesterification to the reactive chromatography. Results from the first objective show a promising applicability of esterification to the reactive chromatography system. However, the productivity is low due to a high affinity of the byproduct, water. Thus, the second objective investigates transesterification as an alternative solution to esterification, since the by-product of transesterification, ethanol, has lower affinity towards the resin compared to water. This work represents one of the first attempts to apply transesterification to reactive chromatography outside of biodiesel production. Results show transesterification has a higher conversion at a lower temperature compared to esterification. In addition, results show improved productivity of the system since the process time decreases to wash out the byproduct.

The final objective is to further improve SMBR based on the previous results. This improvement involves studying homogeneous catalysts and Type II anion exchange resins. Based on numerous literatures about anion exchange resins, it is inevitable for anion exchange resins to lose activity in terms of time when exposed to reactants and atmosphere. To overcome such drawback, homogeneous catalyst and Type II resin is employed and data are demonstrated with sodium alkoxide and Dowex 22. The result shows high conversion and purity of products, which demonstrates the practicality of the process for PMA production.

Altogether this work is focused on finding the best design and operation of the SMBR system for the production of PMA based on a systematic approach. Various types of catalysts are tested to find the one with highest conversion and separation factor. To compare the different systems, model based simulation and optimization is performed. Through this

method, different types of catalysts are compared for an application to reactive chromatography based on simulation without building different SMBR and performing complicated experiments.

CHAPTER 1. INTRODUCTION

The changing nature of the chemical industry implies a transformation of the old vision of chemical engineering as simply changing raw materials to products through reactions and separation into a more elaborate vision of providing the product with markedly higher output, lower consumption of raw materials and energy, zero waste and zero pollution [1]. For the development of new processes and products in a sustainable way, a novel combination of science and technology is required. This can be pursued through process intensification, such as multifunctional reactors in which the reaction and separation are integrated into the same unit, such as reactive chromatography, reactive distillation and membrane reactors [1].

Catalytic distillation is based on the technology where reaction and distillation is combined in one vessel using structured catalysts as the enabling element. It is first considered for esterification process in a series of patents by Backhaus in the 1920s [2]. After the first application, it has been commercially applied to many different areas, such as aromatics alkylation, benzene removal from reformate fractions, selective desulfurization of FCC gasoline fractions, as well as for various selective hydrogenations [3-6]. Membrane reactor is a device which simultaneously performs a reaction (steam reforming, dry reforming, autothermal reforming, etc.) and a membrane-based separation in the same physical device [7]. It also has various applications such as hydrogen production, xylene isomerization, ethanol esterification, methanol production and many others in areas of refinery, food, biotechnology and pharmaceutical industry [8].

Reactive chromatography has also raised considerable interest in the chemical engineering research for multiple reasons. Firstly, for equilibrium limited reactions,

continuous removal of at least one of the reaction products shifts the equilibrium in a direction to increase conversion and reduce by-product formation. Secondly, when the packing material of column is used as a catalyst, catalyst stays inside the column and removal of catalyst from the product stream is not required. Third, chromatography can separate complex mixtures with great precision [9]. The purity requirements of the products are often easier to meet in chromatography compared to other separation methods. Lastly, chromatography can be used to separate delicate products that require special care to avoid harsh process conditions, since the conditions under which chromatography is performed are not typically severe. For these reasons, reactive chromatography is well suited to a variety of uses in the field of biotechnology, such as separating the mixture of proteins or production of biodiesel.

Reactive chromatography, as of today, has developed into an invaluable laboratory tool and an industrial unit for the synthesis and purification of compounds. Over the last 40 years, research has focused on the development of continuous chromatographic reactor in order to enhance productivity and reduce solvent consumption [1, 10].

Among several applications of reactive chromatography, synthesis of esters has been the subject of investigations by many researchers [11, 12]. This is because esters are of great significance in various industrial products including fragrances, flavors, and surface-active agents [13]. In addition, many heterogeneous catalysts including ion exchange resins can be used as a packing material in a chromatography column that functions simultaneously as a catalyst and as an adsorbent for synthesis of esters.

The following sections introduce an ester that has an important industrial value and has potential for improvement in process when applied to chromatographic reactor. In addition,

the basic principle of reactive chromatography and its extension to simulated moving bed reactor (SMBR) are discussed.

1.1 DOWANOL^{TM} PMA [14]

Propylene glycol methyl ether acetate (DOWANOL^{TM} PMA) is second most widely used propylene glycol ether with most of its use as a solvent for industrial paints and coatings in the automotive industry. It is also used in the electronic industry and formulated into various commercial products such as degreasers for the circuit boards. It is very efficient at dissolving resins used in paints, inks, lacquers, and other types of surface coatings. It has high industrial demand, where the U.S. market in 1993 was 72 million pounds [15].

PMA can be synthesized through two types of reactions: i) esterification and ii) transesterification. The esterification reaction of 1-methoxy-2-propanol (PM) and acetic acid in the presence of an acidic catalyst can be represented as in Figure 1. The transesterification is a reaction between PM and ethyl acetate in the presence of basic catalyst and is shown in Figure 2. Both reactions are reversible and equilibrium limited.

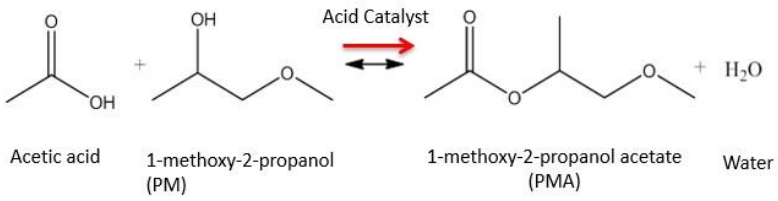

Figure 1 Esterification of acetic acid and PM that produces PMA and water

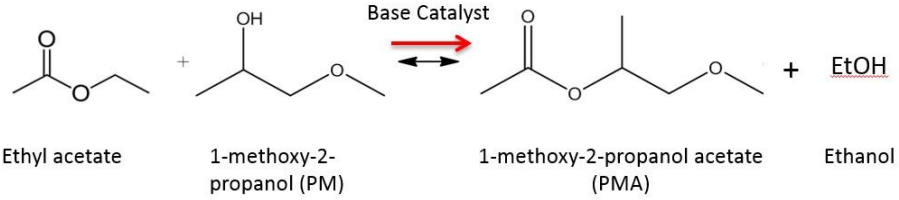

Figure 2 Transesterification of ethyl acetate and PM that produces PMA and ethanol

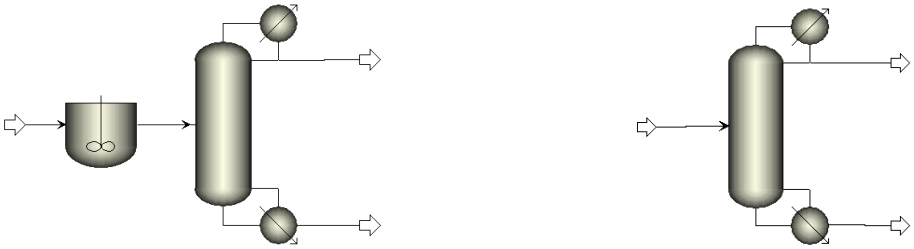

(a) reaction-distillation multi-step **(b) reactive distillation one step**

Figure 3 Conventional methods for the production of PMA

Conventional methods to produce PMA involve reactive distillation as a one-step, or multistep processes of reaction and separation steps as illustrated in Figure 3. However, use of distillation unit for separation limits the production of PMA due to the formation of azeotropes. Hsieh et al. have studied the multiphase equilibria for mixtures containing reactant and products of esterification for PMA synthesis [16]. In addition, Chiavone-Filho et al. investigated the VLE behavior of water and PMA at 353.15 and 363.15K, and observed that maximum pressure azeotropes exist in this binary system [17]. Thus, a distillation process is not suitable for the purification of PMA from reaction mixture.

1.2 Principle of Reactive Chromatography

The reactive chromatography process is a combination of reaction and chromatographic separation inside a single column. Chromatography is an adsorptive separation process, where the components are separated based to their different affinity

towards the adsorbent. For simultaneous reaction and separation, the packing material must be a catalyst that has different affinity towards the reactants and products. Figure 4 illustrates the batch reactive chromatography process for the reaction between reactants A and B that produces products C and D. In this process, the limiting reactant (A) is injected as a sharp pulse into the column that is initially saturated with excess reactant (B). Reactant B is continuously supplied as a desorbent. Two components (A and B) react inside the column with the presence of catalyst and produce two products (C and D). Among the two products, weakly adsorbed component (C) moves faster in comparison to the strongly adsorbed component (D). Based on the different elution time, the products are collected separately by fractionation. Such separation facilitates the reversible reaction to go beyond the thermodynamic equilibrium by continuously separating the products from the reaction zone based on the Le Chatelier's principle. Thus, there is more product formation in these systems with high purities due to their separation from the reactants. Furthermore, the integration of both reaction and separation units into one single unit reduces both capital and operating costs. However, this batchwise operation may not be suitable for large-scale productions.

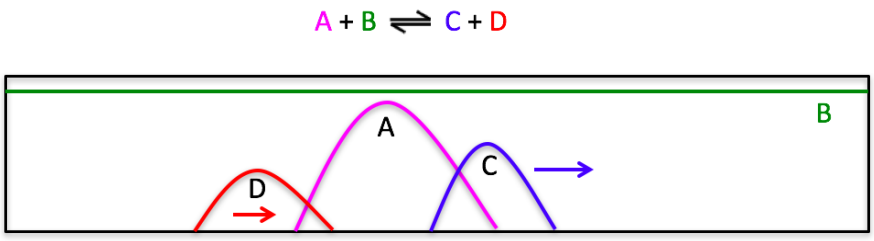

Figure 4 Principle of reactive chromatography

Simulated moving bed reactor (SMBR), on the other hand, is an extension of this process that performs reactive chromatography in a continuous and counter-current fashion.

The SMBR system is described in the next Section.

1.3 Simulated Moving Bed Reactor

Simulated moving bed reactor (SMBR) is an extension of the reactive chromatography process that performs in a continuous and counter-current fashion. Figure 5 shows the standard SMBR unit where chromatographic columns are connected in a cyclic configuration. Similar to single chromatographic reactors, each column is packed with a resin that function both as a catalyst and an adsorbent. For a standard four-zone SMBR, four external streams are present: a feed stream containing the components to be reacted, a desorbent stream, which can be one of the reactants, the extract line containing the more retained product and the raffinate line enriched with the less retained product. For reversible and equilibrium limited reactions in Figure 5, such as A+B↔C+D, both reactants are injected through feed port and one of the reactant (B) is used as a desorbent. Two reactants, injected through the feed port, react inside the column catalyzed by the packing material. Two products, C and D, have different affinity towards the packing material, and Figure 5 shows the case where C is the faster-moving component. The faster-moving component is recovered from the raffinate outlet while the strongly retained component, D, is recovered through the extract outlet. As the reaction proceeds inside the SMBR, the products are continuously removed from the system, thus shifting the equilibrium in the forward direction.

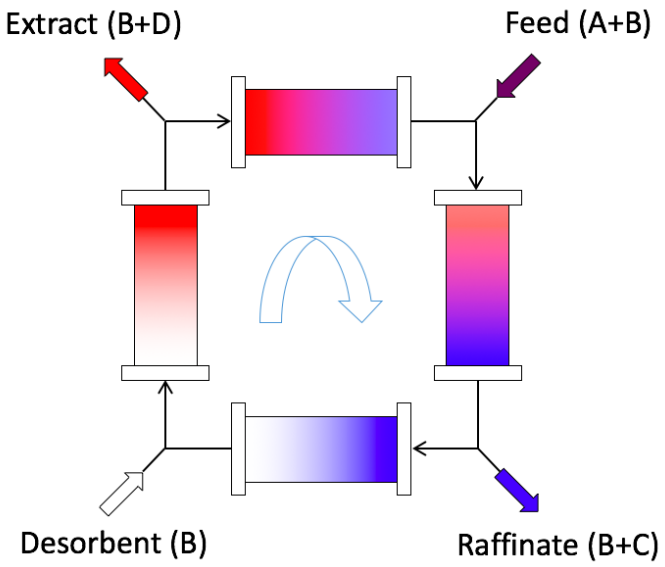

Figure 5 Schematic of Simulated Moving Bed Reactor unit for the production of component C through the reaction of A and B (A+B↔ C+D)

To achieve the desired performance of the SMBR, the operating condition must be determined. Flow rates of each inlet and outlet ports can be controlled independently, and hence there are four degrees of freedom. In addition, the switching time of inlet and outlet ports can be selected separately. These operating conditions are selected such that each sections of SMBR plays a specific role in the process. Separation and reaction are performed in zone II and III, and zone I regenerates the solid phase, and zone IV regenerates the liquid by adsorbing the amount of less retained component not collected in the raffinate.

In order to achieve a complete separation, counter-current motion of solid phase is desired. However, the movement of a stationary phase, which in most cases consists of porous particles in the micrometer range, is technically not possible. Therefore, counter-current flow of both phases is achieved by switching the column periodically upstream in the opposite direction of the liquid flow. In a real plant, the columns are not shifted but all

ports are moved in the direction of the liquid flow by means of valves. In a four-column SMBR, four consecutive switching complete one so-called cycle and brings the external streams back to its initial position. This cyclic operation of SMBR is continuously repeated and ultimately, the SMBR systems arrives at a cyclic steady state (CSS). At the CSS, the concentration profiles still change inside the columns; however, the snapshots of internal concentration profiles at the beginning and at the end of the step are identical, apart from a shift of exactly at the length of one column.

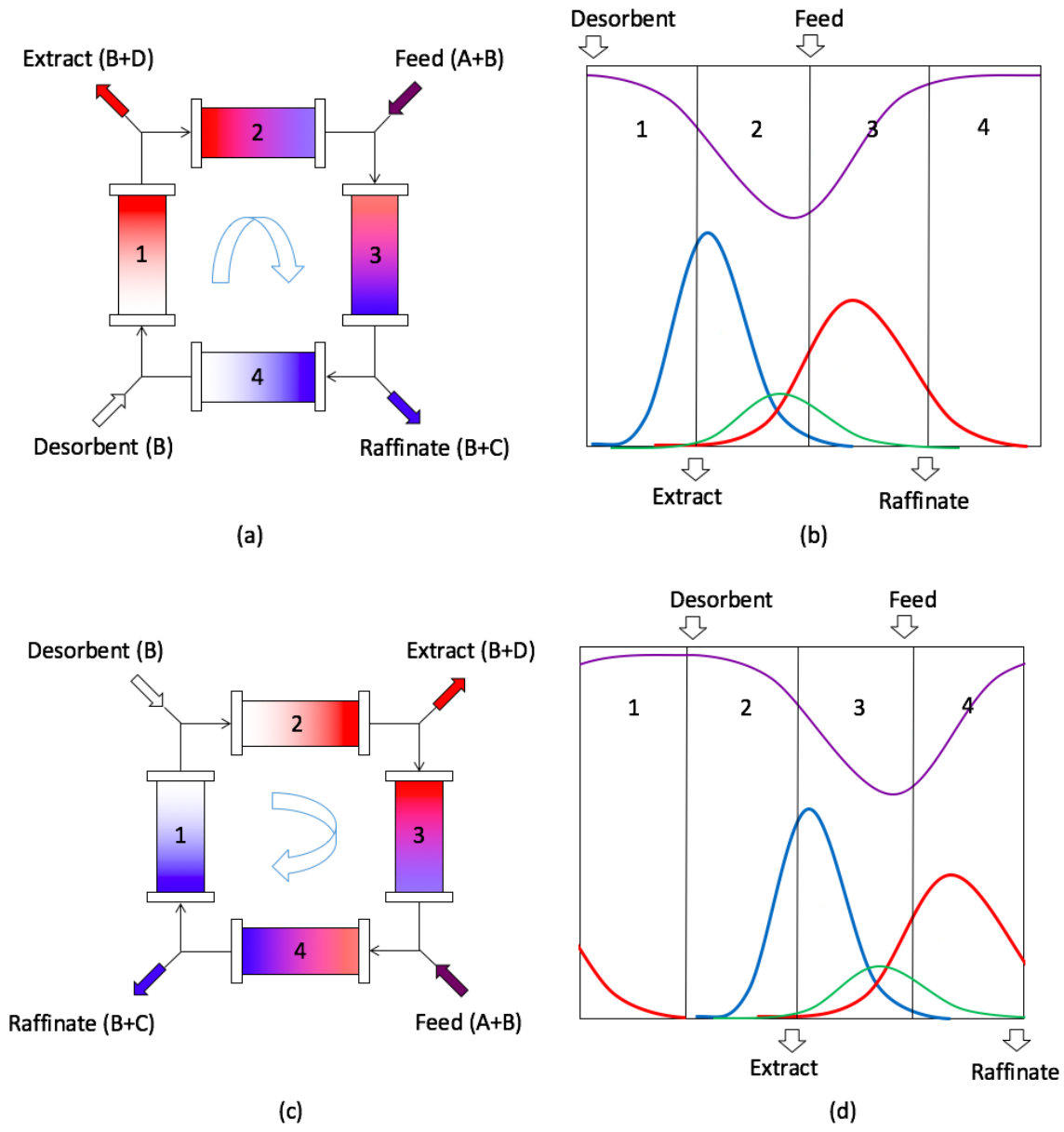

Figure 6 Schematic of Simulated moving bed reactor process with the internal concentration profile at cyclic steady state for reversible reaction of A+B<-> C+D (a) Step 1 (b) the internal concentration profiles at the beginning of Step 1 (c) Step 2 (d) the internal concentration profile at the beginning of Step 2.

Figure 6 illustrates this concept of CSS by showing the internal concentration profiles for two consecutive steps of the SMBR operation at the cyclic steady state for reversible reaction of A+B ↔ C+D. Figure (a) shows the Step 1, where the feed stream is

positioned between columns 2 and 3. In column 3, reactants (A and B) react and produce component C and D. Based on the affinity, the more retained component (D) has to be adsorbed and carried towards the extract port through the movement of the solid, while the less retained component C has to be desorbed and carried by the mobile phase in the direction of the raffinate port. In column 1, the solid phase is regenerated with a fresh eluent by desorption of the strongly adsorbed component. Finally, in column 4, the liquid is regenerated by solid adsorbing the remaining less retained component. It can be seen from Figure (b) that extract stream is positioned at the location where the concentration of component D is at the highest and also the raffinate stream is positioned at where the concentration of component C is high. In this manner, SMBR enables continuous collection of each product at high purity.

The SMBR operates at Figure (a) configuration for one switching time period, and the ports are switched to Step 2. In this step, the positions of all the inlet and outlet ports are moved clockwise by one column length (Figure (c)). As a result, the feed port is positioned in between columns 3 and 4 and desorbent in between columns 1 and 2. Similarly, the raffinate and extract outlet streams are also switched to the outlet of columns 4 and 2, respectively. Figure (d) shows the concentration profiles at the beginning of Step 2. Comparing Figures (b) and (d), the internal concentration profiles at the beginning of Step 2 are exactly identical to Step 1, except for the shift of one column length. Thus, the SMBR system is at a cyclic steady state. This cyclic operation of SMBR is constantly repeated to recover pure products continuously from the raffinate and the extract outlet.

The SMBR has been examined for various reaction systems, with the main focus on reactions of the type $A+B \leftrightarrow C+D$, which is the system studied in this thesis. Examples

are esterification of acetic acid with methanol [18], ethanol[19], and β-phenethyl alcohol [20]as well as the production of bisphenol A[21]. The same reaction type can also be found for hydrocarbons, such as the transfer reaction of sucrose with lactose to lactosucrose [22] and hydrolysis of lactose [10, 23].

Since SMBR enables high throughput and low desorbent consumption compared to conventional chromatography, there has been a continuous effort to find modified SMBR schemes that allow for higher productivity yet meeting the same product specifications. Example of such modification is the process called Hashimoto process [24]. Hashimoto et al. proposed a reactive counter-current chromatographic process for reactions of the type A↔B, where partial deintegration of reaction and separation is applied to conventional SMB process [10]. In this process, adsorption columns and reactors are alternately arranged in one or several sections of the SMB process, which offers the possibility to separate the functionalities separation and reaction [10]. In addition to Hashimoto process, recently developed improved SMB processes, e.g. VariCol,[25] PowerFeed [26], and ModiCon [27], can also be used in reactive chromatography. Application of ModiCon concept to esterification is studied by Agrawal et al. and demonstrated improved conversion and productivity [9]. VariCol concept has been applied to sucrose inversion by Kurup et al. through simulation [28].

The number of operating parameters that affect the performance of SMBR is five: four zone flow rates and the switching time. In a standard SMBR, all of these control parameters are kept constant with respect to time and treated as operating conditions. Since these operating conditions influence both conversion and productivity obtained in the product outlets, the optimal performance of the SMBR systems depends on the

identification of the optimal operating conditions. The optimization strategies that are used for obtaining the optimal operating conditions of SMBR systems are discussed in Chapter 4.

CHAPTER 2 SCOPE OF STUDY

The overarching goal of this work is to develop a novel reactive chromatography process for the production of PMA at an increased productivity and higher conversion compared to batch processes. The development of the process was performed based on experimental works and available mathematical modeling and optimization methods. There are three main objectives in this work:

1. Apply esterification for the development of SMBR with a cation exchange resin to produce PMA
2. Verify the potential of transesterification to be applied to SMBR for the production of PMA
3. Identify alternative solutions to improve SMBR for the production of PMA: Homogeneous catalysis system and Type II resin

The first objective is the topic of Chapter 4, where the esterification is studied for the production of PMA through SMBR. The first approach for PMA production employs ester formation from acid and alcohol with a cation exchange resin as a catalyst and adsorbent. Amberlyst 15 is selected as a cation exchange resin since it has been successfully utilized as a catalyst in various packed bed experiments for esterification [19, 29, 30]. However, the reaction kinetics for the esterification of PMA synthesis has not been previously reported in the literature. Therefore, experiments are first performed with well-stirred batch reactor at different conditions and model parameters are estimated. Then, the application to reactive chromatography is presented. Batch reactive chromatographic experiments are performed at different conditions and reaction parameters are obtained by the inverse method. Using parameters obtained from the experiments, the SMBR is

designed and optimized considering multiple objectives. Finally, SMBR experiments are performed at optimized condition, and the model is validated through comparison with experimental results.

The second objective is the topic of Chapter 5, where the transesterification is studied for the SMBR. Chapter 4 shows a promising applicability of esterification to this system. However, the productivity is low due to a high affinity of the byproduct, water. Thus, Chapter 5 investigates transesterification as an alternative solution to esterification. The by-product of transesterification, ethanol, has lower affinity towards the resin compared to water. However, to the best of our knowledge, no previous research have employed an anion exchange resin in reactive chromatography, although it is discussed in a patent publication by Geier [31]. Thus, Chapter 5 also shows a process of selecting an appropriate resin for the reaction. After the selection of the resin, the procedure is similar to Chapter 4, where the reaction kinetics are first studied in well-stirred batch reactor, then further studied in a single-column chromatographic reactor. Before proceeding to the SMBR experiment, two reactions, esterification and transesterification, are compared based on single-column experiments and model-based simulation result of SMBR. In this way, two reactions can be compared systematically using the model.

The final objective is to further improve SMBR based on the results in the previous chapters. This improvement involves studying homogeneous catalyst and studying other type of ion exchange resins. A lot of previous studies designed SMBR with well-known catalysts and reactions for the purpose of modeling, designing and optimization of chromatographic reactors and sucrose inversion is a good example where it has been tested for many publications investigating different configurations of SMBR [28, 32-34]. On the

other hand, the final objective of this thesis focus on trying different types of resins that have potential for further improving the productivity of the process. The first catalyst is a homogeneous catalyst. Based on numerous literatures about anion exchange resins, it is inevitable for anion exchange resins to lose activity in terms of time when exposed to reactants and atmosphere. What has been observed in Chapter 5 also corroborates those literature results, and deactivation of catalyst was shown. To overcome such drawback, homogeneous catalyst is employed. Chapter 6 shows results of transesterification with sodium alkoxide as a homogeneous catalyst dissolved in the mobile phase. The same anion exchange resin that is used in Chapter 5 in another ionic form is used as an adsorbent without catalytic activity. The second catalyst tested is a Type II anion exchange resin. Type II anion exchange resins, which has a different amine functional group, are not as widely used as Type I resin. This is because in general, Type I resin has higher thermal and chemical stability. However, in case of PMA synthesis, Type II resin is found to have higher chemical stability. For both catalysts, homogeneous and Type II resin, a similar procedure is followed to study the effect of the catalyst. The reactions are performed in single-column chromatographic reactors at different conditions and parameters are estimated through fitting the model. The results are compared in terms of productivity and conversion of reactants.

Altogether this work is focused on finding the best design and operation of the SMBR system for the production of PMA based on a systematic approach. Various types of catalysts are tested to find the one with highest conversion and separation factor. To compare the different systems, model based simulation and optimization was performed. Through this method, different types of catalysts are compared for an application to

reactive chromatography based on simulation without building different SMBR and performing complicated experiments.

CHAPTER 3 EXPERIMENT METHODS

This chapter explains experimental methods that are followed for the rest of this thesis. Experimental procedures are established to characterize reaction kinetics and equilibrium, as well as chromatographic separation.

3.1 Well-stirred batch reactor

Well-stirred batch reactor experiments are performed to study reaction kinetics in a simple setup. Experiments are carried out in a three-necked spherical glass flask of 500 ml capacity fitted with a coil condenser to minimize loss of products. The experimental setup is shown in Figure 7. The temperature is controlled within ±0.1 K by a PID temperature controller in a water bath. Mixing of the reaction fluid is performed by an overhead stirrer to avoid deformation of catalyst by magnetic stirrer.

For heterogeneously catalyzed reactions, PM and catalyst are first placed in a reactor, and then stirring and heating are initiated. When the mixture reaches the desired temperature, the preheated second reactant is added to the reactor. On the other hand, experiments with homogeneous catalysts are initiated by dissolving catalyst into PM for enough time in a reactor, and second reactant is added in the same way. A sample is taken at time zero to determine the initial composition of the reaction mixture. During the sampling procedure, the stirring speed is set to a sufficiently low value to avoid collection of fine particles of the catalyst. About 0.1 ml of liquid sample is withdrawn from the reactor at a regular interval for gas chromatographic analysis. All experiments are conducted until the reaction reach the equilibrium. All experiments in the glass flask reactor have been performed at atmospheric pressure.

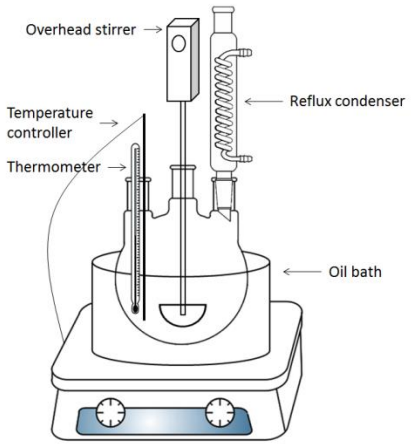

Figure 7 Well-stirred batch reactor setup

3.2 Single chromatographic reactor

Single chromatographic reactor experiments are performed to observe reaction and separation within a single unit. An empty stainless steel column of internal diameter of 0.8 cm and length of 25 cm from Knauer is employed as the vessel for reactive chromatography. The column is packed with heterogeneous catalyst or adsorbent using slurry method. As can be seen from Figure 8 (a), the LC-20 pump from Shimadzu is used to pump the mobile phase through the packed column, and RH-7725i valve from Rheodyne is used to provide an almost rectangular pulse input of reactants. The sample loop and column are kept inside the oven (Shimadzu, CT-20A), which ensures temperature consistency of ± 0.1°C. The effluent from the column is collected with a fraction collector (Shimadzu, FRC-10a) where each sample volume is less than 200 μL. After each experiment, all of the samples are analyzed by gas chromatography. When the reaction temperature is higher than the boiling point of components at atmospheric pressure, a backpressure valve and ice bath are installed after the column to make sure the components cool down to below the boiling point before they are exposed to atmospheric pressure. All tubings connecting to each

instrument are 1/16 inch in the outer diameter and the total dead volume of the system is measured to be 0.343 ml.

For characterizing the conversion of the limiting reactant in a quick and convenient way, the same column is filled with a selected adsorbent - catalyst and an identical amount of limiting reactant is injected at constant conditions. As can be seen from Figure 8 (b), when the conversion of the limiting reactant is tested, the outlet is collected with a graduated cylinder until all components elute out. When basic homogeneous catalysts are present inside the mobile phase, 5 vol% of acetic acid is added to the graduated cylinder to quench the reaction while sampling.

The mobile phase used, PM, is dried before the experiments by adding molecular sieve 3Å into the stock bottle and leaving it overnight. Before making the injections, the column is equilibrated with sufficient amount of dried PM. In addition, a column that has same dimension as reactor is filled with molecular sieve 3Å and installed in front of the reactor when obtaining a chromatogram to help maintain anhydrous conditions. In both cases of (a) and (b), all of the samples are analyzed by gas chromatography.

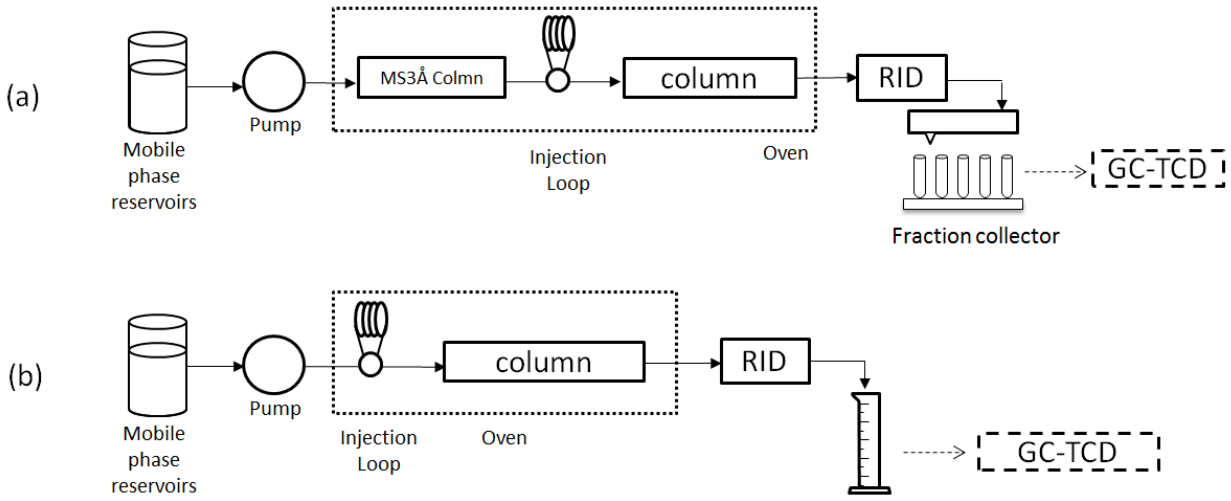

Figure 8 Chromatographic reactor setup for obtaining (a) internal concentration profile (b) overall conversion of limiting reactant

3.3 Porosity Measurement

To estimate the porosity of the chromatographic reactor, dextran (molecular weight approximately 250,000 g/mol) is used as a tracer, which has molecular weight that is large enough not to penetrate into the pores of resins inside the column. Since dextran is not dissolvable in the mobile phase (PM) that is used for this system, the column is first saturated in water, and then dextran dissolved in water is injected into the system. Since the swelling ratio of resins in PM and water does not differ greatly (within 10%), the interstitial volumes measured in these two mobile phases are assumed to be the same, which is validated later in fitting of the models. The retention time obtained in this manner is used to calculate the porosity of the system.

3.4. Analysis

A Shimadzu gas chromatography system GC-2010 equipped with a flame ionization detector and thermal conductivity detector is used to analyze the concentration

of each component in samples. The samples are injected with the AOCi autosampler. The column used for the GC analysis is ZB-1 (Phenomenex), a capillary column with dimensions of 60 m × 0.32 mm × 1.00μm. The method is developed for analysis of all components in a single run. Injector and detector temperatures are maintained at 300 °C and the temperature of the column is varied by the ramp method. The initial temperature is kept at 90 °C and washed for 0.1 min. It is then increased at a rate of 75 °C/min to the final temperature of 300 °C, and then held for another 0.1 min to ensure all the components are purged out between each analysis. Helium is used as a carrier gas. The total run time for each sample is 5.0 min and the split ratio is 50, with the injection volume of 1 μL. A calibration curve is constructed with samples of known concentrations before the experiments, and the resulting curve is used to calculate the concentration of unknown samples. No internal standards are used.

For adsorptive column experiments, where single components are injected, obtaining the chromatogram of single components is possible from a Shimadzu refractive index detector (RID) instead of subjecting the samples to GC analysis. Before the experiment, the RID is calibrated with the mobile phase (PM) and chromatogram is obtained when the chemical is injected.

CHAPTER 4 MODELING AND OPTIMIZATION

This chapter is devoted to the detailed mathematical modeling and the optimization methods for the chromatographic reactor and simulated moving bed reactor (SMBR) process. The mathematical modeling is based on first principles.

4.1. Adsorption Isotherm

When a mixture of components is injected into a reactive chromatography column, each component adsorbs onto the resin to an extent depending on their affinities towards the resin. The equilibrium is determined by the isotherm, which gives the correlation between the loading of the solute on the adsorbent q_i at different fluid phase concentrations C_i. In contrast to the well-developed thermodynamic methods for determining gas/liquid equilibriums, theoretical determination of adsorption isotherms in liquid chromatography is not yet feasible for most applications. Therefore, both the linear and non-linear isotherms are taken into consideration. The linear adsorption isotherm is often used in the range of low liquid phase concentration where a linear relationship between q_i and C_i holds [35]. For the linear adsorption isotherm, the stationary phase concentration is expressed by:

$$q_i^{eq} = H_i C_i \quad (1)$$

where H_i is the adsorption equilibrium constant and q_i^{eq} is the solid phase concentration that is in equilibrium with C_i. On the other hand, a nonlinear isotherm can describe equilibria in a wider range of concentrations. The nonlinear Langmuir isotherm is as shown below:

$$q^{eq} = \frac{H_i C_i}{1+\sum_{j=1}^{n} b_j C_j} \quad (2)$$

where b_j is nonlinear isotherm coefficients.

4.2 Single Column Model

4.2.1 Heterogeneously Catalyzed System

Different kinds of modeling approaches for the single column reactive chromatography are nicely summarized and discussed by Guichon et al. [36] and have been applied to various systems. In this work, the isothermal, lumped kinetic rate model with a linear driving force (LDF) is used, given as the following set of equations.

Mass balance in liquid phase:

$$\frac{\partial C_i}{\partial t} + \frac{1-\varepsilon}{\varepsilon} k_{m,i}\left(q_i^{eq} - q_i\right) + u\frac{\partial C_i}{\partial x} = D_{ax}\ \frac{\partial^2 C_i}{\partial x^2} \quad (3)$$

where t is time, x is the space coordinate, ε the total porosity, $k_{m,i}$ the solid-liquid mass transfer coefficient, and D_{ax} is the axial dispersion coefficient. q_i^{eq} is the solid phase concentration that is in equilibrium with C_i which is given by the adsorption isotherm. The change in the adsorbent volume due to swelling is ignored, and the superficial liquid velocity of the liquid u is assumed to be constant. The total volume is assumed to be constant, which is an approximation. Our studied system is mostly diluted by one component, the mobile phase, and thus, the change of the total volume is assumed to be negligible.

Mass balance in solid phase is described as :

$$\frac{\partial q_i}{\partial t} = k_{m,i}\left(q_i^{eq} - q_i\right) + \mu_i r \quad (4)$$

where μ_i is the stoichiometric reaction coefficient and r the reaction rate.

For reversible reaction where component A and B react to produce component C and D, assuming the reactions are first order in all components, and the activities of components can be represented by their concentrations, the net reaction rate is expressed as:

$$r = k_f(q_A\, q_B - \frac{q_C\, q_D}{K_{eq}}) \quad (5)$$

where K_{eq} is the equilibrium constant of the reaction which will be determined from a well-stirred batch reactor.

The above partial differential equations require initial and boundary conditions, which are discussed below.

The initial conditions are defined at $t = 0$ as follows:

$$C_i\left[t = 0, x\right] = 0 \qquad (6)$$

$$q_i\left[t = 0, x\right] = 0 \qquad (7)$$

The boundary conditions are,

$$C_i\left[t, x = 0\right] = C_{\text{in},i}(t) \quad (8)$$

The inlet concentrations are,

$$C_{\text{in},i}\left[t, x = 0\right] = 0,\ 0 < t < t_d \qquad (9)$$

$$C_{\text{in},i}\left[t, x = 0\right] = C_{f,i},\ t_d \le t \le t_d + t_p \qquad (10)$$

$$C_{\text{in},i}\left[t, x = 0\right] = 0,\ t > t_d + t_p \qquad (11)$$

where $C_{f,i}$ is the concentrations of injected components, t_d is the time corresponding to dead volume, and t_p is the pulse injection time.

4.2.2. Homogeneously Catalyzed System

For homogenously catalyzed system, the same LDF model is used to describe the chromatographic reactor. The difference is the reaction occurs inside the liquid phase with a homogeneous catalyst. Thus, the reaction term presents in liquid phase mass balance as follows:

$$\frac{\partial C_i}{\partial t} + \frac{1-\varepsilon}{\varepsilon} k_{m,i}\left(q_i^{eq} - q_i\right) + u\frac{\partial C_i}{\partial x} - \mu_i r = D_{ax}\ \frac{\partial^2 C_i}{\partial x^2} \quad (12)$$

Mass balance in solid phase is

$$\frac{\partial q_i}{\partial t} = k_{m,i}\left(q_i^{eq} - q_i\right) \quad (13)$$

The reaction rate equation is represented by concentration of each component in liquid phase as given below:

$$r = k_f(C_A C_B - \frac{C_C\, C_D}{K_{eq}}) \quad (14)$$

The above partial differential equations have the same initial and boundary conditions as in the previous section by equation 6-11.

4.2.3. Reaction Equilibrium

Assuming the reactions are first order in all components, and the activities of components can be represented by their concentrations, the chemical reaction equilibrium constant of the reaction is given as follows:

$$K_{eq} = \frac{C_{PMA} C_{EtOH}}{C_{PM} C_{EtAc}} \quad (15)$$

The value of K_{eq} is calculated based on the final concentration from the well-stirred batch reactor experiments. The activity coefficients are assumed to be 1 in the above equation

for the sake of model simplicity, and it should be noted that this assumption may contribute to the potential error of the model.

This constant can also be expressed in terms of temperature by Van't Hoff equation:

$$ln\frac{K_{eq}(T_1)}{K_{eq}(T_2)} = \frac{\Delta H}{R}(\frac{1}{T_1} - \frac{1}{T_2}) \quad (16)$$

By fitting the above equation at different temperatures, the reaction enthalpy (ΔH) is obtained as a constant that is independent of temperature.

4.2.4. Activation Energy

The temperature dependence of the reaction rate constant can be represented in a classical manner by the Arrhenius equation:

$$lnk_f(t) = lnk_0 - \frac{E_a}{RT} \quad (17)$$

where k_0 is the frequency factor and E_a is the activation energy, which is considered a potential energy barrier that has to be passed by the reactants. By fitting the above equation to experimental data, the activation energy E_a and the frequency factor k_0 can be obtained as a constant that is independent of temperature.

4.2.5 Selectivity

To compare the separation ability of each resin, selectivity (α) of two components, *i* and *j* can be defined as follows:

$$\alpha = \frac{t_{R,j} - t_0}{t_{R,i} - t_0} \quad (18)$$

The overall retention time of a retained component *i* and *j* are $t_{R,}$ and t_0 is the total dead time of the pulse injection system and column.

4.3 Inverse method

4.3.1. Inverse method for well-stirred batch reactor

In this study, the inverse method is used for estimating the model parameters. For well-stirred batch reactor experiments, the concentration data are fitted to reaction kinetic models. The least-square technique is used where we minimize the sum of the square of the difference between the concentrations predicted by the model and the experimental observations. The objective function is formulated as

$$S = \sum_{k=1}^{N} (C_{exp,k} - C_{model,k})^2 \quad (19)$$

where $C_{exp,k}$ is the experimentally observed concentration of each component at the k-th data point, and $C_{model,k}$ concentration estimated by the model, and N the total number of experimental data. The minimization was achieved by the MATLAB nonlinfit function.

4.3.2. Inverse method for chromatographic reactor

For single column experiments, the concentration profiles of the model for pulse-injection experiments are fitted to the experimental chromatograms to find the optimal values of model parameters. There are total of twelve model parameters to be calculated: total porosity, two reaction kinetic constants, four adsorption constants, dispersion coefficient, and four mass transfer coefficients. The same least-square technique is used where we minimize the sum of the square of the difference between the model and the experimental observations. The objective function, is formulated as

$$\min_{H_i,k_{m,i},D_{ax},k_1,K_{eq},e} \sum_{k=0}^{N_{exp}} \sum_{i=1}^{N_{comp}} \sum_{l=1}^{N_{t,i}^k} (C_{i,l}^{k,\mathrm{mod}} - C_{i,l}^{k,\mathrm{exp}})^2 + r \sum_{m=1}^{N_{reg}} \left(\frac{q_m^{\mathrm{mod}} - q_m^{init}}{q_m^{init}}\right)^2 \quad (20)$$

where the superscript k refers to the experiment index, *exp* refers to the experimental values, N_{exp} refers to the total number of experiments, and N_{comp} refers to the total number of

components. In the second term, N_{reg} refers to the total number of regularization parameters and Θ refers to the individual parameters. The superscripts *mod* and *init* refer to the values predicted from the model and the values obtained from the initial experiments and ρ is a Tikhonov regularization parameter which is a small positive value [37]. The Tikhonov regularization is necessary to penalize deviation of selected parameters from the initial experiment results [38]. In this study, initial values of some parameters are obtained from well-stirred batch reactor experiments and adsorption experiments. From these experiments, we obtain initial values of the equilibrium constant K_{eq} and adsorption constant of two products, mass transfer coefficients of two products in Θ^{mod}; i.e. $\Theta^{mod}{}_{reg} = [K_{eq}, H_{PMA}, H_{Byproduct}, k_{m,PMA}, k_{m,Byproduct}]^{T}$. The parameter ρ is found by carrying out several trial-and-error runs and identifying the best compromise between the model fitting and the deviation of Θ^{mod} from Θ^{init}

4.4 SMBR

Since the SMBR system consists of multiple chromatographic columns that are interconnected in a cyclic conformation, the mass balance equations at the connecting ports should be defined.

Mass balance between j^{th} and $(j + 1)^{th}$ column:

$$C_i^{j+1}(0,t)u^{j+1} = C_i^j(L,t)(u^j - u_{Ex}^j - u_R^j) + C_{i,F}u_F^{j+1} + C_{i,D}u_D^{j+1} + D_{ax}\left.\frac{\partial C_i^j(x,t)}{\partial x}\right|_{x=0} \quad (21)$$

where $u^j_{Ex,}$ $u^j_{R,}$ $u^j_{F,}$ and u^j_D are the velocities of extract, raffinate, feed and desorbent streams respectively.

Flow balance at the inlet and outlet ports :

$$u^{j+1} = u^j - (u_R^j + u_{Ex}^j) + (u_D^{j+1} + u_F^{j+1}) \qquad i = 1,\ldots N_{Comp}, \qquad j = 1,\ldots N_{Column} \quad (22)$$

where the symbol N_{Comp} refers to the total number of components and N_{Column} is the total number of columns.

In an SMBR, the counter-current movement of the solid phase is simulated by shifting of inlet and outlet ports. After repeating this operation for a number of times in the start-up period, the SMBR system arrives at a cyclic steady state (CSS). At the CSS, the snapshots of internal concentration profiles at the beginning and at the end of the step are identical, apart from a shift of exactly one column length [9]. In this formulation, the concentration profiles at the beginning of the step in the j^{th} column are identical to the concentration profiles at the end of the step in the $(j + 1)^{th}$ column[39-41]. The formulation is written as:

$$C_i^j(x,0) = C_i^{j+1}(x,t_{step}) \qquad i = 1,...N_{Comp},\ j = 1,...,N_{Column} - 1 \tag{23}$$

$$q_i^j(x,0) = q_i^{j+1}(x,t_{step}) \qquad i = 1,...N_{Comp},\ j = 1,...,N_{Column} - 1 \tag{24}$$

$$C_i^{N_{Comp}}(x,0) = C_i^1(x,t_{step}) \qquad i = 1,...N_{Comp} \tag{25}$$

$$q_i^{N_{Comp}}(x,0) = q_i^1(x,t_{step}) \qquad i = 1,...N_{Comp} \tag{26}$$

4.5 Optimization Strategy

4.5.1 Objective functions

The multi-objective optimization problem is formulated by i) maximizing the production rate of PMA in the raffinate outlet ii) maximizing the conversion of the reaction. In addition, constraints are set to minimize the amount of byproduct in the raffinate outlet to ensure the purity of the product, PMA. Similarly, it is also desired to maximize the PMA recovered in the raffinate outlet. To satisfy this requirement, the PMA recovery from the

raffinate outlet is enforced to be more than 90% as shown in equation 16. The degrees of freedom for this optimization problem are five: switching time (t_{step}), feed concentration (C_F), and four zone flow rates (u^j, j =1,2,3,4). It needs to be mentioned that the optimization of feed concentration (C_F) is critical to maximize the conversion as discussed previously in Agrawal et al.[9]

The overall optimization problem is as follows:

Maximizing PMA production rate (g/h):

$$\max Pr = \frac{A_{cs} MW_{PMA}}{t_{step}} \sum_{j=1}^{N_{Col}} \int_0^{t_{step}} C^j_{PMA,R}(L,t) u^j_R(t) dt \quad (27)$$

Maximizing conversion of limiting reactant:

$$\max X = 1 - \frac{\sum_{j=1}^{N_{Col}} \int_0^{t_{step}} C^j_{EtAc,R}(L,t) u^j_R(t) + C^j_{EtAc,Ex}(L,t) u^j_{Ex}(t) dt}{\sum_{j=1}^{N_{Col}} \int_0^{t_{step}} C^j_{EtAc,F} u^j_F(t) dt} \quad (28)$$

PMA recovery in the raffinate stream outlet:

$$Recov_{PMA} = \frac{\sum_{j=1}^{N_{Col}} \int_0^{t_{step}} u^j_R(t) C^j_{PMA,R}(L,t) dt}{\sum_{j=1}^{N_{Col}} \int_0^{t_{step}} u^j_R(t) C^j_{PMA,R}(L,t) + u^j_{Ex}(t) C^j_{PMA,Ex}(L,t) dt} \geq 90\% \quad (29)$$

Bounds on the zone flow rates:

$$u_L \leq u^j(t) \leq u_U \quad (30)$$

where *Pr*, *X* and *Recov* are the objective functions, A_{cs} is the area of cross-section of the column and MW_i is the molecular weight of i^{th} component and $C_{i,R}$ and $C_{i,Ex}$ are the concentrations of i^{th} component in the raffinate and extract outlet, respectively. We have upper bounds on the zone velocities so that the pump does not reach the maximum pressure drop in the SMBR system. The symbols u_L and u_U refers to the lower and upper bounds and their corresponding values in this study are 0 m/hr and 8 m/hr, respectively.

4.5.2 Solution strategy

The optimization of the two objectives is achieved by using an epsilon-constrained method [9]. In this approach, maximization of conversion *X* in Equation (28) is replaced by the following constraint:

$$X \geq \epsilon \quad (31)$$

By varying the value of ϵ and repeatedly solving the optimization problem, a solution set that maximizes PMA production against different conversions is obtained.

The optimization problem involves both special and time domains. In this study, we apply a full-discretization approach where special domain is discretized into 40 finite elements, and the temporal domain is discretized using Radau collocation on finite elements. Each step is discretized into five finite elements and three collocation points. The discretized equations are incorporated within a large scale nonlinear programming (NLP) problem, which is solved using an interior-point solver IPOPT [42] in AMPL (A Mathematical Programming Language) [43].

CHAPTER 5 ESTERIFICATION FOR THE PRODUCTION OF DOWANOL PMA

5.1 Motivation

This chapter provides a case study of applying a chromatographic reactor to an equilibrium-limited reaction for an important industrial application, and presents the potential to develop a SMBR system.

Among several applications of reactive chromatography, esterification of a carboxylic acid with an alcohol with the presence of an acid catalyst has been the subject of wide investigations by many researchers [11, 12]. This is because esters are of great significance in various industrial products including fragrances, flavors, and surface-active agents [44]. Many heterogeneous acid catalysts including cation exchange resins can be used as a packing material in a chromatography column that functions simultaneously as a catalyst and as an adsorbent. Heterogeneous catalysts avoid the drawbacks of homogeneous catalysts such as corrosion and catalyst recovery loss.

This chapter focuses on the production of propylene glycol methyl ether acetate (DOWANOL^{TM} PMA) through esterification of acetic acid with 1-methoxy-2-propanol (PM), or DOWANOL^{TM} PM. No previous study has evaluated the kinetics of esterification for PMA synthesis, and this is the first study to apply it to reactive chromatography. This type of esterification is very slow without the presence of a catalyst, but the reaction rate increases dramatically under an acidic condition. In addition, the reaction is limited by equilibrium, and therefore separation of products from the reaction sites increases the conversion. More traditional reactive separation methods, such as reactive distillation, could not be readily applied to this system due to the presence of azeotropes and the thermal

instability of the ion exchange resins.

We investigate a potential application of reactive chromatography for this reaction. As a heterogeneous catalyst, we use a cation exchange resin, AMBERLYST^{TM}15. This resin works as a catalytic adsorbent that separates the products from the reactants. In the proposed reactive chromatography process, PM is supplied as the mobile phase and also as the excess reactant to a packed column with AMBERLYST^{TM}15. The limiting reactant, acetic acid, is injected to the column as the feed. As acetic acid travels through the column, the reaction occurs, producing the two products, PMA and water. One of the products, water, is selectively adsorbed on the resin, thus driving the reaction forward. When the other product PMA reaches the outlet of the column, it can be collected at a high purity, which is followed by collection of water.

There are two different classes of adsorption based reaction mechanisms considered in previous studies: Eley–Rideal and Langmuir–Hinshelwood. Some studies are focused on determining the model that gives the best prediction [45-48]. For the esterification reactions, several papers have reported that Langmuir– Hinshelwood model successfully predicted the experimental data [12, 19, 29, 49, 50]. In this study, this model is used to for the reaction for the synthesis of PMA.

Despite the benefit of reactive chromatography for equilibrium-limited reactions, it is rarely used for an industrial application. Many literature studies on reactive chromatography are verified with reactions that are already understood well, where a careful study of reaction kinetics is not necessary. In this chapter, production of PMA is considered, where reaction kinetics studies are unavailable in literature. The potential application of reactive chromatography to PMA synthesis may have substantial economic

benefit for the industrial demand, which motivates us to eventually develop a simulated moving bed reactor (SMBR) system for large-scale production.

5.2. Materials and Methods

5.2.1. Materials

PM (1-methoxy-2-propanol, >99%) and PMA (propylene glycol methyl ether acetate,>99%) are purchased from Alfa Aesar, and acetic acid (99%) is purchased from BDH chemicals. All of chemicals are used without further purification. Sulfonated cation exchange resin, AMBERLYST^{TM}15 is supplied from The Dow Chemical Company in a wet condition. Before use, the resin is dried at 373.15 K for 12 h and sieved. The result of sieving and properties of AMBERLYST^{TM}15 are summarized in Table 1.

Table 1. Physical and chemical properties of cation exchange resin, AMBERLYST™15[51]

Matrix type	Styrene –DVB (Macroreticular)	
Operating pH	0-14	
Ionic form	H+	
Concentration of active sites	≥ 1.7eq/L	
Moisture (%)	52-57	
Max. Operating temperature (K)	393.15	
Surface area (m^2/g)	53	
Total pore volume (cm^3/g)	0.40	
Average pore diameter (Å)	300	
Bulk density (g/L)	770	
	Mass fraction	Size(μm)
Size distribution	0.001	< 300
	0.015	300-500
	0.093	500-600
	0.164	600-707
	0.351	707-850
	0.376	> 850

5.2.2 Methods

5.2.2.1. Experimental methods

Experimental methods that are described in Chapter 3 are followed. As shown in Table 2, the temperature of the reaction for batch experiment is varied from 50°C to 90°C and each experiment is conducted until the reaction reached the equilibrium.

Table 2 Batch experiment conditions

Run	Temperature (K)	Catalyst loading (g/ml of mixture)	Initial reactant molar ratio (acetic acid/PM)	Resin size	Stirring speed (rpm)
1	363.15	0.1	1.8	707-1000(µm)	270
2					400
3					300
4	343.15				
5	333.15				
6	323.15				
7	363.15	0.1	2.5		
8			1		
9			0.6		
10			0.3		
11		0.2	1.8		
12		0.05			
13		0.1	1.8	300-707(µm)	

5.2.2.2. Mathematical model

In addition to the models explained in Chapter 4, a simplified well-stirred batch reactor model is used in this chapter. Well-stirred batch experiments are performed in order to get the initial values of reaction rate constants (k_1, K_{eq}). Only for this experiment, the reaction rate model of batch reactor is simplified by assuming the equilibrium between the liquid and the solid phase:

$$q = q^{eq} \quad (32)$$

This assumption will be verified from the experimental validation in Section 5.3.1.1, where the change of catalyst size or stirring speed does not affect the reaction rate. From this observation, we assume mass transfer does not play a significant role on the overall reaction rate. The same assumption was made for several previous studies, where esterification was studied with the ion exchange resins and equilibrium between the solid and liquid phase was assumed [29, 52-54]. Based on the above statements, reaction rate model, Eq. (5), is rewritten with the equilibrium assumption (Eq. (32)) and linear adsorption isotherm (Eq. (1)) as follows:

$$r^{batch} = k_1 \left(H_{AA} C_{AA} H_{PM} C_{PM} - \frac{H_{PMA} C_{PMA} H_{water} C_{water}}{K_{eq}} \right) m_{cat} \quad (33)$$

While in the batch reactor, resins are fluidized and agitated and thus the equilibrium assumption given in Eq. 32 may hold, the same assumption would not be valid in reactive chromatography where the resin particles are packed in a column and mass transfer becomes more prominent. Therefore, in the reactive chromatography model, the equilibrium assumption given in Eq. 32 was dropped and the linear driving force model (Eq. (4)) was used. It is to be noted that the estimated parameters from the simplified model were used only as initial guesses for the fitting of reactive chromatography model. Final

parameters at the end of the chapter are obtained from the reactive chromatography models (Eqs. (3)–(5)).

5.3. Results and discussion

5.3.1 Well-stirred batch reactor experiment result

5.3.1.1 Significance of external and internal mass transfer resistance.

To obtain the reaction kinetic model, the effects of the intraparticle and extraparticle mass transfer resistances were investigated. Figure 9 shows the batch wise experimental kinetic data for the PMA reaction at stirring speeds of 270 rpm and 400 rpm. There was no difference between two plots, which indicates the extraparticle mass transfer resistance was assumed to be negligible in this range. Figure 10 shows the result of two experiments using different sizes of resin particles. Both plots matched each other well, indicating negligible effect of internal mass transfer resistance for the range of the resin size. Similar findings were reported in the literature for esterification with ion exchange resins [55-57]. Hence, all further batch experiments were conducted with the ion-exchange resin within the size range of 707–1000 μm and the stirring speed of 300 rpm.

5.3.1.2. Effect of catalyst loading

In order to see the effect of catalyst loading, the amount of catalyst was varied between 0.1 and 0.2 (g-dry-catalyst/ml mixture) at the temperature of 363.15 K, acid to alcohol feed molar ratio of 1.8:1 and stirring speed of 300 rpm. **Error! Reference source not found.** Figure 11 shows that with increasing catalyst concentration, the initial reaction rate increased and the equilibrium was reached faster, but the final conversion was not affected significantly. This result confirms our expectation that the catalysts only affect the reaction rate but not the equilibrium, which was reported also by others [58].

5.3.1.3. Effect of initial reactant molar ratio

The effect of the initial molar ratio of acetic acid to PM was changed from 0.6 to 1.8 and the results are compared in Figure 12. The catalyst loading was maintained at 0.1 g/ml and the temperature at 363.15 K. As can be seen from Figure 12, higher molar ratio of reactants resulted in higher PMA yields. Similar results are also reported by previous studies of esterification [56, 58].

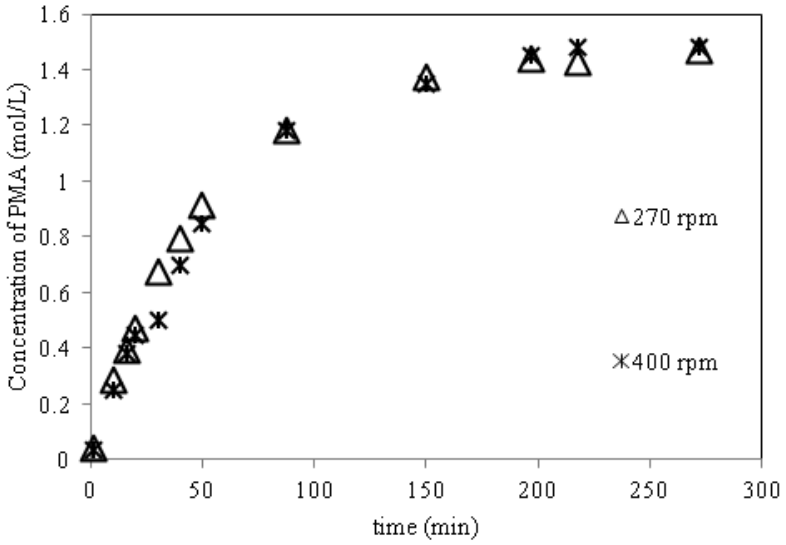

Figure 9 Well-stirred batch experiment at stirring speeds of 270rpm and 400rpm. Temperature 90°C, Initial reactant molar ratio 1.8:1, catalyst loading 0.1g/mL (Run #1 and 2 in Table 2)

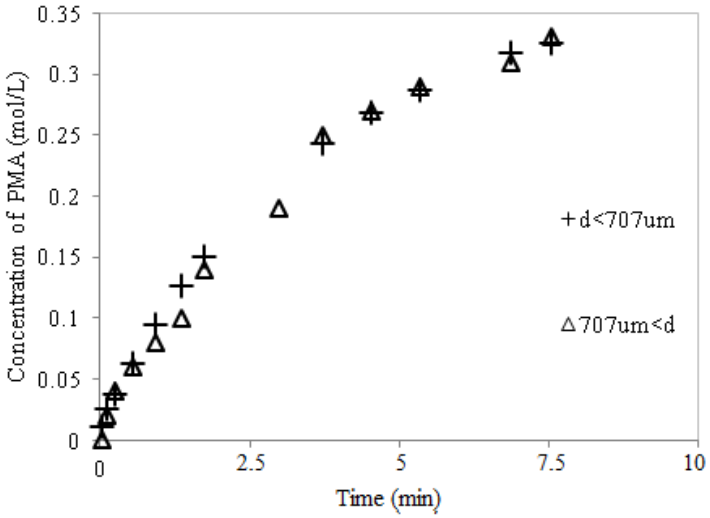

Figure 10 Well-stirred batch experiment with different size of catalyst particle. Temperature 90°C, Initial reactant molar ratio 1.8:1, Catalyst loading 0.1g/mL (Run #3 and 13 in Table 2)

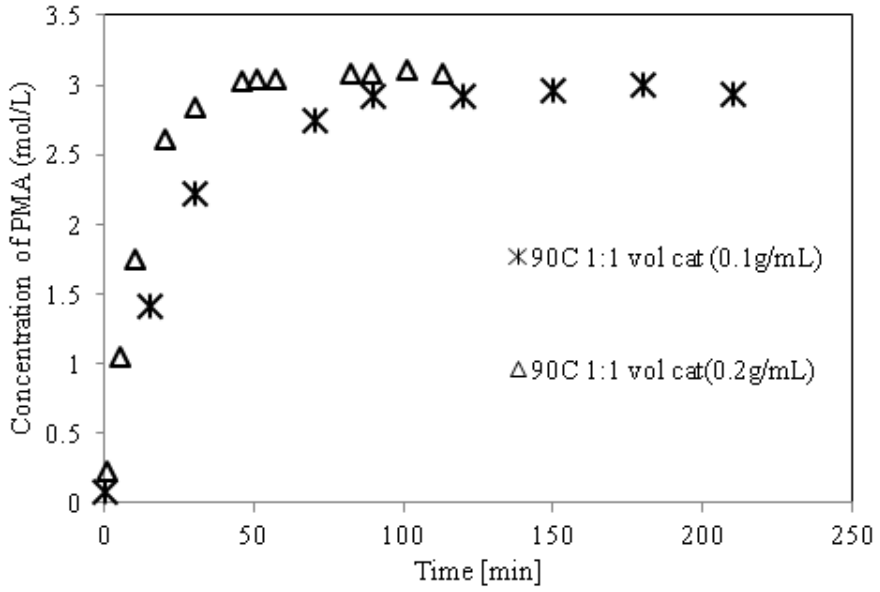

Figure 11 Well-stirred batch experiment with different catalyst loadings. Temperature 90°C, Initial reactant molar ratio 1.8:1 (Run #3 and 11 in Table 2)

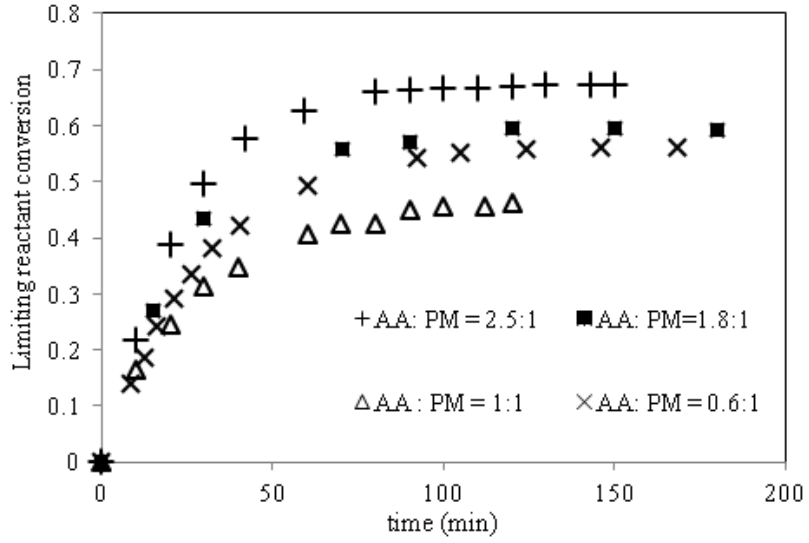

Figure 12 Well-stirred batch experiment with different initial reactant molar ratio. Temperature 90°C, Catalyst loading 0.1g/mL (Run #3,7,8, and 9 in Table 2)

5.3.1.4. Effect of the reaction temperature

In order to investigate the effect of temperature on the reaction rate, the temperature was varied between 323.15 K and 363.15 K with the catalyst loading of 0.1 g-dry-catalyst/ml-mixture, and initial reactant molar ratio of 1.8:1. As shown in Figure 13, the initial reaction rate increased with temperature, which has been observed in numerous reports [44, 45, 52]. Table 3 shows the values of K_{eq} obtained at final equilibrium states at each temperature. The final conversions at 60 °C, 70 °C and 90 °C did not differ greatly and the effect of temperature was more significant at the initial reaction rate than the final conversion.

The value of ΔH was found to be 4.642 kJ/mol from the Van't Hoff equation. The value of ΔH is small, as was found in some previous studies of esterification where equilibrium constants are not a strong function of temperature [45]. From these observations, the experiments were designed and analyzed under the assumption that the effect of temperature is more crucial on the initial reaction rate than on the final conversion.

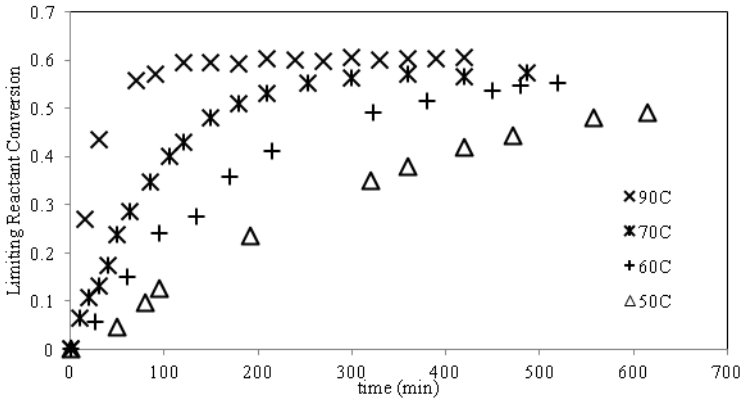

Figure 13 Well-stirred batch experiment at different temperatures. Initial reactant molar ratio is 1.8:1, Catalyst loading 0.1g/mL, (Run #3,4,5,6 in Table 2)

Table 3 Equilibrium constant at different temperature, and heat of reaction

Temperature (K)	K_{eq}	$ln\ (K_{eq})$	$\Delta H(kJ/mol)$
323.15	0.5286	-0.6375	4.642 ±0.24
333.15	0.6804	-0.3851	
343.15	0.7398	-0.3014	
363.15	0.7863	-0.2404	

5.3.1.5. Reaction rate model fitting and comparison

As mentioned above, with the assumption of adsorption equilibrium, the reaction rate model was simplified for the batch experiment as shown in Eq. 5.2. Conversion data at different temperatures in Figure 13 were fitted and forward reaction rate constants (k_1) were obtained as a function of temperature. Arrhenius equation was used to find k_0 and E_a values which were shown in Table 4. On the other hand, adsorption constants (H_i) were independent of temperature and concentration. As a result, only two sets of parameters were obtained regardless of temperature or concentration variance, which were the product of H_{AA} and H_{PM} and the product of H_{PMA} and H_{water}. The results are shown in Table 4. The relatively tight confidence intervals for these parameters may be due to linear approximation around the optimal solution [59]. Figure 14 shows the result of fitting, and the good agreement between experimental data and model is observed.

Reaction rate constants in Table 4 were used as initial guesses for the fitting of reactive chromatography in Section 5.3.2. This was because having reliable initial guess is crucial for the optimization problem when there are several parameters to be fitted. On the other hand, the products of adsorption constants in Table 4 ($H_{AA}H_{PM}$ and $H_{PMA}H_{water}$) which were obtained for the solvent composition specific to this experiment under the assumptions discussed above, were not used for the fitting of reactive chromatography. In

order to get more reliable adsorption constants, separate pulse injection experiments were performed.

Table 4 Reaction rate constants and adsorption constants and their 95% confidence intervals obtained by fitting Equation 13 to Figure 8

Parameter	Value
$\ln(k_0)$[L/(g-cat.mol.min)]	16.739 ±2.56
E_a/R [1/K]	7407.7 ±396.2
$H_{AA}H_{PM}$	0.0177±0.002
$H_{PMA}H_{water}$	0.0178±0.002

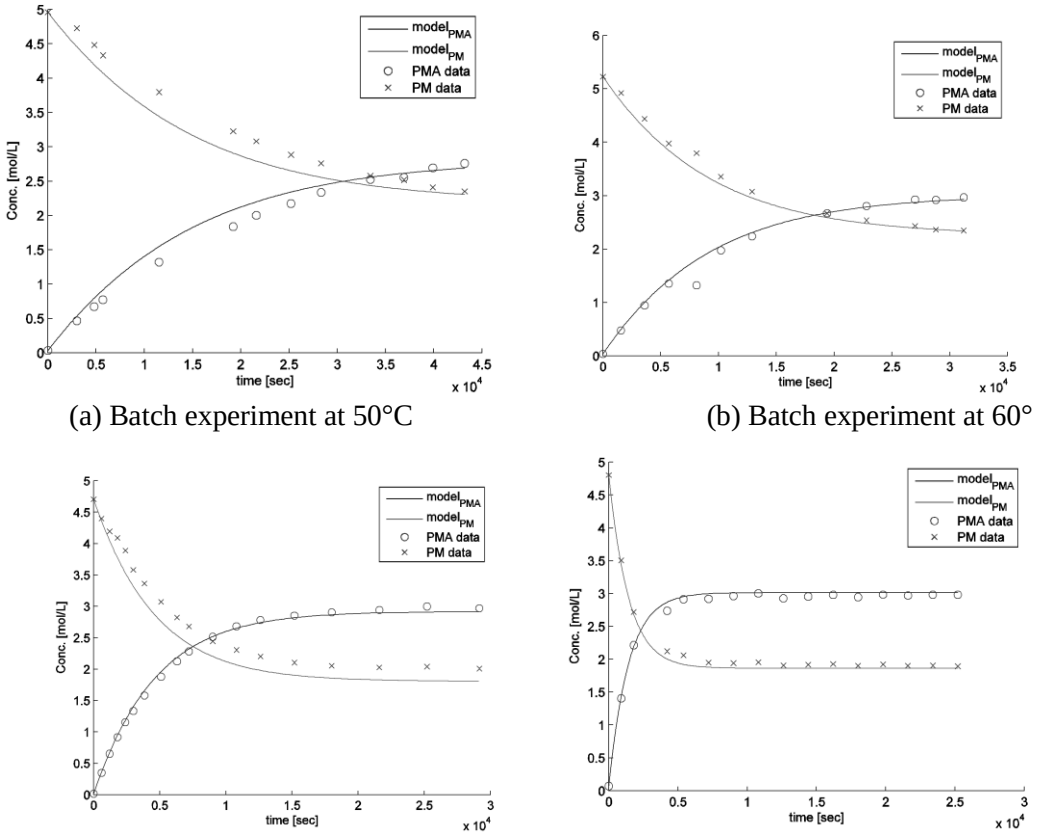

(a) Batch experiment at 50°C (b) Batch experiment at 60°

(c) Batch experiment at 70°C (d) Batch experiment at 90°C

Figure 14 Comparison of experimental data from Figure 8 to model fitting of equation 13 (a) 50°C (b) 60°C (c) 70°C (d) 90°C

5.3.2. Adsorption experiment (pulse injection)

In order to determine the adsorption constants of each component (PMA, acetic acid, water), a pulse of each chemical was injected into a preheated packed column while keeping the flow rate of the mobile phase (PM) constant. Figure 15 shows the result of pulse injection experiments.

As can be seen from Figure 15 (a), water showed a high retention time due to its strong affinity towards AMBERLYST^{TM}15. To elute out the water completely, approximately 4.8 bed-volumes of the mobile phase were necessary. In order to find the type of adsorption isotherm, models of both linear and non-linear isotherms, Eqs. (1) and

(2) were fitted to the data. As a result of fitting, the objective function values of two models were very close to each other. In addition, constant b_i of the nonlinear adsorption model was estimated to be nearly zero, which indicates that the constant b_i was unessential for the model and the linear isotherm was sufficient for the parameter estimation. Similar fitting results were observed for the PMA peak. In this chapter, the linear adsorption isotherm was used for the further modeling of the chromatography. Figure 15(a) shows only the linear model compared to the experimental data.

Figure 15(b) shows the fitting of the PMA chromatogram with the linear adsorption model. The peak shape of PMA pulse injection is nearly symmetric, which was another factor that supports the linearity of the adsorption isotherm [60]. The estimated parameters, adsorption equilibrium constants H_i and mass transfer coefficients $k_{m,i}$ of water and PMA, are shown in Table 5.

In order to obtain the adsorption parameter of the limiting reactant, acetic acid, the reaction must be suppressed. In our study, the temperature was kept low, 25 °C, and the flow rate was doubled to reduce the residence time to 6.28 min. Two experiments were performed by varying the injection volume, where we observed the peak shape was asymmetric. One may suspect that this peak asymmetry is due to nonlinearity of the isotherm. However, retention times of different injection volumes are nearly the same, as shown in Figure 15(c), which may weaken the possibility of isotherm nonlinearity.

The peak asymmetry of acetic acid may be explained by unsuppressed reaction. It was not possible to get a good fitting with the experimental data even when nonlinear (Langmuir) isotherm was assumed, while the reaction was ignored in the model. This may indicate that the reaction was not suppressed completely. GC analysis showed no trace of

PMA or water, but it was possible that the concentrations were lower than the minimum detection limit, considering the small volume of acetic acid injected. In this chapter, acetic acid adsorption parameter was not estimated from this experiment. Instead, they were obtained from a reactive chromatography experiment discussed later.

In this chapter, we consistently use the linear isotherm for all components. Nevertheless, we cannot exclude the possibility that the adsorption equilibria are nonlinear. To investigate this problem further, more extensive experiments such as breakthrough tests are necessary. It should also be noted that obtaining the adsorption equilibrium and mass transfer parameters of the mobile phase PM is necessary, but cannot be realized by a similar experiment. We must rely on model fitting of PM to experimental data in reactive chromatography experiments, as discussed in the next section.

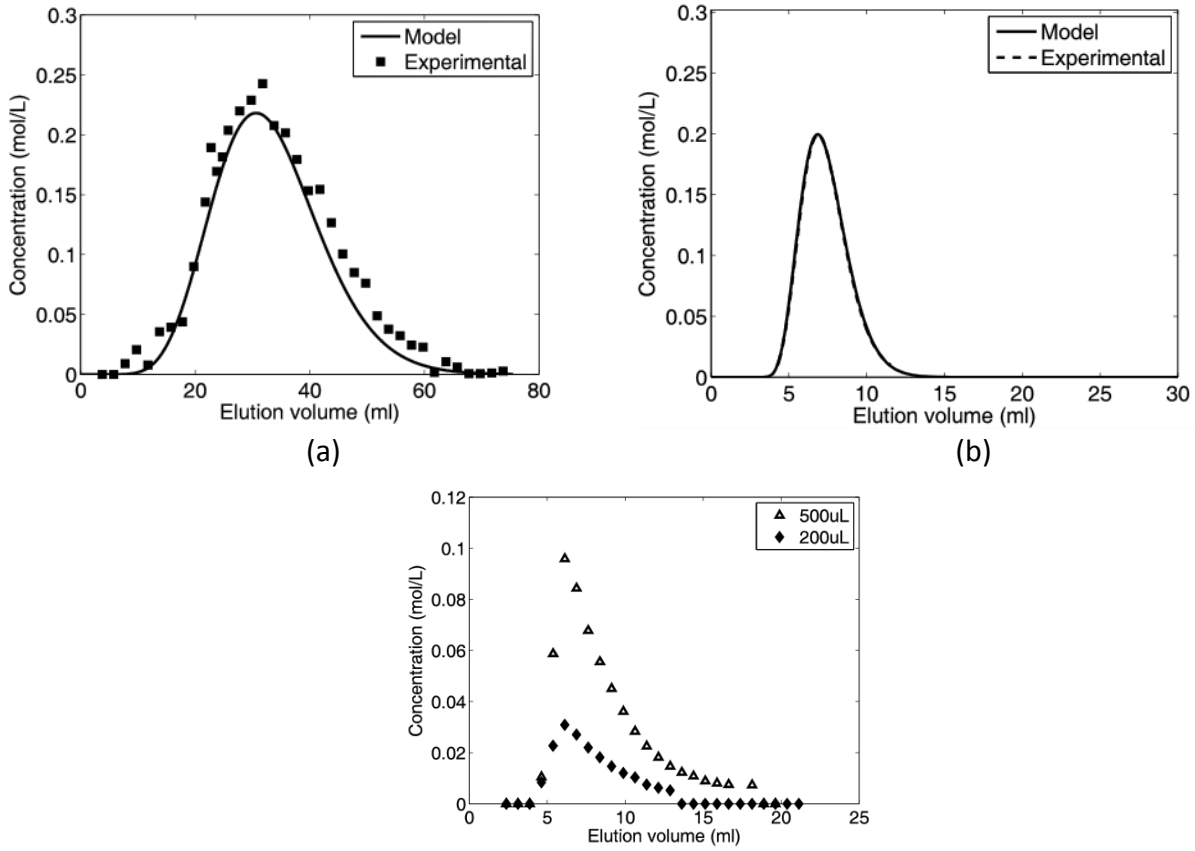

Figure 15 Injection of single component into chromatographic column (a) Injection of 1.0mL water at 85°C flow rate 1.0mL/min (b) Injection of 1.0mL PMA at 85°C flow rate 1.0ml/min, measured by RID (c) Injection of acetic acid at 25°C with two different volumes, 200µL, 500µL flow rate 2.0ml/min.

Table 5 Values of H_i *and*, k_m obtained from fitting adsorption data to linear isotherm model.

	PMA	Water
H_i	0.33	4.26
$k_m(\text{min}^{-1})$	2.98	0.69

5.3.3 Reactive chromatography experiment

5.3.3.1. Effect of feed concentration

The injection volume of acetic acid was varied to evaluate the effect on the reaction conversion and the separation performance. Figure 16(a) shows the injection of 5.0 ml of pure acetic acid into the column saturated by PM. The injection volume was approximately 40% of total volume of the column.

The resulting chromatogram of PMA in Figure 16(a) shows a peak with two local maximum concentrations. We assume this peak shape is a result of combination of two peaks of PMA from two reaction zones in which PMA was synthesized. A schematic diagram to explain this is shown in Figure 17. The formation of two PMA peaks could be explained due to the large amount of acetic acid injected and lack of sufficient mixing between the two reactants. When pure acetic acid was injected, two reactive fronts developed at the leading and trailing boundaries between PM and acetic acid. The acetic acid in the center of the pulse was not completely in contact with PM due to volumetric excess. As a result, two peaks of PMA were formed inside the column and thus the particular peak shape of PMA was observed.

In order to obtain one symmetric peak of PMA, the volume and the concentration of the injected acetic acid was diluted in PM to 50 vol%, and the injection volume was reduced to 1.0 ml, while the flow rate and temperature were kept constant. In this experiment, one sharper peak of PMA was formed and is compared in Figure 16(b). Such a strategy of diluting the feed has been done previously in the literature with different concentrations of injected feed in order to find the optimal concentration that gives the best separation performance [59, 61]. However, to the best of our knowledge, this is the first

study that observed a deformed peak of the product when a pure reactant was injected in a large volume due to the formation of two reaction sites.

Based on the chromatogram of each component, the orders of affinity towards the resin were determined as follows: water > PMA > acetic acid. This is because components with stronger affinity elutes out at a slower speed. The difference in the affinity between acetic acid and PMA is relatively small. As a result, the separation of PMA and acetic acid is relatively poor, and thus a high conversion must be achieved to drive the reaction to extinction of acetic acid. On the other hand, there exists significant difference in affinity between PMA and water, and water is retained inside the column strongly. As a result, water is separated from the reaction site. This separation of product from the reaction locus results in the esterification to proceed towards the complete conversion of the acetic acid, overcoming the thermodynamic equilibrium.

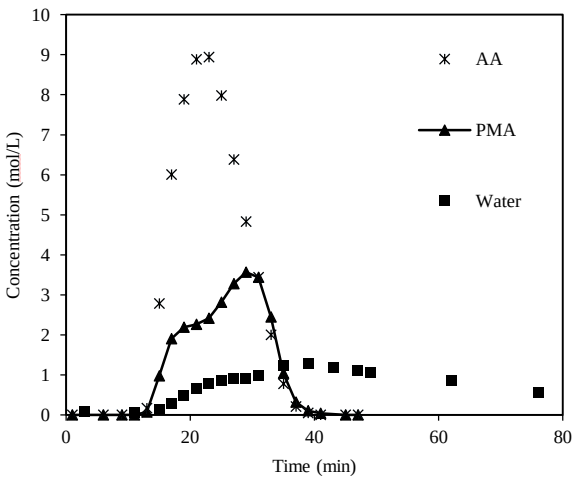

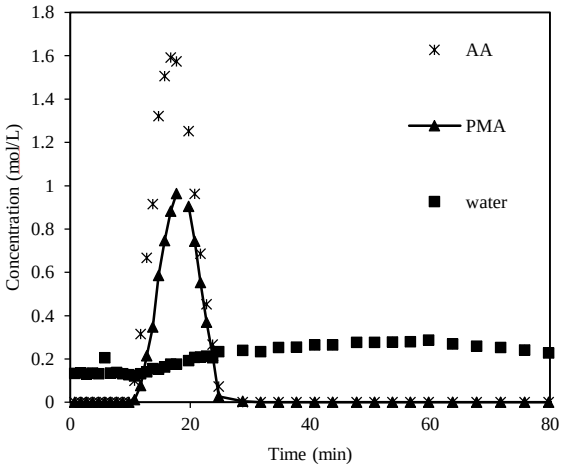

(a) 100% acetic acid, injection volume 5.0mL **(b) 50% acetic acid, injection volume 1.0mL**

Figure 16 Injection of 100% acetic acid and 50% acetic acid into chromatographic reactor. Temperature 85°C, flow rate 0.5ml/min.

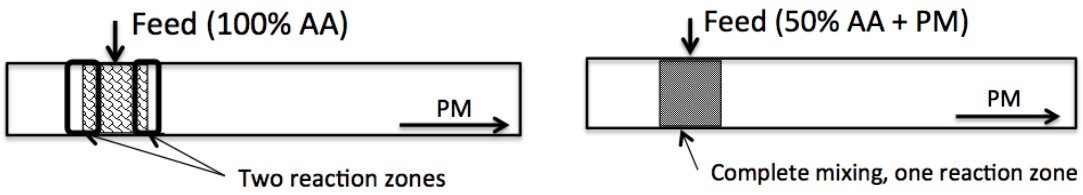

(a) (b)

Figure 17 Schematic diagram of acetic acid injection at different concentration (a) Injection of 100% acetic acid, forming two reaction zones (b) 50%

5.3.3.2. Effect of flow rate and injection volume

The flow rate primarily influences the residence time and dispersion. Therefore, the feed flow rate of the reactants plays an important role in the optimization of PMA synthesis in reactive chromatography. Experiments were carried out to quantify the influence of the flow rate on the conversion.

Table 6 shows the conversion at different feed flow rates and injection volumes, while keeping the temperature at 110 °C and concentration of the acetic acid at 50 vol%. As can be seen in Table 6, the conversion of acetic acid depends strongly on the residence time. When the flow rate is decreased from 1.0 ml/min to 0.5 ml/min, the conversion increased from 34.4% to 83.6%. This is because the contact time of reactants with the catalyst was increased. Furthermore, when the flow rate is decreased further to 0.2 ml/min and the injection volume was decreased to 0.05 ml, the conversion was nearly 100%, which was infeasible in the batch reactor. This result demonstrates that reactive chromatography achieves such a high conversion by separating the products from the reactants, which leads to a conversion that exceeds the equilibrium limit. However, since the retention time increased, it takes a longer time to wash out the water from the resin and complete one batch run. Thus the trade-off between a shorter batch time (higher throughput) and a higher conversion must be considered in process development.

It should be pointed out that removal of water, which has the strongest affinity to the resin, can be the bottleneck in the process economics. To flush out the water, a large amount of the mobile phase must be consumed. Furthermore, the batch time—the time interval between feed injections—is determined by the time to flush out water.

Table 6 Influence of flow rate and injection volume on conversion at 110 °C

Flow rate [ml/min]	Injected acetic acid [ml]	Conversion [%]
1	0.5	34.4 (±3.1%)
0.5	0.5	83.6 (±2.3%)
0.2	0.05	>99.9

5.3.3.3. Effect of temperature

The influence of temperature was investigated, which may affect adsorption, reaction equilibrium, reaction kinetics, and mass transfer. Among these factors, effects on the adsorption were previously studied with PMA and water by injecting each component through column at different temperatures from 60 °C to 85 °C. The outlet profiles were identical regardless of temperature. Based on these preliminary results, adsorption of PM and acetic acid were also assumed to be independent of temperatures. Furthermore, the reaction equilibrium is also insensitive to temperature change, as discussed in Section 5.3.1.4. Thus we focus our analysis on the influence on reaction kinetics in reactive chromatography.

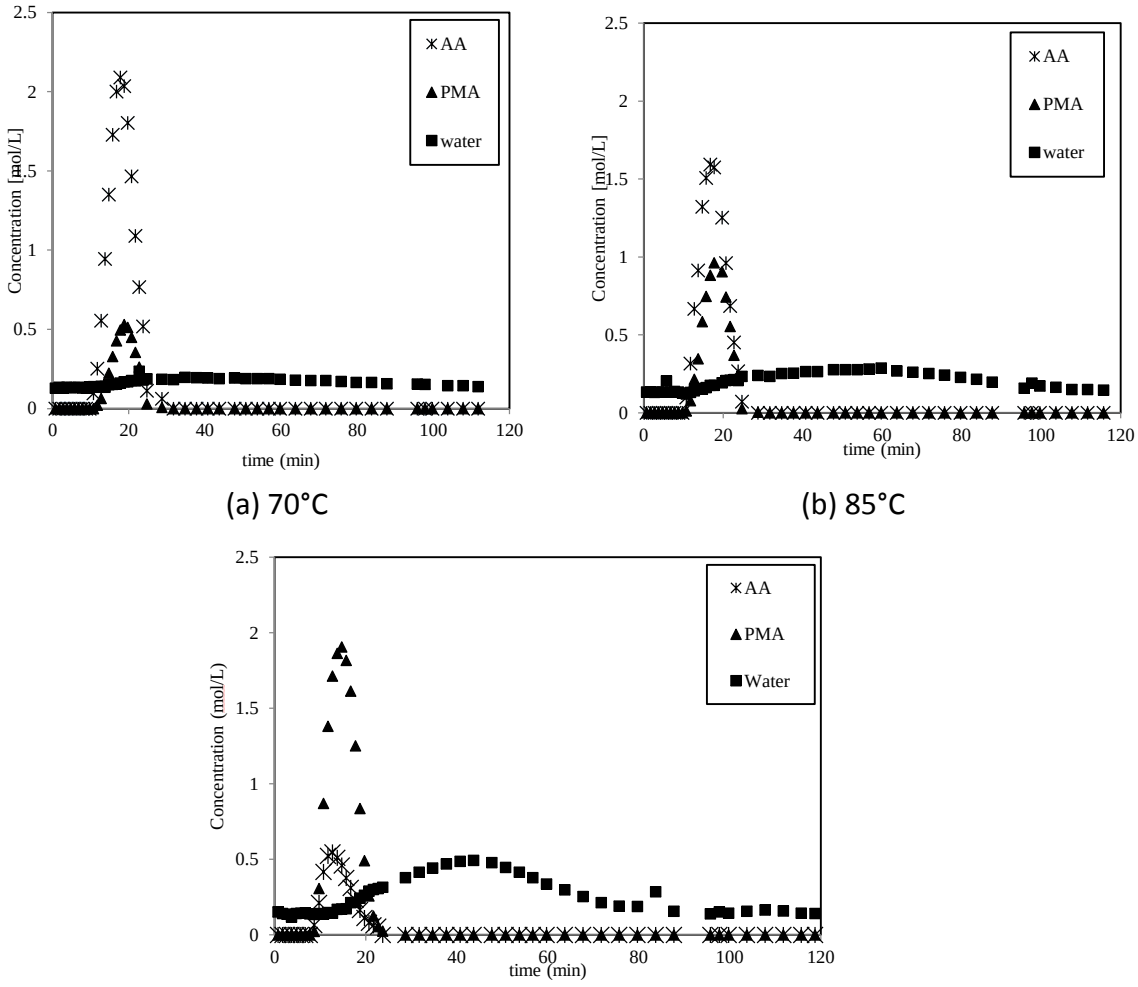

Figure 18 Injection of 50 vol% acetic acid into chromatographic reactor at different temperatures. (a) 70 °C, (b) 85 °C, and (c) 110 °C. Flow rate is 0.5ml/min.

In order to see the effect of temperature on the reaction kinetics inside the chromatographic reactor, temperature was varied from 70°C to 110°C while the flow rate was kept at 0.5ml/min and feed concentration at 50 vol%. We did not carry out an experiment at a temperature exceeding 110°C, since we observe significant amounts of byproducts in GC chromatography analysis, which affected the conversion. Furthermore, the maximum operating temperature of the resin was 120°C. Due to these restrictions, only the data under 110°C are discussed. The reaction proceeded with an excess amount of PM since it was used as a mobile phase.

As can be seen from Figure 18, the peak area of PMA increased as the operating temperature increased. The conversion of the limiting reactant, acetic acid, was calculated based on the peak area of remaining acetic acid and the initially injected amount of acetic acid. As can be seen from Table 7, the conversion increased from 22% to 83% depending on temperature.

The effect of temperature on the conversion increase is more significant in chromatographic reactor compared to the well-stirred batch reactor. The conversion inside the batch reactor increased only slightly from 59% to 60% by increasing the temperature from 70°C to 90°C. On the other hand, conversion inside the reactive chromatography increased significantly from 22% to 43% at 70°C and 85°C. This is because in the stirred batch reactor, the reaction reaches the equilibrium eventually, where the effect of temperature is not significant. On the other hand, inside the chromatographic reactor, the products are continuously separated from the reaction site, which drives the reaction to exceed the equilibrium limit. As a result, the reactants continue to react, where the temperature plays a significant role, resulting in a higher increase of conversion.

Table 7 Conversion of acetic acid calculated based on chromatogram from Figure 18. Compared batch conversions are the result from Figure 14. Values are the average of two replicated experiments.

Reactive chromatography		Well-stirred batch reactor	
Temperature (°C)	Conversion	Temperature(°C)	Conversion
70	0.22 ±0.02	70	0.59±0.02
85	0.43 ±0.02	90	0.60±0.02
110	0.83 ±0.02	110*	0.62

*Calculated from Van't Hoff equation

It is worth mentioning that we consistently observe a positive baseline of water of approximately 0.1 mol/L. It could not be removed even if the mobile phase PM was dehydrated with a molecular sieve. One of the causes was the absorption of moisture by

PM, which was confirmed by the GC analysis of water content in PM. Another possibility is that the mobile phase, PM, went through side reactions with the catalyst and formed a small amount of water as a byproduct. We observed that flowing only the mobile phase through the packed column showed a constant amount of water collected at the outlet even without injection of the acetic acid.

5.3.4 Parameter estimation for reactive chromatography

In order to obtain the full set of model parameters, the two pulse injection experiments of 50vol% and 75 vol% acetic acid concentrations in PM at 110°C with 5ml injection loop were fitted to the model. Including two experimental chromatograms in model was expected to increase the reliability of the estimated parameter set. By carrying out this fitting, the adsorption equilibrium constants of acetic acid and PM can be obtained, which were very difficult to obtain only from the adsorption experiments. All other model parameters which have been already obtained in this chapter—adsorption equilibrium constants H_{PMA} and H_{water}, porosity ϵ, mass transfer coefficients $k_{m,i}$, reaction rate constant k_1, and equilibrium constant K_{eq}—were not fixed in the reactive chromatography model, but re-estimated from the reactive chromatograms to check the consistency.

In our parameter estimation analysis, it was found that the equilibrium constant K_{eq} is very insensitive to the fitting, and this parameter cannot be estimated from the reactive chromatography experiment. Thus the parameter value from the batch reaction experiment must be utilized. In this study, we modify the objective function of least square minimization form Chapter 4 as follows:

$$\min \sum_{k=1}^{N} \left(C_{\exp,k} - C_{\mathrm{cal},k} \right)^2 - \rho \left(K_{eq}^{\mathrm{model}} - K_{eq}^{\mathrm{batch}} \right)^2 \quad (34)$$

where ρ is a Tikhonov regularization parameter [62] which is a small positive value, and K_{eq}^{batch} is the value of the equilibrium constant obtained from batch reaction experiment. The equilibrium constant K_{eq} at 110°C was calculated to be 0.860 by extrapolating the Van't Hoff plot. The regularization for K_{eq}^{model} was necessary to penalize deviation from the batch experiment result, since this parameter was found to be very insensitive to the fitting of the model to the reactive chromatography data. The initial guess for the reaction rate constant k_1 was taken from batch experiment result and those of the adsorption parameters (H_i and k_m) were taken from the pulse injection experiment in Table 5.

Table 8 (a) and (b) show the optimal model parameters as a result of parameter estimation analysis. It can be seen that some of the adsorption equilibrium constants deviate slightly from the values obtained from the pulse experiments shown in Table 5. In addition, there was a minor deviation in the estimated porosity from the experimentally measured value in water using dextran (0.310), which was probably caused by the minor swelling ratio difference of the resin in water versus in PM. Unless these parameter deviations were not allowed, the model did not fit well with the experimental data. It is to be noted that some parameters are correlated and reliability of the parameter values should be investigated further. Addition of experimental data and further modifications of the models may be necessary to understand and resolve these minor inconsistencies of model parameter values.

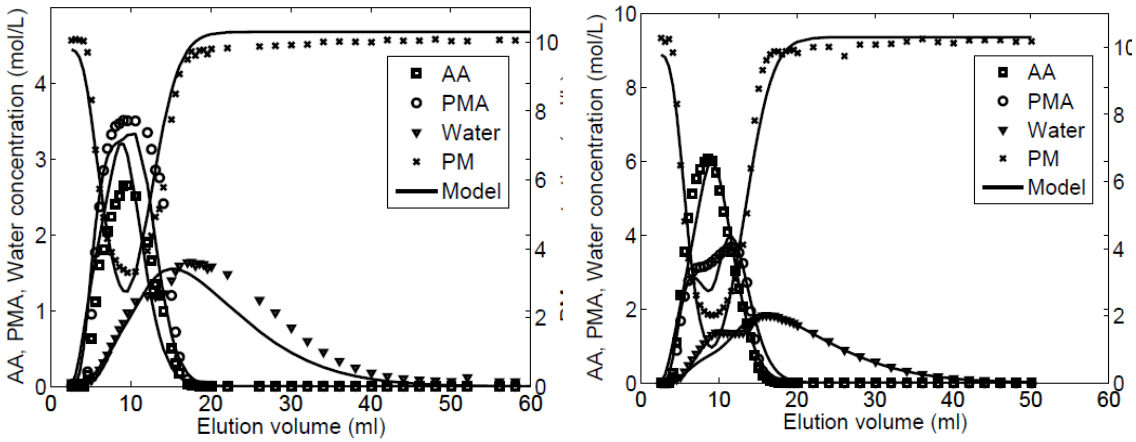

(a) Feed composition: 50-50vol% AA and PM

(b) Feed composition: 75-25vol% AA and PM

Figure 19 Model fitting results: comparison of the elution profiles predicted by the model and the experimental chromatograms obtained by injecting a pulse of acetic acid and PM at 110°C, 5ml injection and at 0.5ml/min flow rate.[9]

Figure 19 shows the fitting of the models with the experimental chromatograms. The concentration profiles of acetic acid, PMA and water are plotted on the left y-axis while PM concentration is shown on the right y-axis. The solid lines represent the experimental data. The water concentration has been modified by subtracting the initial water content that was present throughout the data. As can be seen from the figure, the model fits the concentration profile reasonably well. It should be noted that the concentration of PM, which is both a mobile phase and excess reactant, is also fitted well.

Table 8 Parameters estimated from reactive chromatography experiment at 110°C

(a) Component specific parameters

	H_i	$k_{m,i}$ [min^{-1}]
PM	0.226	1.772
Acetic acid	0.474	0.350
PMA	0.001	1.505
Water	1.648	0.286

(b) Other parameters

$k_1 m_{cat}$ [L/(mol·min)]	K_{eq} (regularized in objective function)	ϵ
0.195	0.862	0.334

This study demonstrates that the use of reactive chromatography for PMA synthesis would enhance the overall process performance compared to conventional batch systems in terms of increasing the reaction conversion. The improvement is realized by the separation of the species involved thereby reducing the capital and energy cost of additional separation. The next goal of this study is to extend the single-column reactive chromatography to a multi-column process of the simulated moving bed reactor system, where even higher degrees of conversion and separation of components can be targeted.

5.3.5 SMBR Optimization [9]

The result of SMBR optimization using the parameters from Table 8 are presented in this section. The specification of the SMBR columns is given in Table 9. The multi-objective optimization problem of the SMBR that has been discussed in chapter 4 is implemented in the AMPL modeling environment and solved using the IPOPT solver. The multiple objectives are: i) maximize the production rate of PMA in the raffinate outlet and

ii) maximize the conversion of acetic acid. In this study, two-dimensional projections of this Pareto plot is presented. The projection investigates the trade-off between the maximum production rate of PMA against the conversion of acetic acid.

Figure 20 shows the trade-off between the PMA production rate against the conversion of acetic acid. As can be seen from this figure, the conversion was increased up to 95% of acetic acid, which is a significant improvement compared to single column experiments. The figure also shows the decrease of the production rate of PMA through the raffinate outlet with increase in the conversion of acetic acid. Thus the higher conversion of acetic acid is not favorable to high production rates of PMA. This also can be explained from the optimal operating conditions listed in Table 10. In order to achieve higher conversion, the residence time must increase inside the SMBR. This lead to a slower flow rate and longer switch time [63]. Specifically, the desorbent flow rate decreases from 6.00ml/min to 3.20ml/min as conversion increases from 70% to 85%. A similar trend can be observed for the extract, feed and recycle flow rate.

Table 9 SMBR system details

Parameter	Value
N_{comp}	4
N_{column}	4
Configuration	1-1-1-1
Column length (L)	0.5m
Internal diameter (D)	0.015m
u_L	0m/h
u_U	10m/h

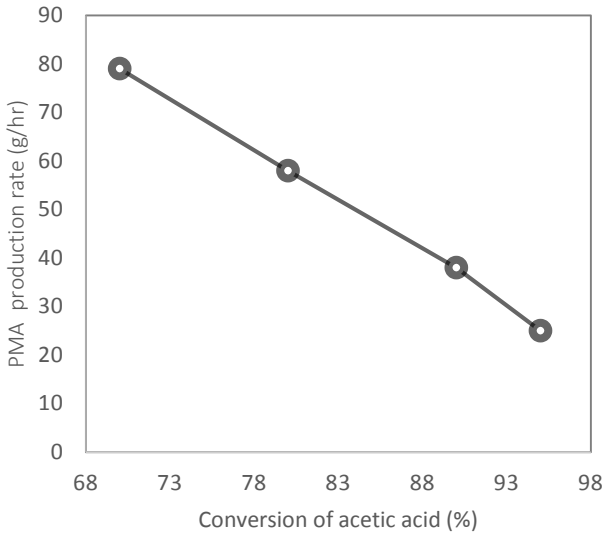

Figure 20 Pareto plot of the multi-objective SMBR optimization problem: PMA produced through the raffinate outlet in g/hr against the percentage conversion of acetic acid [9].

Table 10 Optimal operating conditions of SMBR from the multi-objective optimization analysis for maximizing PMA production rate and acetic acid conversion [60].

Conversion	70%	85%	95%
Desorbent flow rate [ml/min]	6.00	3.20	1.60
Extract flow rate [ml/min]	5.80	3.10	1.60
Feed flow rate [ml/min]	1.27	0.72	0.38
Recycle flow rate [ml/min]	0.70	0.40	0.20
Switch time [min]	18.6	29.3	51.3

5.4 Conclusions

The goal of this chapter was to apply the esterification of acetic acid with PM to reactive chromatography, and further show the improvement through simulating the result from SMBR system. In order to obtain parameters, the kinetics of esterification was studied under well-stirred batch reactor and chromatographic reactor. Batch reactor experiments were performed at different temperatures, initial reactant ratios, catalyst particle size, and agitation rate. It was found that the reaction conversion was limited by the equilibrium, and

the final conversion in a batch reactor could not be improved significantly by increasing the temperature. Simplified reaction rate model was fitted to the batch experimental data and reaction rate constants were obtained. Adsorption constants were obtained by performing a pulse injection experiment in a packed column. Reactive experiments were performed using a chromatographic reactor by injecting different concentrations of acetic acid with varying temperature and flow rate. It was found that when a large volume of pure reactant was injected into the column, two reaction zones could be formed, which could be observed as a deformed peak.

The parameters obtained from single column experiments are used to carry out model-based optimization of SMBR. In some optimal operating conditions, the conversion from SMBR reached 95% which was infeasible from the batch reactor. This optimization demonstrated that SMBR can be applied to the synthesis of PMA for the increase of conversion by exceeding the thermodynamic equilibrium. However, the productivity was sacrificed with a low flow rate and productivity.

There are several questions which must be addressed before scaling up this reactive chromatography process. The mathematical model of reactive chromatography must be validated carefully with more experimental data. In particular, we consistently assumed that the isotherms of all components were linear, which must be verified at higher concentrations. Furthermore, we found that flushing out water from the column can be the bottleneck for process economics.

CHAPTER 6 HETEROGENEOUS TRANSESTERIFICATION WITH TYPE I RESIN FOR THE PRODUCTION OF PMA

6.1. Motivation

In this chapter, transesterification reaction is studied for the production of PMA through chromatographic reactor. Transesterification is an alternative reaction to esterification that produces PMA and a by-product ethanol (EtOH) through the reaction between PM and ethyl acetate (EtAc). An advantage of transesterification over esterification is the ease of by-product removal; the by-product in transesterification, EtOH, has reduced affinity for the adsorbent and elutes from the column faster than water in esterification. Since water has a strong affinity towards cation exchange resins, the retention time is very long and the resulting concentration profile is very broad as can be seen from Chapter 5. Thus, a large volume of desorbent is required to push water out of the system [14]. Work described in Chapter 5 found that the productivity of the esterification process was severely limited by the amount of time required to remove water retained inside the column. On the other hand, the by-product of transesterification (EtOH) elutes faster than water, while still enabling sufficient separation of the products, leading to increased productivity. This way, the length of the column can be shortened and the amount of desorbent to remove the by-product can be minimized.

Transesterification has many applications, especially in biodiesel production, and a number of studies have been conducted previously on heterogeneously catalyzed reaction for biodiesel production [64]. Those studies include transesterification between palm oil and methanol catalyzed by KF/Ca-Mg-Al [65], production of ethyl oleate with ion

exchange resins [66], transesterification of triolein [67], methyl acetate- butanol [68, 69] and methyl acetate – hexanol [70] using ion exchange resins.

In addition to the study of transesterification reaction, various types of process development have been performed for transesterification. Some of the examples includes reactive distillation columns [71-75] and bubble columns [76, 77]; both configurations benefit from combining the reaction and separation into a single unit.

However, to the best of our knowledge, no previous research have employed an anion exchange resin in reactive chromatography, although it is discussed in a patent publication by Geier [31]. Anion exchange resins, which act as base catalysts, are effective for transesterification. This chapter is important for applying reactive chromatography to transesterification other than biodiesel for the first time, and it also provides a detailed case study for designing a reactive chromatography process for a reaction where the reaction equilibrium or kinetics are unknown.

In this chapter, we demonstrate the applicability of transesterification to reactive chromatography for the PMA production. To analyze the reaction equilibrium and kinetics, batch reaction experiments were performed in a well-stirred batch reactor with different catalysts. Various types of heterogeneous and homogeneous catalysts were employed. In addition, the effect of water concentration on the final conversion was tested by performing a well-stirred batch reactor experiment with a homogeneous catalyst, sodium hydroxide. Since existing information available for transesterification in reactive chromatography is very limited, several anion exchange resins are tested for swelling ratio and catalytic activity to find the best heterogeneous catalyst.

This chapter also discusses the advantage of transesterification over esterification from the previous chapter. The transesterification has the advantage of higher conversion at a lower temperature, which results in higher productivity. Furthermore, the faster retention time of by-product, EtOH, also contributes to high productivity of the process due to the shortened batch time. However, we have observed deactivation of anion exchange resin after few runs of experiments.

6.2. Materials and Methods

6.2.1 Materials

PM (1-methoxy-2-propanol, >99%), PMA (propylene glycol methyl ether acetate, >99%) and ethyl acetate (HPLC grade, 99.5+%) were purchased from Alfa Aesar, and ethanol (anhydrous, 99.5+%) was purchased from Acros Organics. All of chemicals were used without further purification. Sodium hydroxide (NaOH, 99.99%) in ultra-dry state and powder form was purchased from Sigma Aldrich. Molecular sieve 3Å was purchased from Alfa Aesar, in beads form with the size distribution of 1-2mm.

Sodium alkoxide was one of the homogeneous catalysts that was used for the comparison of different catalysts. It was produced in the lab based on the reaction shown in Figure 21. The reaction was performed as follows: PM was stirred with solid NaOH, and then molecular sieve 3Å was added afterwards. This enabled a conversion of sodium hydroxide by removing water from the solution. The solution was left overnight before use in experiments to ensure water removal. Each solution was analyzed by gas chromatography to confirm the water concentration is below 0.005vol%.

Properties of anion exchange resins considered in this chapter are summarized in Table 11. Anion exchange resin, AMBERLITE^{TM} IRA900 in chloride form, and DOWEX

MARATHON™ A in hydroxide form were purchased from Sigma Aldrich and AMBERLITE™ IRA904 in chloride form was provided from the Dow Chemical Company in a wet condition. For a comparison with anion exchange resin, a cation exchange resin, AMBERLYST™ 15 with particle size of 707-850 μm, was used for the experiment. DIAION PA316 was purchased from Mitsubishi Chemical. Resins in chloride forms (AMBERLITE™ IRA904 and AMBERLITE™ IRA900) were converted to hydroxide form by flushing the resin with 12 BV of 5wt% NaOH solution at 0.1 BV/min and 18 BV of DI water at 0.1 BV/min.

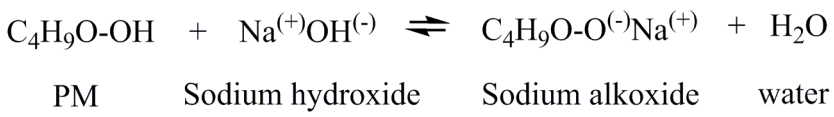

Figure 21 Reaction equation for the formation of sodium alkoxide

Table 11 Properties of ion-exchange resins that are used in experiments

	Resin type	Base polymer and structure	Functional group	Particle size(μm)	Max operating temp (°C)	Total exchange capacity (meq/ml) in OH^- form
AMBERLYST™ 15	Cation exchange	Styrene-DVB Macroreticular	sulfonic acid (strongly acidic)	707-850	120	1.8 (H^+) form
DOWEX MARATHON™ A	Anion exchange	Styrene-DVB Gel	quaternary ammonium (strongly basic)	525-625	60(OH^-) 100(Cl^-)	1.0
AMBERLITE™ IRA904	Anion exchange	Styrene-DVB Macroreticular	quaternary ammonium (strongly basic)	368-850	60 (OH^-) 75(Cl^-)	0.7
AMBERLITE™ IRA900	Anion exchange	Styrene-DVB Macroreticular	quaternary ammonium (strongly basic)	650-820	60 (OH^-) 75(Cl^-)	1.0
DIAION® PA316	Anion exchange	Styrene-DVB Macroreticular	quaternary ammonium (strongly basic)	300-1180	60(OH^-) 80(Cl^-)	1.3

6.2.2 Experimental methods

The experimental procedures explained in chapter 3 are followed for well-stirred batch reactor experiments, single chromatographic reactor experiments, porosity measurements and analysis. In this chapter, additional experiment of swelling ratio test was performed to measure the volume of resin beds at different solvents. To measure the swelling ratio, a graduated empty glass column of internal diameter of 1.5 cm and height of 23 cm (Omnifit Benchmark columns, Diba industries) was filled with dry resin to about 50% of the column height. Each resin was dried at resin's maximum temperature inside a vacuum oven for overnight before experiment. After the initial height of dry resin bed was measured, solvent was pumped from the bottom of the column so that the resin bed could be fluidized with at least 5 column volumes of the solvent. The fluidized resin was then left to settle by gravity. The height of the settled resin in the solvent was measured. Each experiment was performed in duplicate. The same procedure was repeated for different solvents.

6.2.3. Modeling method

The mathematical models explained in chapter 4 are used for modeling. Linear adsorption isotherm is used with single column model for heterogeneously catalyzed system.

6.3 Results and discussions

6.3.1. Well-stirred batch reactor experiment

6.3.1.1 Effect of catalyst

Four different catalysts were employed for the well-stirred batch reactor experiment at identical conditions to observe the effect of the catalyst on the reaction. Two heterogeneous catalysts were selected, one that has a gel structure (DOWEX

MARATHON™ A) and another that has a macroreticular structure with the minimum swelling ratio which will be discussed in section 6.3.2.1 (AMBERLITE™ IRA904 OH^-). In addition to heterogeneous catalysts, homogeneous catalysts (sodium alkoxide and NaOH) were also tested to see the effect of different types of catalyst. It should be noted that while NaOH in PM forms a mixture of small amount of sodium alkoxide, the majority remains as NaOH. All of the batch experiments were performed at 40°C and initial reactant volumes were 100 ml of EtAc and 100 ml of PM, where the composition is very close to the equimolar ratio. The water concentration of each sample was measured at each time point and averaged over the duration of the experiment to see how it influences the final conversion.

As can be seen from Figure 22, the reaction equilibrium was reached after approximately 150 minutes for all catalysts. It can be seen that DOWEX MARATHON™ A, sodium alkoxide and AMBERLITE IRA904 OH^- achieved the final conversion of approximately 27%. On the other hand, the conversion of NaOH was lower than those of the other catalysts. This can be attributed to the neutralization of catalysts with the presence of water in the mixture which will be discussed in detail in Section 6.3.7. NaOH and PM are very hygroscopic, which can also be interpreted from the high water concentration of samples shown in Table 12. Since batch experiments are performed while exposed to atmosphere, it is hard to control the water concentration of reaction mixture when catalysts are hygroscopic. As a result, NaOH deactivates through neutralization before the reaction reaches the final equilibrium.

On the other hand, the conversions for DOWEX MARATHON™ A and sodium alkoxide were relatively high even at low catalyst concentrations. This is because DOWEX

MARATHON^{TM} A, which is a gel-type resin and has higher capacity (Table 1), was not completely neutralized. In the experiment of sodium alkoxide, water in the solution was nearly completely removed by adding molecular sieve 3Å and thus neutralization was minimized. This hypothesis is further analyzed in Section 6.3.7. Based on this experiment, sodium alkoxide showed the highest initial reaction rate. However, a homogeneous catalyst requires additional separation unit at the outlet of reactor. Further investigations must be performed to quantify the advantages and disadvantages of homogeneous catalysis for transesterification in reactive chromatography and will be discussed in the following chapter.

From these well-stirred batch reactor experiments, it has been noted that a careful handling of water concentration is required when hygroscopic catalysts such as NaOH is used. This will be discussed again in section 6.3.4, the water concentration at the outlet of the column was kept below 0.005 vol% throughout the reactive chromatography experiments.

In this chapter, the value of K_{eq} was calculated only from experiments performed with AMBERLITE^{TM} IRA904 OH^-, Marathon A and sodium alkoxide, which show consistent final conversion values (Table 12). The values of $\frac{C_{PMA}C_{EtOH}}{C_{PM}C_{EtAc}}$ for AMBERLITE^{TM} IRA904 OH^-, DOWEX MARATHON™ A and sodium alkoxide will be employed as the equilibrium constant K_{eq} for the parameter estimation for reactive chromatography experiments in section 6.3.6.

Table 12 Conversion of transesterification reaction at 40°C inside well-stirred batch reactor using four different catalysts

	Catalyst	Catalyst Concentration [g/200ml]	Average water concentration [vol%]	Conversion [%]	$\frac{C_{PMA}C_{EtOH}}{C_{PM}C_{EtAc}}$
Heterogeneous catalysts	DOWEX MARATHON™ A (OH form)	9.0	0.015	27.6	0.1365
	AMBERLITE™ IRA904OH^-	40.0	0.04	26.4	0.110
Homogeneous catalysts	Sodium alkoxide	0.49	0.0057	27.6	0.1423
	NaOH	0.10	0.021	15.5	N/A

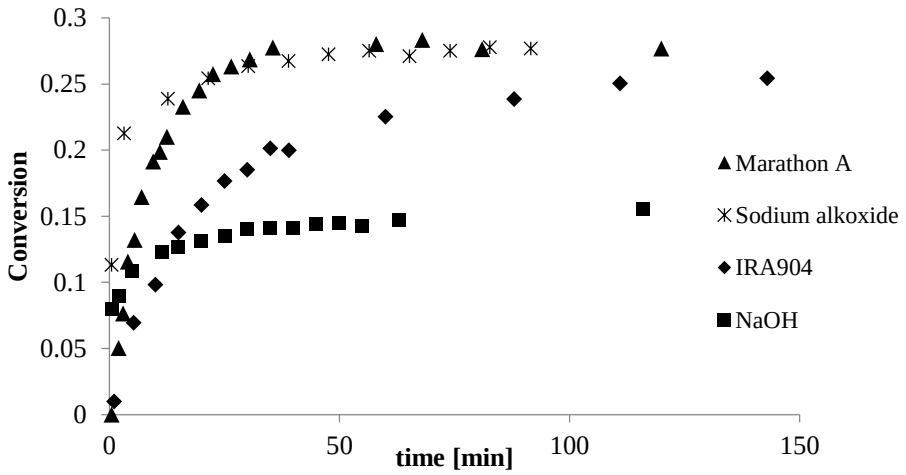

Figure 22 Conversion of transesterification reaction inside well-stirred batch reactor with four different catalysts

6.3.1.2 Effect of water concentration

As discussed in section 5.3.1.1, water concentration plays an important role for base-catalyzed transesterification due to the potential for catalyst deactivation via a neutralization mechanism [78]. In this section, the effect of water is studied with a homogeneous catalyst, NaOH, by varying water concentration inside the well-stirred batch reactor. In this experiment, a predetermined amount of water was added into the reactor at the beginning of each run. Figure 23 shows the conversion of transesterification reaction

at 40°C with the same amount of NaOH (0.1g/200ml reaction mixture) while the water concentrations are varied between 0.02 and 0.14 vol%. It can be seen that when water concentrations are high (0.12-0.14%), the catalyst deactivates fast and the reaction no longer proceeds once the conversion reaches 6%. On the other hand, when water concentrations are low (0.02-0.03%), the reaction proceeds until it reaches the higher conversion of 12-15%, but far below the expected equilibrium based on the reaction conditions.

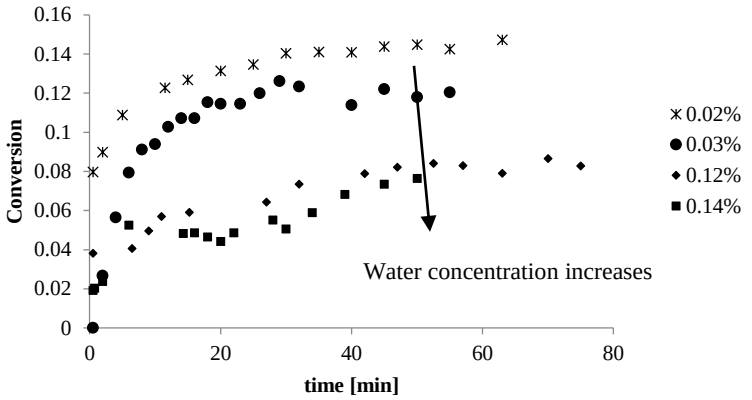

Figure 23 Conversion of transesterification reaction using NaOH as a homogeneous catalyst while varying water concentrations inside the well-stirred batch reactor

6.3.2 Selection of catalyst for reactive chromatography

Due to the lack of literature on reactive chromatography for transesterification, multiple resins had to be screened to select the catalyst that is applicable to the studied system. In this chapter, two properties of catalysts are studied: the swelling ratio and the conversion.

6.3.2.1 Swelling ratio test

A well packed column is of fundamental importance to carry out reactive chromatographic experiments. Especially, presence of headspace in the packed column can lead to flow mal-distribution and consequently highly unpredictable behavior could be seen.

On the other hand, if a resin swells too much inside a fully packed column, it could result in breakage of the resin or of the column. To pack columns with less dispersive characteristics, swelling ratios of resin beds in different solvents are investigated.

Figure 24 shows the result of four different resin beds; AMBERLITE™ IRA904 OH^-, AMBERLITE™ IRA900, DOWEX MARATHON™ A and DIAION PA316. In addition to PM, EtAc and water were used in the volume measurement tests, which were found to have the most significant influence on the resin volume. The resin bed volumes in these solvents are normalized by that in PM, which is the excess reactant and mobile phase in reactive chromatography. As can be seen from the graph, AMBERLITE™ IRA904 OH^- showed smallest bed volume changes of within 5% in different solvents. In other resins, such as AMBERLITE™ IRA900 and DOWEX MARATHON™ A, the bed volume change was more significant when the solvent was exchanged from PM to EtAc, which exceeded 40%. DIAION PA316 also showed a significant bed volume change of 38% when the solvent was exchanged from EtAc to water. As discussed previously, such large swelling and shrinkage may cause an internal dead volume and thus undesirable mixing in chromatographic reactor. From these observations, AMBERLITE™ IRA904 OH^- was chosen for the packing material in this chapter.

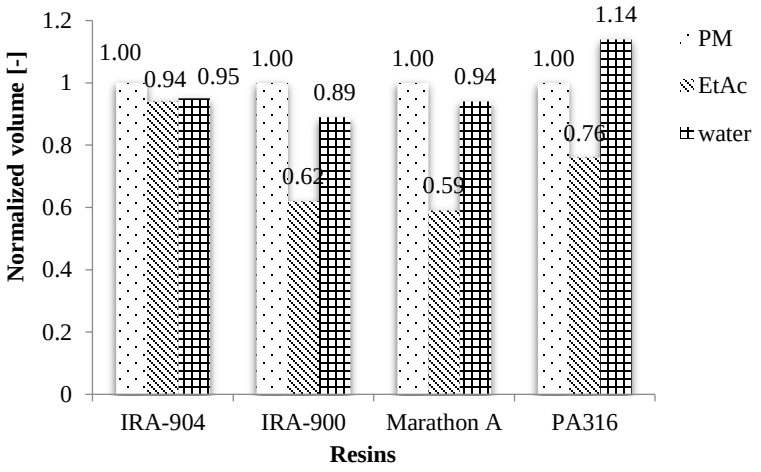

Figure 24 Normalized resin bed volumes saturated in different solvents. The volume of resins beds in PM is 1.0.

6.3.2.2 Catalyst activity test

The catalytic activity of the selected resin in a reactive chromatography process is one of the most important properties since higher activity leads to a higher conversion and productivity. To quantify the conversion in a reactive chromatography, tests were performed by packing a column (0.8 cm internal diameter × 25 cm length) with a selected catalyst and injecting the same amount of reactant (1ml 100%EtAc). All of columns were packed with the resin slurry using PM as solvent without a solvent exchange step to change the resin volume.

The final conversion was calculated based on the remaining EtAc that was unreacted and eluted from the outlet of the column and is shown in Figure 25. As can be seen from the graph, all three of resins, AMBERLITE™ IRA900, DOWEX MARATHON™ A, and DIAION PA316 showed similar conversions, which were approximately 78%.

On the other hand, IRA-904 OH^- achieved a lower conversion, 45%. This low conversion could be attributed to reduced reaction rate related to the exchange capacity; as

can be seen from Table 11, AMBERLITE^{TM} IRA904 OH^- has the lowest value of exchange capacity, which also indicates a lower number of active sites functioning as a catalyst.

To compare the performance of anion exchange resin to that of cation exchange resin, the activity of AMBERLYST^{TM} 15 was tested. The conversion was 14.3%, which is significantly lower. This experiment demonstrated the advantage of base catalysts over acid catalysts for transesterification for glycol ether esters, which has been previously shown for biodiesel production [66].

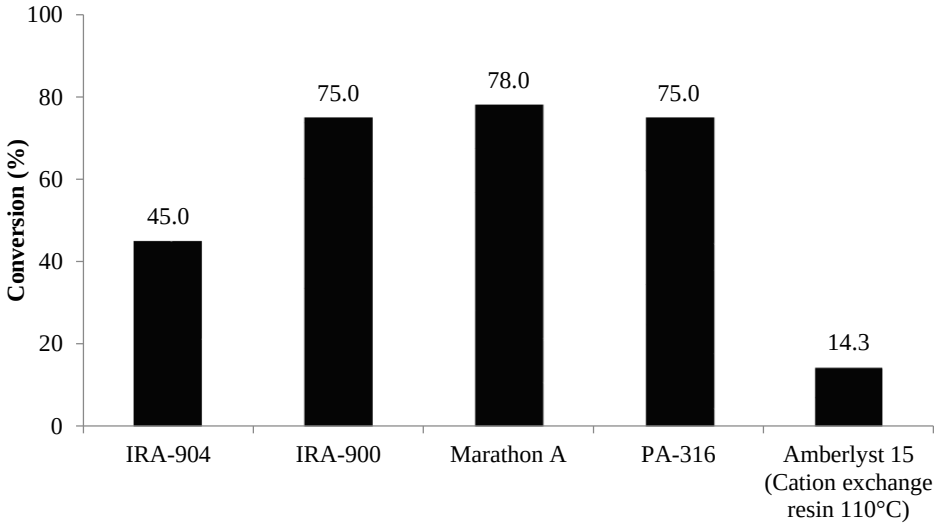

Figure 25 Conversions of EtAc when 1 ml of 100% EtAc was injected into chromatographic reactors filled with each resin. The experiment was performed at 40°C, 0.5 ml/min flow rate of desorbent, PM.

For the selection of a resin to be used for the reactive chromatography experiment, both the swelling ratio and the conversion were considered. In our study where a trade-off between conversion and swelling was observed, more emphasis was placed on the swelling ratio, and AMBERLITE^{TM} IRA904 OH^- was selected. To overcome the relatively low conversion, we attempt to optimize the operating conditions.

6.3.3. Adsorption experiment

To study the selectivity of the resin, an adsorption experiment was performed with an AMBERLITE^{TM} IRA904 OH^- packed column. Each of the two products, PMA and EtOH, was separately injected with the volume of 100 µL into the PM saturated column at 40°C at the PM flow rate of 0.5 ml/min. As can be seen from Figure 26, good separation is observed between PMA and EtOH based on the different retention times which give selectivity separation factor of 1.6.

The linear isotherm was fitted to the chromatogram. Using the inverse method, the fitting result showed that the model predicted the isotherm very well. The relatively good fit without introducing nonlinearity to the isotherm may be due to the relatively low concentrations of the injected components. It should be mentioned that in the SMBR process, the concentrations of each component may increase and the assumption of linear isotherm may not be satisfied. In such a case, a nonlinear isotherm may need to be employed. The plot of linear isotherm is shown in Figure 26 and estimated parameters are shown in Table 13.

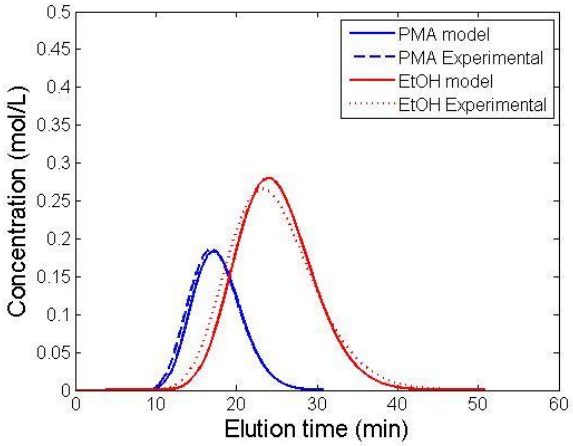

Figure 26. Adsorption experiment of two products, PMA and EtOH. Both products are separately injected at 40°C, at the PM flow rate of 0.5 ml/min.

Table 13. Estimated parameters of PMA and EtOH by fitting linear isotherm to the injection experiment from Figure 26

Estimated Parameters	PMA	EtOH
H_i	0.539	0.944
k_m[min^{-1}]	2.945	2.05

6.3.4 Reactive chromatography experiments

For reactive chromatography experiments, the effects of the feed concentration and temperature were studied. In all experiments, a stainless steel column packed with AMBERLITE^{TM} IRA904 OH^- was used, and the column was regenerated with a NaOH solution each time before the experiment. The conversion was checked before each experiment to ensure the consistency of the column activity. A detailed explanation of regeneration will be discussed in section 6.3.7. Before injection of EtAc, the outlet PM flow of the column was analyzed and water concentration was confirmed to be below 0.005vol%.

6.3.4.1. Effect of feed concentration

To study the effect of the feed concentration, two different feed mixture were prepared: one that contains 50 vol% of EtAc and 50 vol% of PM (denoted as 50% EtAc), and another that contains only 100% EtAc. Each of these mixtures in 1 ml was injected into the system at 40°C at the PM flow rate of 0.5 ml/min.

The results are shown in Figure 27. It can be seen that while the peak heights of the components change with the feed concentration, the shapes and retention times remained unchanged. On the other hand, the conversion of EtAc is correlated negatively with the feed concentration; the conversion increased from 65% to 74% when the feed is diluted

from 100% to 50%. This could be due to the insufficient mixing of EtAc with PM at 100% EtAc injection, which results in a lower conversion. A similar observation was made in the previous chapter with esterification [14]. In this chapter, only two feed concentrations were tested, and optimization of feed concentration [9] was not performed but left as future work. Finally, we note that there is no significant change in retention times when the feed concentration is varied from 100% EtAc to 50% of EtAc.

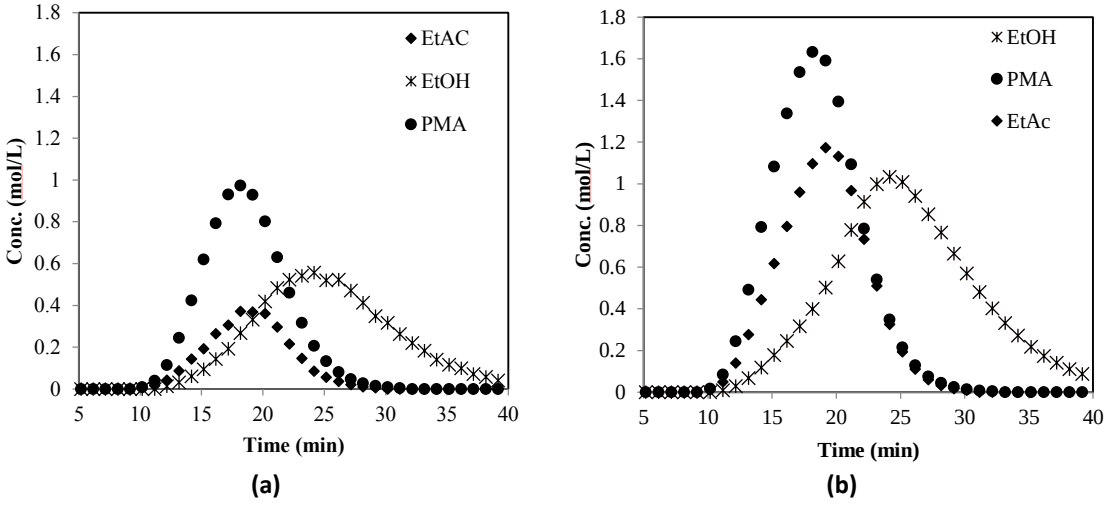

Figure 27 Injection of 1 ml of EtAc into the reactor at 40°C while PM flows at 0.5ml/min. (a) 50% EtAc/PM (b) 100% EtAc

6.3.4.2 Effect of temperature

To study the effect of temperature on the transesterification reaction in reactive chromatography, the temperature is varied from 40°C to 60°C, the temperature limit of the thermal stability of AMBERLITE^{TM} IRA904 OH^-. Figure 28 shows the result of injection of 1 ml 50% EtAc into the system at the PM flow rate of 0.5 ml/min. The conversion is 80% at 60°C, which is slightly higher than that at 40°C, 74%. This increase in the conversion is due to the endothermicity of the reaction. However, the effect of the temperature on the final conversion is relatively minor; only 6% points increase is observed when temperature

is increased from 40°C to 60°C. In addition, according to the experiments where deactivation is observed, the catalyst deactivates faster at 60°C, which counteracts the benefit of the high conversion. It should also be noted that the retention times of components are not affected by the temperature within the studied range as shown in Figure 28.

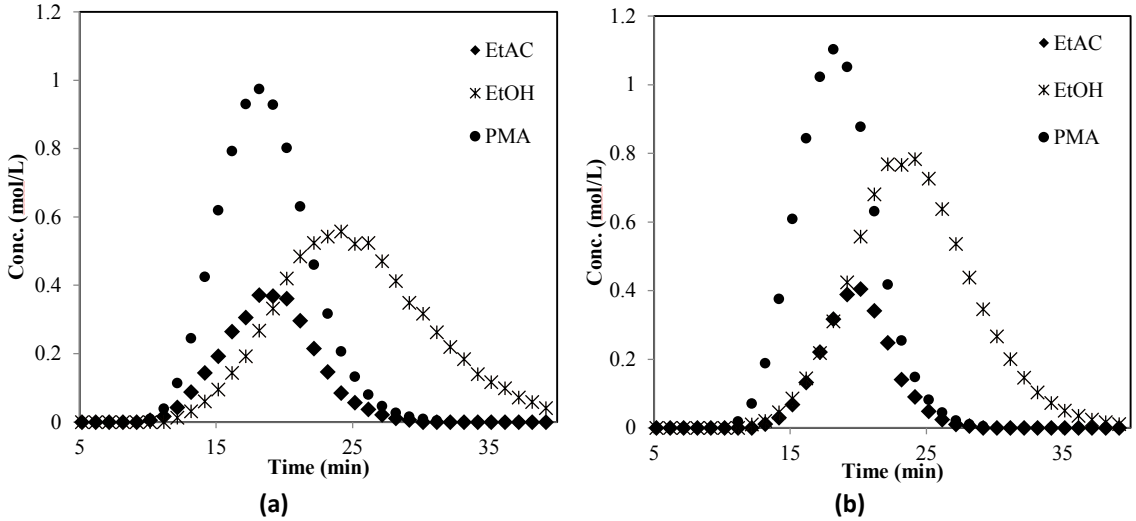

Figure 28 Injection of 1ml of 50% EtAc/PM into the system at different temperatures at the PM flow rate of 0.5ml/min (a) 40°C (b) 60°C

6.3.5 Comparison of esterification and transesterification

It is worth comparing esterification and transesterification to produce the same ester by reactive chromatography, which has never been addressed in past studies. The comparison mostly focuses on the conversion and the separation performance, which are critical for the productivity of the system. It should be noted that all the comparison was made with an assumption that anion exchange resin does not deactivate. As mentioned earlier, deactivation of anion exchange resin was observed and will be discussed in detail in section 6.3.7. All the transesterification experiments were performed with fully regenerated resin. All of esterification data are referenced from Chapter 5.

Figure 29 shows the effect of temperature on two reactions. It can be seen that relatively higher conversion was achieved with the transesterification even at low temperatures. On the other hand, for the esterification, the process had to be operated at the high temperature of 110°C to achieve a comparable conversion. At the highest temperatures, both reactions reached a similar conversion of approximately 80%. However, transesterification would not benefit from increasing the temperature any further since the conversion is relatively insensitive to temperature. In addition, the basic resin has low thermal stability, where the maximum temperature is limited to 60°C. Thus, the stability of the catalyst is better with the acidic catalyst, but the basic catalyst has an advantage of low operating temperature for the same conversion.

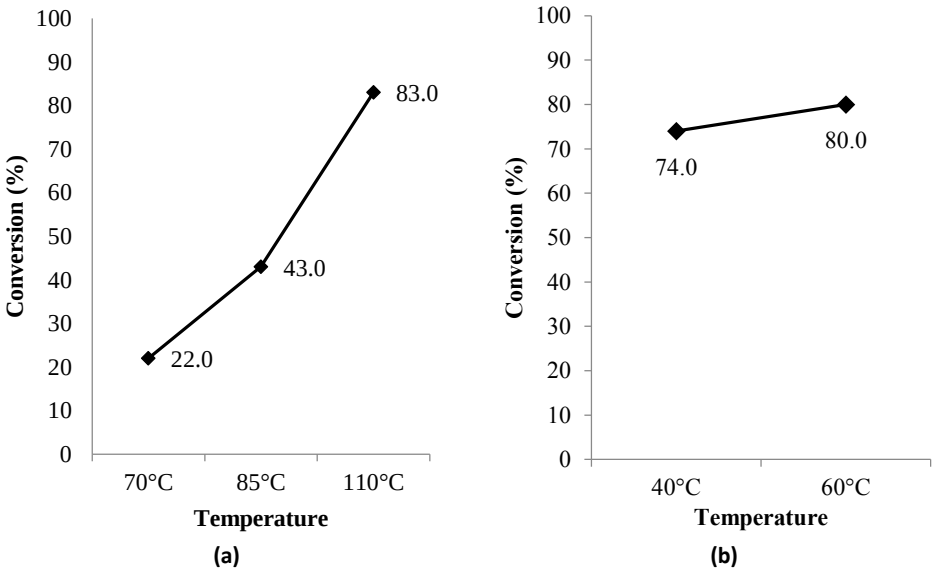

Figure 29 The effect of temperature on the esterification and the transesterification applied to the reactive chromatography. (a) The esterification reaction conducted with AMBERLYST™ 15 resin by injecting 1 ml of 50% acetic acid at the PM flow rate of 0.5 ml/min[14] (b) The transesterification reaction conducted with IRA904 OH^- by injecting 1 ml of 50% EtAc at the PM flow rate of 0.5 ml/min

Figure 30 shows the effect of feed concentrations for the esterification and transesterification reactions. For both reactions, the conversion increased when the reactant

in the injected feed was diluted to 50% from 100%. The increase in conversion could be due to a better mixing of injected reactants with the desorbent or an excess amount of desorbent compared to the injected reactants. To find the optimal concentration, further parameter estimations and optimizations are required.

Another difference between the two reactions is the elution time of the most retained components. For esterification, water has the strongest affinity toward the resin, and it takes a large amount of desorbent to wash out water. [14, 70]. On the other hand, in transesterification, EtOH is not as strongly retained as water while EtOH can be effectively separated by the anion exchange resin, which results in higher efficiency.

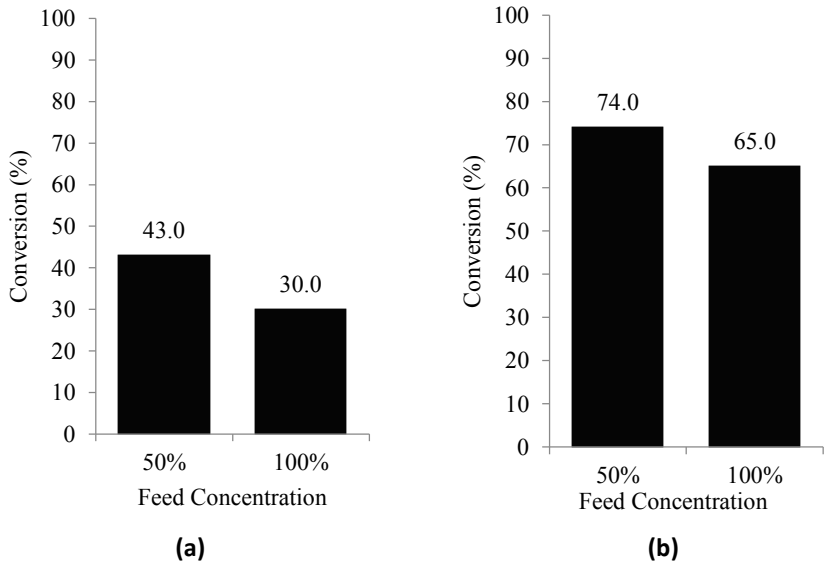

Figure 30 The effect of feed concentrations to the esterification and the transesterification by reactive chromatography (a) The esterification reaction conducted with AMBERLYST™ 15 resin at 85°C by injecting 1ml of acetic acid at the PM flow rate of 0.5ml/min[14] (b) The transesterification reaction conducted with IRA904 OH^- at 40°C by injection 1ml of EtAC at the PM flow rate of 0.5ml/min

6.3.6 Parameter estimation

Based on the experimental data collected from reactive chromatography, models given in chapter 4 were fitted to estimate parameters using the inverse method. It has been

observed that the resin deactivates rapidly at 60°C, and thus only the experiments performed at 40°C were fitted to estimate parameters.

Figure 31 shows the result of fitting two experiments at 40°C by injecting 1 ml of EtAc at different concentrations at the PM flow rate of 0.5 ml/min. The result shows a good fit of the model to the experimental data, and the estimated parameters are shown in Table 14. It can be seen from this table that all values of the fitted parameters are reasonably close to the initial values, which were obtained from separated experiments obtained as follows: the initial values for parameters of PMA and EtOH are from pulse injection experiments in section 6.3.3. Initial reaction rate constant k_1 is obtained from parameter estimation of well-stirred batch reactor experiment. The equilibrium constant K_{eq} is obtained from Table 2 as a result of the same batch reactor experiments. The initial value of axial dispersion coefficient, D_{ax}, is obtained from dispersion coefficients of esterification system inside chromatographic reactor packed with AMBERLYST^{TM} 15, which has similar properties. The initial parameters of PM and EtAc was also taken from esterification system in Chapter 5 [32].

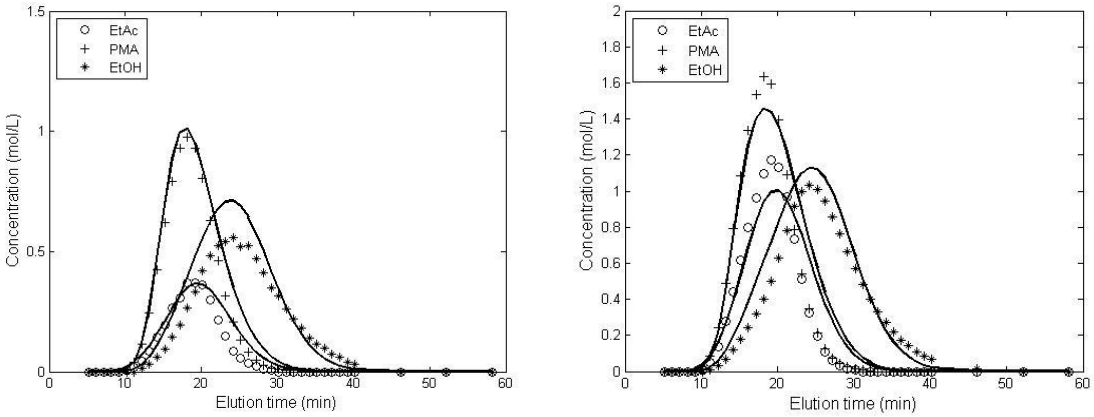

Figure 31 The result of fitting the model to the experimental data. Experiments are conducted at 40°C by injecting 1 ml of EtAc of different concentrations while PM flows at 0.5 ml/min (a) 50% EtAc/PM (b) 100% EtAc

Table 14 Estimated parameters from model fitting shown in Figure 31

Parameters	Fitted Value	Initial value	Lower bound	Upper bound
H_{PM}	0.51	0.5	0.0	5.0
H_{EtAc}	0.79	0.5	0.0	5.0
H_{PMA}	050	0.54	0.0	5.0
H_{EtOH}	0.89	0.94	0.0	5.0
k_{PM} [1/min]	1.24	1.00	0.0	10.0
k_{EtAc} [1/min]	0.93	1.00	0.0	10.0
k_{PMA} [1/min]	4.02	2.95	0.0	10.0
k_{EtOH} [1/min]	1.63	2.05	0.0	10.0
k_1 [mol/L/min]	0.04	0.04	0.0	10.0
K_{eq}	0.19	0.13	0.01	1
D_{ax} [m^2/min]	0.09×10^{-4}	2.73×10^{-4}	0.0	50×10^{-4}

6.3.7 Catalyst deactivation and regeneration

Throughout the experiments using the chromatographic reactor, the deactivation of catalyst was observed when using anion exchange resin. To investigate the deactivation of the catalyst, an accelerated deactivation test was carried out in the form of a continuous fixed bed reactor mode of operation.

The experimental setup for the accelerated deactivation test is shown in Figure 32. The number of pumps was increased to two for the two reactants, PM and ethyl acetate, which were pumped into the column simultaneously at the same flow rate. The reactants, PM and EtAc, were dehydrated before the experiments by adding molecular sieve 3Å into the stock bottle and leaving it overnight. At the outlet, samples were collected about every hour. The conversion of each sample was plotted against the retention time as shown in Figure 33. As can be seen from the plot, conversion decreased to less than 25% of the initial conversion after 11 bed volumes of reactants were injected. It should be noted that even the highest conversion at the beginning of the experiment did not reach equilibrium since the residence time was not long enough.

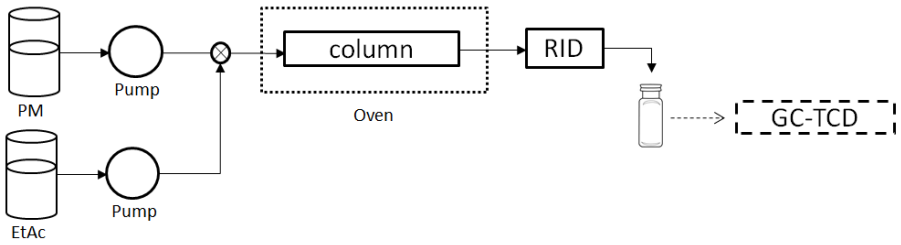

Figure 32. Setup for catalyst deactivation test with AMBERLITE™ IRA904 OH^-

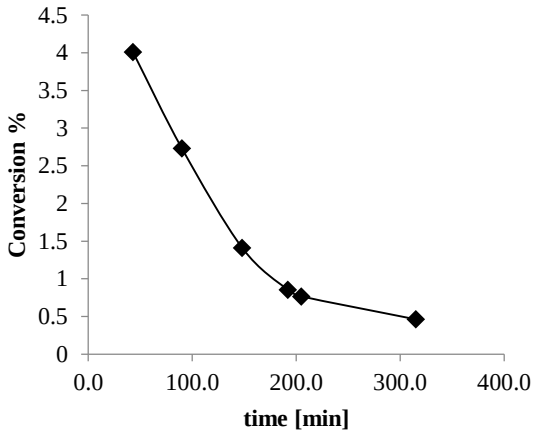

Figure 33. Reactant conversion at the outlet of the column vs. the retention time for deactivation test. Flow rates of PM and ethyl acetate are both 0.3ml/min, and temperature is at 40°C

After the conversion decreased to 0.5%, the column was regenerated in-situ by washing the column with 5 wt% NaOH in water for 12 bed volumes, which is followed by 18 bed volumes of water. After the regeneration, water in the column was replaced by PM. The same conversion test was performed with the regenerated column, which confirmed that the conversion returned to the initial value with the fresh resin, 4%. This set of experiments indicates that AMBERLITE™ IRA904 OH^- loses activity when a large amount of reactants was injected, but it is possible to regenerate the catalyst to regain the initial activity.

A possible reason for the deactivation is a neutralization of active sites due to presence of water, which produces acetic acid when reacted with ethyl acetate as shown in Figure 34. To verify this hypothesis, a set of experiments was performed as follows: the

column was intentionally deactivated by washing it with EtAc followed by water, which is assumed to generate acetate ion and deactivate the resin. With the deactivated resin prepared in this manner, the same conversion test was performed, which showed 0% conversion.

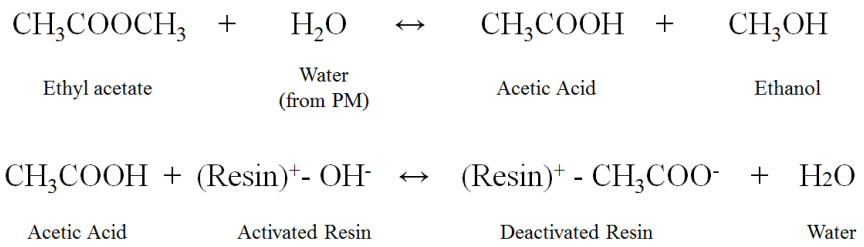

Figure 34 Deactivation mechanism of AMBERLITE™ IRA904 OH^- which is initiated by small amount of water present in PM

To ensure the consistent activity of the column, the column was regenerated every time before each experiment in this chapter. The regeneration step was consistent as discussed in the previous paragraph, and the conversion test was performed before each experiment to ensure the constant activity of the reactor.

It should be noted that the deactivation can be a critical issue in a continuous reactive chromatography process such as SMBR. A potential solution could be adding a separate regeneration zone. In such a design, one extra column goes through a regeneration step while the remaining columns perform reaction and separation. When one step is finished, the regenerated column can be replaced with a deactivated column through port switching. A similar design has been suggested in previous studies, such as Xie et al. for isolation of six sugars from biomass hydrolysate [79], and Paredes et al. [80] for plasmid DNA purification.

6.4. Conclusion

In this chapter, reactive chromatography was applied successfully to produce PMA through transesterification of EtAc and PM while an anion exchange resin was employed as both catalyst and adsorbent. Various catalysts were tested and screened. To investigate the reaction equilibrium, heterogeneous and homogeneous catalysts were compared at a well-stirred batch reactor experiment. The result showed that the conversion at thermodynamic equilibrium is around 27% at 40°C, when started from a 50-50 volume mixture of reactants. Hygroscopic catalysts with hygroscopic solvent, such as NaOH in PM, showed continual deactivation from the start of the reaction, owing to the acid produced from the reaction between water and EtAc. The well-stirred batch reactor experiment showed the importance of controlling the water concentration to prevent catalyst from deactivation.

The most suitable catalyst for the reactive chromatography was found based on the swelling ratio of the resins in different solvents and different degrees of conversion. AMBERLITE^{TM} IRA904 OH^- was selected based on a swelling ratio for a good packing of the column.

Using the anion exchange resin selected in this chapter, AMBERLITE^{TM} IRA904 OH^-, the selectivity was tested by injecting PMA and EtOH into the column packed with the catalyst. The result showed a good separation between the two products, and adsorption parameters were estimated by fitting the model to the chromatogram. Reactive chromatography experiments were conducted at different feed concentration and temperature. The results show the strong influence of temperature and feed concentration on the performance of chromatographic reactors. Based on the obtained data of reactive

chromatography at different conditions, parameters were estimated by fitting the model to experimental chromatograms in Section 6.3.6. The model predicted the experimental data very well, and all values of the fitted parameters are reasonably close to the initial values, which were obtained from separated experiments.

Transesterification in reactive chromatography was compared to esterification in the previous chapter. It was found that transesterification is relatively insensitive to temperature. In addition, diluting the feed increased the conversion, which is consistent with the previous chapter on esterification. The comparison emphasized the advantage of transesterification where the higher conversion was achieved at lower temperature, and removal of strongly adsorbed component can be carried out in a shorter amount of time, which leads to a higher productivity.

However, deactivation of anion exchange resin was observed throughout the study. It was found that presence of even a small amount of water in the system is detrimental to the activity of basic catalysts. Nevertheless, regeneration of the catalyst to the initial activity was possible and validated in our experiment. It should be noted that to perform transesterification in a continuous chromatography system, the design may need to be modified to allow regeneration operations, which is out of scope for this chapter. The following chapters (chapter 7,8) suggest alternative catalysts that could be used to avoid deactivation.

CHAPTER 7. HOMOGENEOUS TRANSESTERIFICATION FOR PMA PRODUCTION

7.1. Motivation

The previous chapter studied anion exchange resin for the PMA production, but found that the resin deactivates throughout the batch reactive chromatography process. Anion exchange resin has been widely used for transesterification [66, 67, 81-85]. However, it has been shown in many published works that anion exchange resin deactivates [66, 83, 86-89]. Kim et al. showed the decrease of base site densities by 5-20% from the initial values of macroporous anion-exchange resins after 9 hours of batch run [81]. They concluded that one of the major deactivating agents was water. Meher et al. and Schuchardt et al. claimed that all materials involved in transesterification should be substantially anhydrous to meet desired ester yields in all base-catalyzed biodiesel production [90-92].

Several approaches attempted to overcome this drawback of deactivation [66, 83, 86-89]. Shibasaki-Kitakawa suggested a three-step regeneration protocol that should be performed between batch runs to maintain the catalytic activity of anion exchange resins [66]. Kim et al. showed that a trace amount of CH_3ONa was found to exhibit synergetic effects with the anion resin catalysts (Marathon A and Marathon MSA), attributed to the regeneration of active catalytic sites in a basic environment [83]. However, most of these approaches are applied only to packed-bed reactors or well-stirred batch reactors, and a solution to the deactivation inside the continuous chromatographic reactor has not been found so far.

In this chapter, a new approach is proposed to combine the merits of homogeneous catalyst and anion exchange resin for chromatographic reactors. Sodium alkoxide is used

as a homogeneous catalyst, which circumvents the problem of deactivation of heterogeneous catalyst. Fresh homogeneous catalyst is fed continuously into the reactor. In this way, a process can be performed continuously without interrupting the run with regeneration steps. A packed column with an anion exchange resin in Cl^- ionic form, which is non-reactive, was employed. The resin performs separation and overcomes the deactivation since the functional group is not basic any more. By combining the homogeneous catalyst and anion exchange resin, the process also overcomes the drawback of a homogeneously catalyzed system for establishing a continuous process [93].

As in the previous chapter, transesterification of PM and ethyl acetate by reactive chromatography is studied. To analyze reaction equilibrium and kinetics, batch reaction experiments are performed in a well-stirred batch reactor at different temperatures and catalyst concentrations. The adsorptive separation is analyzed by injecting the two products, PMA and EtOH, separately into the column packed with a separation medium, IRA904 Cl^-, while PM is supplied as a mobile phase. Finally, transesterification is performed in a chromatographic reactor at different temperatures, catalyst concentrations, and residence times (different flow rates and column lengths) to study the effect of those conditions on the conversion and separation.

The resulting chromatograms are fitted to a single reactive chromatography model and parameters are further used to optimize the simulated moving bed reactor (SMBR). We use a transport dispersive model with a linear driving force for the adsorption rate. The model parameters are estimated from the batch reactor experiments and single-column pulse injection experiments by the inverse method. The parameters and models are validated by simulating an experiment result at different reactor dimension. These

parameters are used to further design a continuous system, i.e. the simulated moving bed reactor (SMBR).

Figure 35 shows the schematic of a SMBR operation with homogeneous catalyst which are used for the optimization. The basic operation steps are identical with SMBR explained in Chapter 1. In this chapter, the homogeneous catalyst is injected through desorbent, S, and also partially through feed when the feed stream contains desorbent. As a result, catalysts are also collected from raffinate and extract. Thus, there should be an additional separation unit at the outlet of the SMBR process to remove the catalyst when applied to industrial process. In addition, at the outlet of the raffinate stream, a suitable quenching material needs to be added when collecting the raffinate stream to suppress the backward reaction.

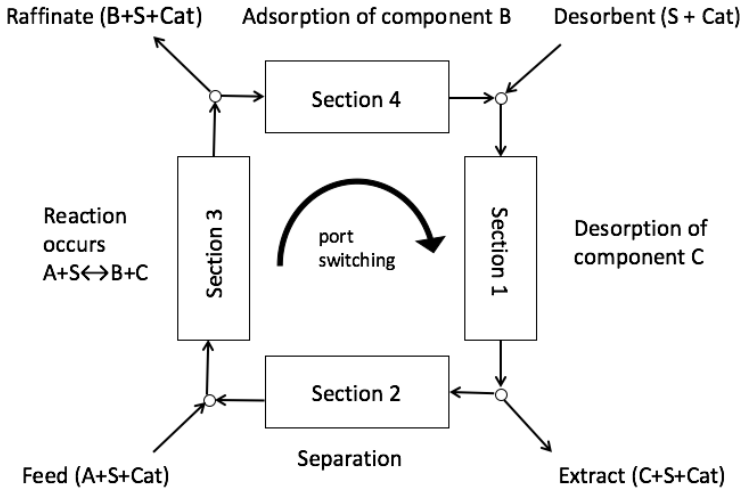

Figure 35 Schematic of a SMBR operation

The goal of this chapter is to develop an optimized process for the production of PMA through reactive chromatography, and further present the potential to develop a SMBR system. The approach combines the utilization of a homogeneous catalyst and anion-exchange resin to overcome the deactivation of the resin. The resulting model and parameters are validated through comparison of simulation and the experimental data. By

applying the concept of SMBR to the system, the optimized design of SMBR yields a significantly improved conversion compared to the well-stirred batch reactor.

7.2. Materials and Methods

7.2.1 Materials

The homogeneous catalyst, sodium alkoxide was synthesized in the lab based on the reaction shown in Figure 21. The reaction was performed as follows: PM was stirred with solid NaOH, and then molecular sieve 3Å was added afterwards. This enabled an excess conversion of sodium hydroxide by removing water from the solution. The solution was left overnight before use in experiments to ensure water removal. Each solution was analyzed by gas chromatography to confirm the water concentration is below 0.005 vol%. The adsorbent Amberlite^{TM} IRA904 was provided by the Dow Chemical Company in the Cl^- form. The resin was washed with water for 10 bed volumes (BVs) and washed with dehydrated PM before used for packing a column.

7.2.2 Experimental setup and procedure

The experimental procedures explained in Chapter 3 are followed for well-stirred batch reactor experiments, single chromatographic reactor experiments, and analysis.

7.3 Results and discussion

7.3.1 Well stirred batch reactor experiment

7.3.1.1 Effect of catalyst loading

To see the effect of catalyst loading, the amount of catalyst is varied between 1.7 g/L and 3.4 g/L at 40°C, and acetate to alcohol molar ratio of 1:1. Figure 36 shows that with increasing catalyst concentration, the initial reaction rate increases and the equilibrium is reached faster. As expected, the final conversion is not affected by catalyst loading

significantly. In all cases, the same value of the equilibrium constant K_{eq} is obtained based on Eq (11), which is 0.14 ± 0.02. The maximum concentration of the catalyst, 3.4 g/L, is determined by the solubility of the catalyst to the reactant, PM.

7.3.1.2 Effect of temperature

To investigate the effect of temperature on the reaction rate, the temperature is varied between 40°C to 60°C with the catalyst loading of 3.4 g/L, and initial reactant mole ratio of 1:1. As shown in Figure 37, with increasing temperature, the increase in initial reaction rate is minimal. In addition, nearly the same equilibrium conversion of ethyl acetate is obtained in the investigated temperature range. The reason is that the heat of reaction for transesterification reaction is small; i.e., the equilibrium constants are not a strong function of temperature. From these observations, the experiments are designed and analyzed under the assumption that the effect of temperature is minimal on the reaction kinetics at high catalyst concentration.

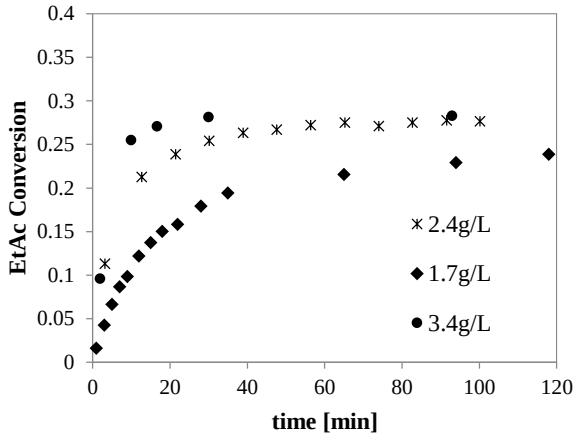

Figure 36 Effect of the amount of catalyst, 1.7g/L,2.4g/L, and 3.4g/L at 40°C. The initial molar ratio of EtAc/PM=1

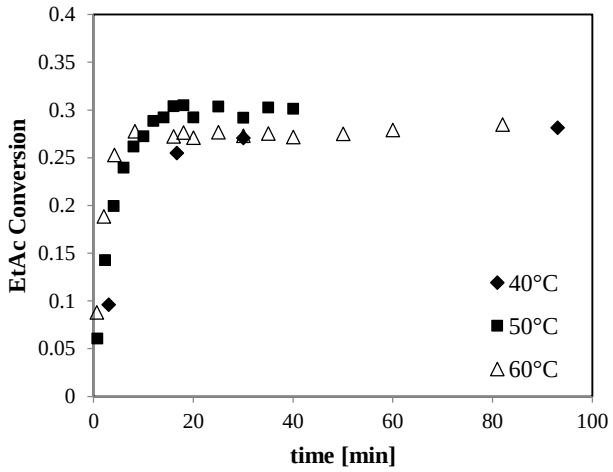

Figure 37 Effect of temperature, 40°C,50°C and 60°C on the conversion of EtAc, at 3.4 g/L of catalyst concentration and initial molar ratio of EtAc/PM = 1

7.3.2. Adsorption experiments (pulse injection of non-reacting components)

To determine the adsorption constants of two products (PMA, EtOH), a pulse of each component is injected into a preheated packed column at different flow rates and concentrations, and Figure 38 shows the result of pulse injection experiments. For various concentrations of each component, rather symmetrical peaks are observed at the same specific retention times. This indicates that the linear equilibrium model is adequate [52] in the concentration ranges of the experiments. Thus, the adsorption equilibrium constants, $H_{i,}$ and mass transfer coefficients, $k_{m,i}$ of ethanol and PMA are obtained by fitting linear adsorption isotherm model to the chromatograms. Table 15 summarizes the determined constants for all components.

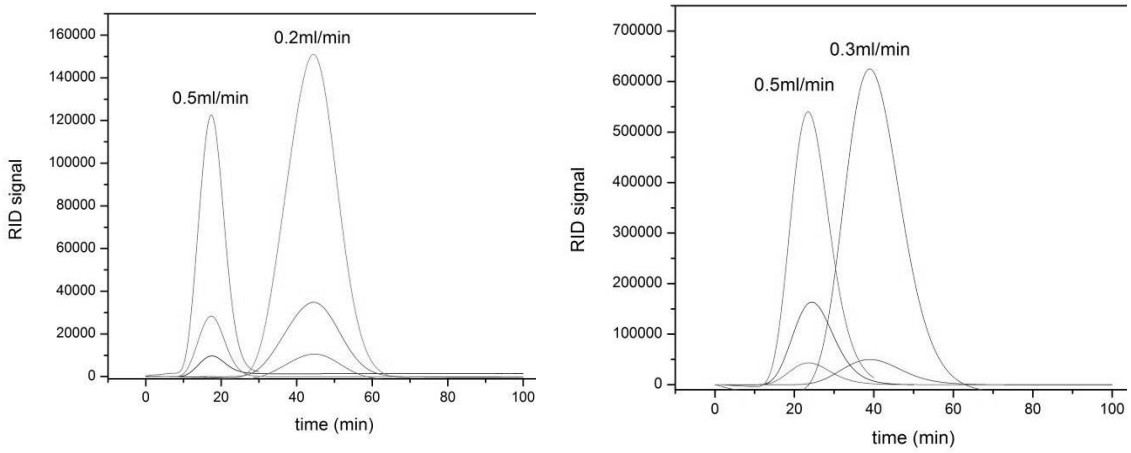

(a) PMA (b) EtOH

Figure 38 Elution profiles of (a) PMA and (b) EtOH at different flow rates and various injection concentrations (C^{inj} = 10vol%, 30vol% and 100vol%). PM was used as a mobile phase

In this study, we consistently use the linear isotherm for all components. Nevertheless, we cannot exclude the possibility that the adsorption equilibria are nonlinear. To investigate the problem further, experiments at higher concentrations may need to be performed to improve the predictability of the model at the conditions of higher concentrations, such as those in the SMBR process. In addition, it should be mentioned that the adsorption equilibrium constant of mobile phase PM, was not possible to obtain from pulse injection experiment, and thus the model is fitted to the reactive chromatograms to estimate this parameter.

Table 15 Adsorption parameters obtained by fitting Equation (1),(2) and (3) to Figure 38

Parameters	Value
H_{PMA}	0.412
H_{EtOH}	0.948
$k_{m,PMA}$ [1/min]	1.957
$k_{m,EtOH}$[1/min]	2.098
D_{ax} [m^2/min]	0.5201×10^{-4}

7.3.3 Reactive chromatography experiments

7.3.3.1. Effect of catalyst concentration

Figure 39 shows the effect of catalyst concentration on the conversion and separation performance. An experiment was performed at two different catalyst concentrations, 1.7 g/L and 3.4 g/L at 40°C while the flow rate of mobile phase was kept at 0.5 ml/min. Based on the constant retention times of each component, the separation is not affected by the catalyst concentration. A conversion is calculated based on the area under the peak of ethyl acetate and subtracting the amount from the injected volume, which is 1 ml. A conversion increases from 37% to 52% when catalyst concentration is increased. This result corresponds with the batch experiment result shown in Figure 36, where the initial reaction rate increases with higher catalyst concentrations.

Based on the chromatogram of each component, the orders of affinity towards the resin are determined as: ethanol > ethyl acetate > PMA. This is because components with stronger affinities elute out more slowly. Here, the difference in affinity between ethyl acetate and PMA is relatively small. Thus, a high conversion of ethyl acetate is necessary to obtain pure PMA from the separation; otherwise, unreacted ethyl acetate may contaminate the PMA product. This high conversion will be the objective of SMBR design in the later section. On the other hand, the separation between PMA and ethanol is more significant, which directs the transesterification reaction toward the complete conversion exceeding the thermodynamic equilibrium.

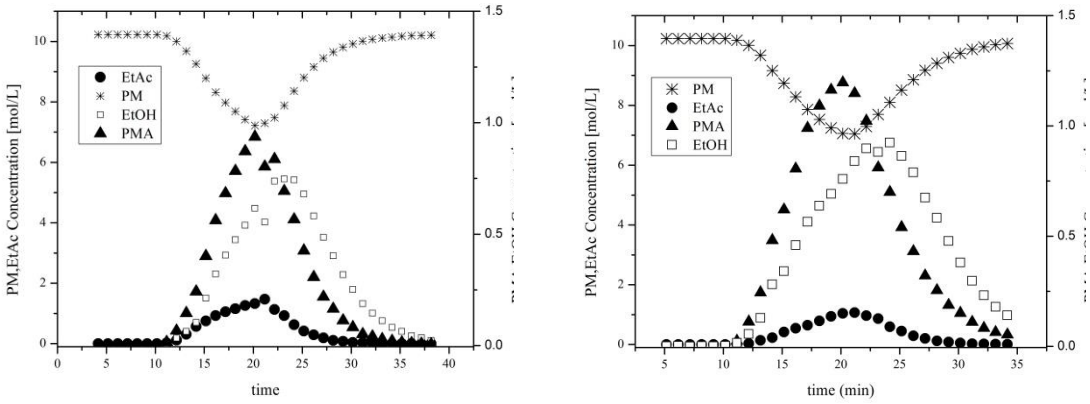

Figure 39 Influence of catalyst concentration on the transesterification reactions at 40°C. (a) C_{cat} =1.7 g/L (b) C_{cat} = 3.4 g/L (PM flow rate = 0.5 ml/min, feed concentration = 100%, injection volume = 1 ml, column length 25 cm)

7.3.3.2 Effect of temperature

To investigate the effect of temperature, the experiment was performed at 40°C and 60°C with the catalyst concentration of 3.4g/L while keeping the flow rate at 0.5 ml/min. The effect of temperature on the conversion and separation can be seen from Figure 40. The temperature mainly affects adsorption, reaction equilibrium, reaction kinetics and mass transfer. It has been verified that the adsorption is not affected by temperature from our previous study within the considered temperature range [94]. In addition, the reaction equilibrium has been shown to be not affected by temperature from our well-stirred batch reactor experiment in section 5.1.2.

As can be seen from Figure 40, the peak area of PMA increases little as the operating temperature increases. Based on the remaining ethyl acetate, the conversion increases from 52% to 57% when temperature is changed from 40°C to 60°C. A similar result is observed from well-stirred batch reactor experiment, where the temperature range of 40°C to 60°C has minimal effect on the final conversion and initial reaction rate.

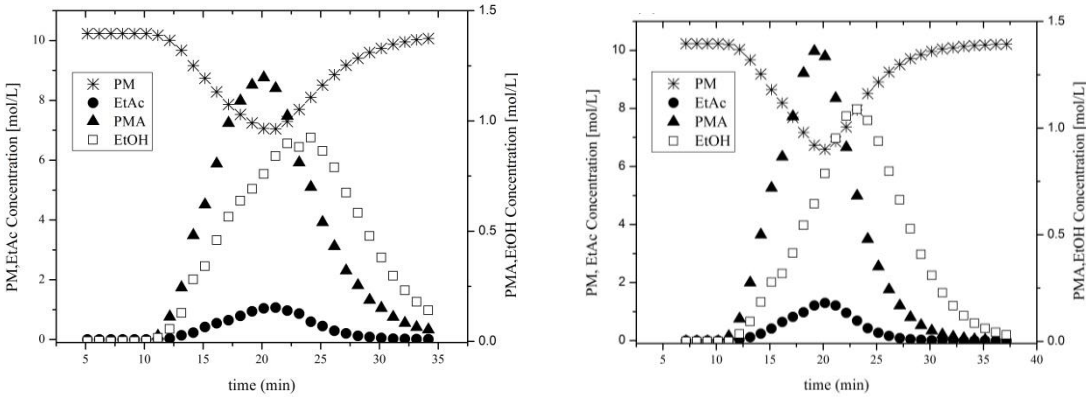

Figure 40 Influence of temperature on the transesterification reactions (a) 40°C (b) 60°C (Catalyst concentration 3.4g/L, PM flow rate = 0.5 ml/min, feed concentration = 100% EtAc, injection volume = 1 ml, column length 25 cm)

7.3.3.3. Effect of flow rate

The flow rate primarily influences the residence time and dispersion. To investigate the effect of flow rate on the conversion, the transesterification was performed at different flow rates. Figure 41 shows the resulting chromatograms where the flow rate was varied from 0.5 ml/min to 2 ml/min while keeping the temperature at 40°C and catalyst concentration at 1.7 g/L. Based on the retention time difference of PMA and ethanol, the separation between the two products was improved when the flow rate was decreased. The conversion was also increased when the flow rate was decreased. This is because i) the contact time of reactants with the catalyst was increased and ii) better separation of product from the reaction mixture due to improved resolution, increased the conversion by exceeding the thermodynamic equilibrium. The conversions are compared at different residence times in Figure 43.A similar effect of flow rates are observed from the previous literature, where resolution is significantly improved when the flow rate is decreased [53].

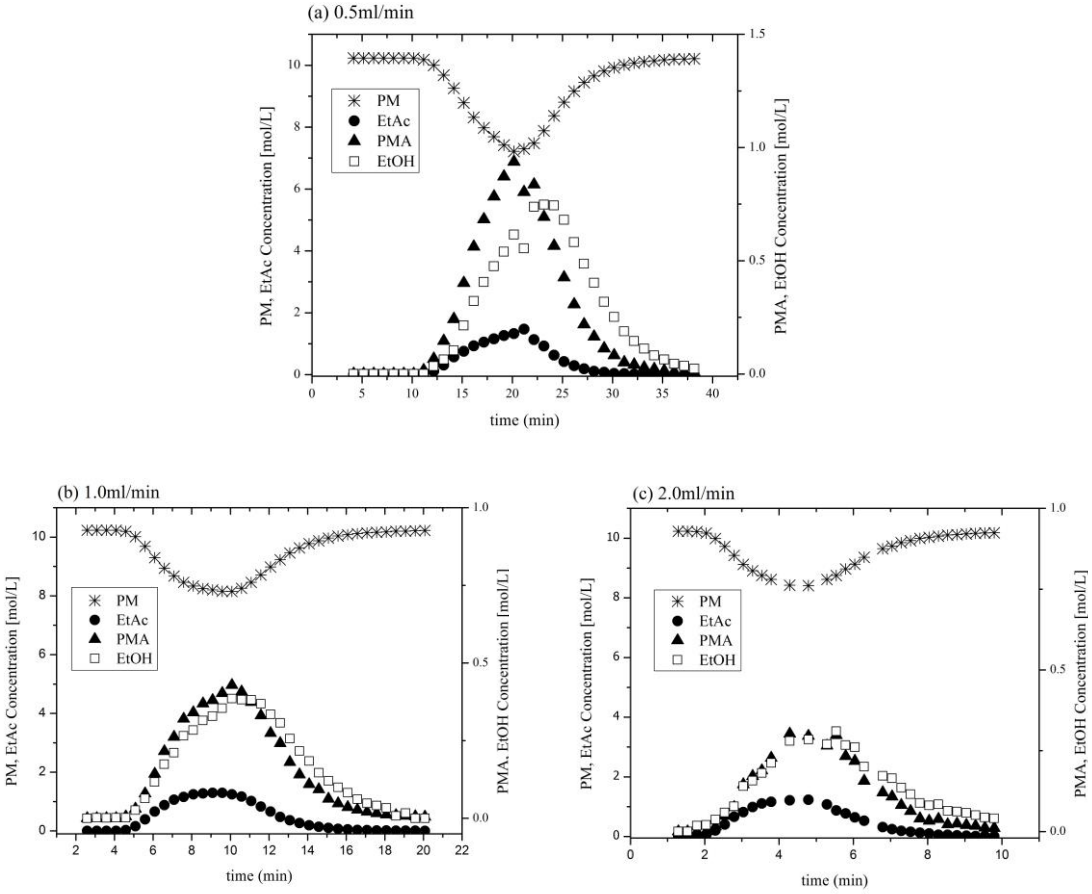

Figure 41 Influence of flow rate on the transesterification reactions. (a) 0.5ml/min (b) 1ml/min (c) 2ml/min (feed concentration 100 vol%, temperature 333.15 K, injection volume 1 ml, column length 25 cm, catalyst concentration 1.7 g/L).

7.3.3.3. Effect of column length

Figure 42 shows a chromatogram of transesterification performed at an increased length of reactor column. The length of the reactor was increased to 50 cm from 25 cm, the standard length for all previous experiments. As can be seen from the graph, separation between the two products was improved by increasing the column length. The conversion of reactant was also increased by 9% points.

Figure 43 summarizes the conversions in terms of residence times, which are varied by flow rates and column length. The conversions are increased as residence times are increased, as expected, due to increased reaction time and improved separation. However,

since the retention time increased, it takes a longer time to complete one batch run. Thus the trade-off between a shorter batch time (higher throughput) and higher conversion must be considered in process development [14].

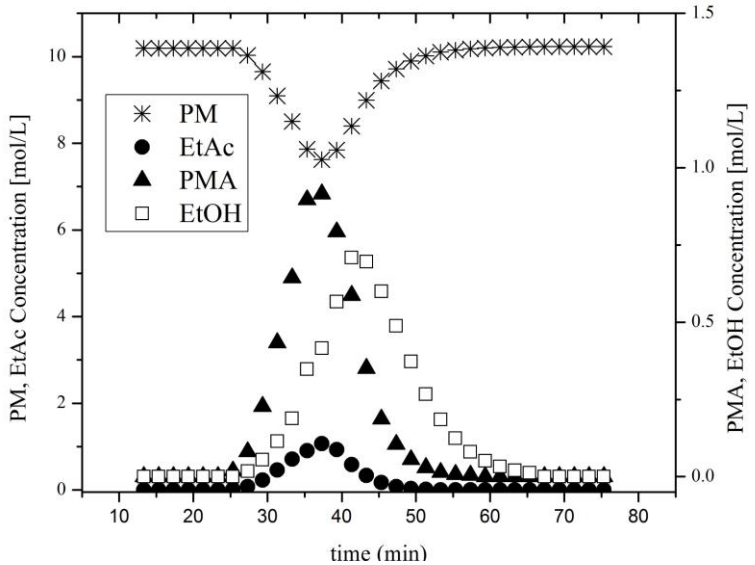

Figure 42 Elution profile of transesterification reaction at higher reactor column length, 50 cm (feed concentration 100vol%, temperature 333.15K, injection volume 1 ml, flow rate 0.5 ml/min).

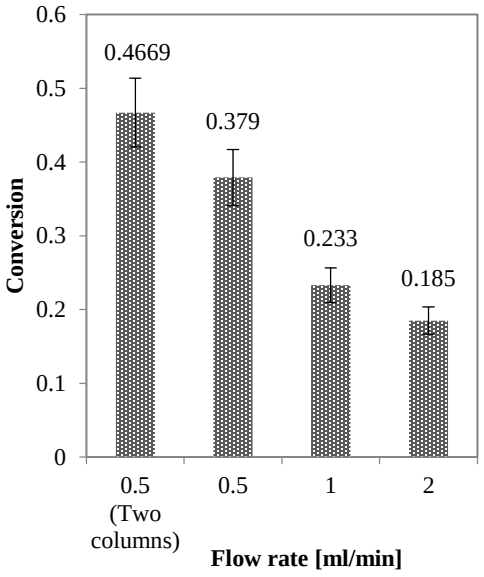

Figure 43 Influence of residence time on the conversion of ethyl acetate (feed concentration 100vol%, temperature 40°C, injection volume 1 ml).

7.4 Modeling result and discussion

7.4.1 Single column parameter estimation and model validation

Based on the experimental data collected from reactive chromatography, models given in section 3 were fitted to estimate parameters using the inverse method. Since the effect of temperature on the final conversion was minimal, only the experiments performed at 40℃ were fitted to estimate parameters. Parameters obtained here will be used to simulate the SMBR process in the following section.

To increase the reliability of the estimated parameter set, two experimental chromatograms at different flow rates (0.5 ml/min and 1 ml/min) were fitted simultaneously. By carrying out this fitting, the adsorption equilibrium constant of mobile phase (H_{PM}) can be obtained, which cannot be obtained from the adsorption experiments only. All other parameters which have been already obtained in this study - adsorption equilibrium constants, H_{EtAc}, H_{PMA} and H_{EtOH}, porosity ε, mass transfer coefficients $k_{m,i}$, equilibrium constant K_{eq} were not fixed in the reactive chromatography model, but re-estimated from the reactive chromatograms through Tikhonov regularization. The regularization of these parameters was necessary to penalize large deviation from the batch experiment result and adsorption experiment results in Table 15.

Figure 44 shows the fitting of the models with the experimental chromatograms. As can be seen from the figure, the model fits the concentration profile reasonably well for both experiments. The concentration profiles of reactants, EtAc and PM, are plotted on the left y-axis while product concentration, PMA and EtOH, is shown on the right y-axis. The solid lines represent the concentration profiles from the model and markers represent the experimental data.

Table 16 shows the optimal model parameters as a result of the parameter estimation analysis. The values of all the estimated parameters were between their lower and upper bounds, which indicates that the optimized solution was not restricted by the bounds. It can be seen that the adsorption equilibrium constants are consistent with the values obtained from the pulse experiments shown in Table 15.

However, the fitted porosity is larger than its initial value from porosity measurement experiment. This discrepancy is because PEG6000 was used as a tracer for the experiment to measure the porosity; it measures the interparticle (interstitial) porosity $\varepsilon_{b,}$ while the porosity used in the model represents the total porosity, ε_{t}., i.e. both the interparticle and internal porosity. Our previous study also observed a larger value of the porosity compared to the one from the experiment using dextran (molecular weight approximately 250,000 g/mol) with Amberlyst^{TM} 15 [63]. It should also be noted that the concentration of the catalyst could not be measured, and the estimated values of Henry's constant H_{catalyst} and mass transfer coefficient k_{catalyst} may still be uncertain.

These model parameters, obtained by fitting experiments at the flow rates of 1 ml/min and 0.5 ml/min with the column length of 25 cm, were also validated against another experimental run. The model prediction was compared with the elution profiles of the experiment at increased column length, 50 cm, at the flow rate of 0.5 ml/min. The results are shown in Figure 45 and as can be seen from the figure, the model was able to predict the elution profiles of all components closely. From these observations, we believe that the parameter set shown in Figure 44 is reliable enough to be used for further optimization of SMBR.

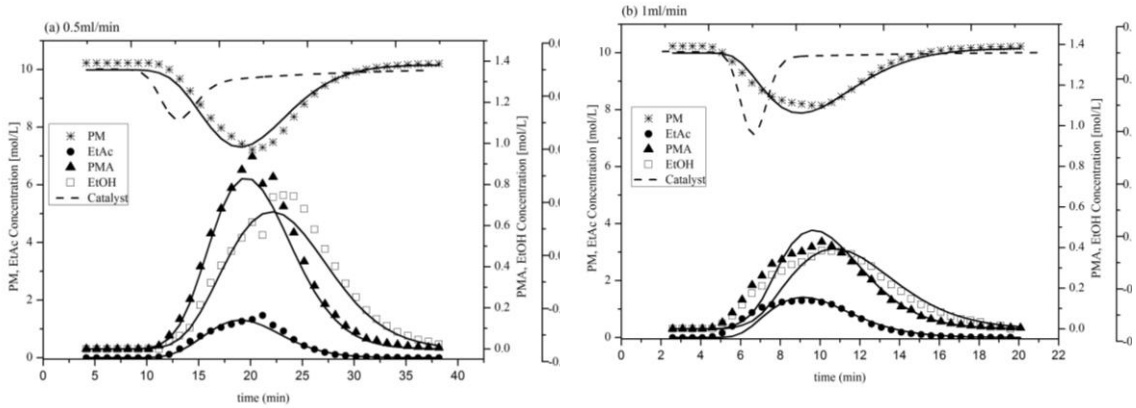

Figure 44 Model fitting results: comparison of the elution profiles predicted by the model and the experimental chromatograms obtained by injecting a pulse of ethyl acetate at 40°C and 1.7g/L catalyst concentration. (a) Flow rate: 0.5ml/min and (b) flow rate: 1ml/min

It should to be noted that the set of experiments for fitting was carefully selected so that they have different flow rates and column length. This is to confirm that the model is reliable for predicting results at different flow rates and switching times, which are the critical variables for SMBR optimization.

Table 16 Model parameters obtained by fitting the model to the two reactive chromatography experiments in Figure 44. The lower and upper bounds of the parameters that were imposed in the *fmincon* function are also listed.

Model Parameters	*Fitted Value*	*Initial value*	*Lower bound*	*Upper bound*
H_{EtAc}	0.5327	0.663	0.01	1
H_{PM}	0.5236	0.500	0.01	1
H_{PMA}	0.4983	0.412	0.01	1
H_{EtOH}	0.8926	0.948	0.01	1
$H_{Catalyst}$	0.4973	0.500	0.01	1
k_{EtAc} [min^{-1}]	1.6641	1.670	0.1	6
k_{PM} [min^{-1}]	1.2957	1.600	0.1	6
k_{PMA} [min^{-1}]	1.8736	1.957	0.1	6
k_{EtOH} [min^{-1}]	1.7001	2.098	0.1	6
$k_{catalyst}$ [min^{-1}]	0.1100	1.600	0.1	6
k_1 [$L^3/mol^2/min$]	0.5138	0.3841	0	0.1
K_{eq}	0.1379	0.120	0.01	1
D_{ax} [m^2/min]	0.5132×10^{-4}	0.1×10^{-4}	0.01	10
ε	0.4642	0.420	0.2	0.8

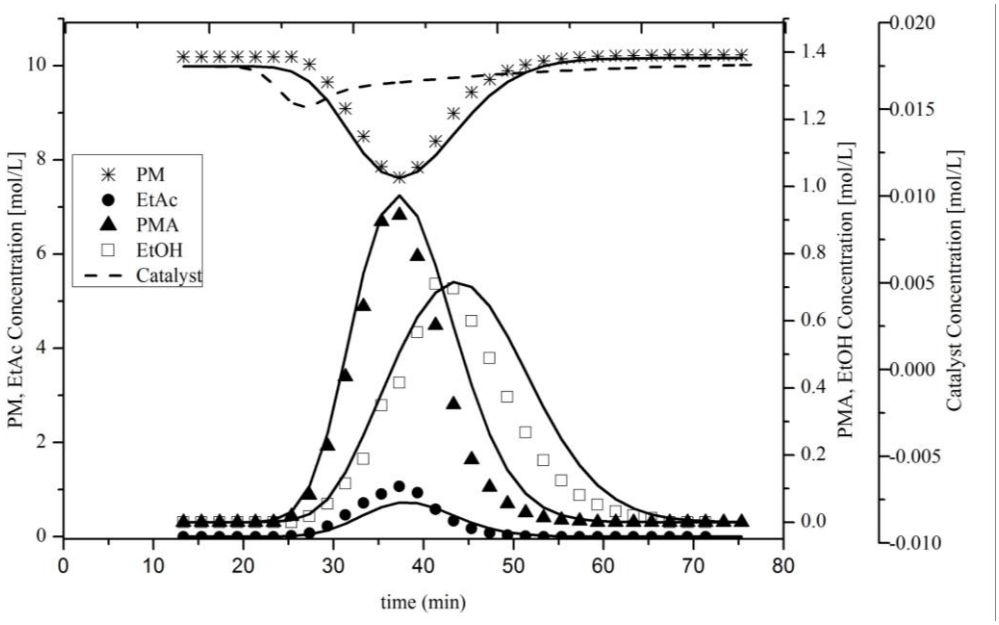

Figure 45 Comparison of the elution profiles predicted by the model and the experimental chromatogram obtained by injecting a pulse of 100% EtAc at 40°C, 1ml injection at 0.5ml/min flow rate, 1.7g/L catalyst concentration, using 50cm length column reactor.

7.4.2 SMBR Optimization

The multi-objective optimization problem of the SMBR in Section 4 is implemented in the AMPL modeling environment and solved using IPOPT solver. The specification of the SMBR columns used for optimization is given in Table 17.

Table 17 SMBR system details

Parameter	Value
N_{comp}	5
N_{Column}	4
Configuration	1-1-1-1
Column length (L)	0.5 m
Internal diameter (D)	0.015 m
U_L	0.0 m/h
U_U	10 m/h
C_{cat}	3.4g/L

The objectives for the optimization problem are i) to maximize the conversion of acetic acid and ii) to maximize the production rate of PMA in the raffinate outlet. The maximization problem of PMA production rate (Eq 13) was solved at four different

conversion constraints (ϕ); 0.7, 0.8, 0.9 and 0.95. Relatively high conversion values (ϕ) are chosen so that the advantage of SMBR process can be shown effectively compared to batch processes. Each optimal solution of this optimization problem lies on the Pareto front of the multi-objective problem (Figure 46).

Figure 46 shows the trade-off between the PMA production rates against the conversion of ethyl acetate. As can be seen from this figure, the production rate of PMA through the raffinate outlet decreases upon an increase in the conversion of ethyl acetate. A similar correlation of conversion and production rate has also been discussed in previous studies by Shan et al. and Agrawal et al. [9, 63]. To increase the conversion, the residence time must increase and thus flow rates decrease and switching time increases. This can be confirmed from Table 18 and Figure 47, flow rates decrease and switching time increases as conversion constrains are increased. Note that this trend was also observed from the single column experiment, where decrease of flow rate and increase of column length increased conversion (Figure 43). Table 18 also shows the feed concentrations in vol% of EtAc diluted in PM at different conversions. It can be seen that as a higher conversion is desired, concentration of ethyl acetate must be increased and flow rates must be decreased.

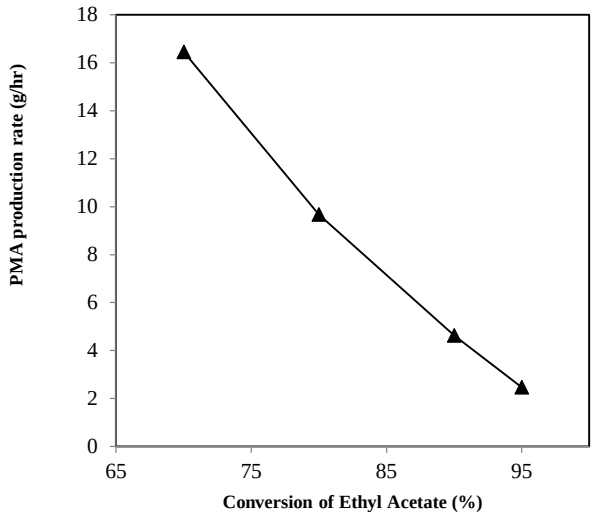

Figure 46 Pareto plot of the multi-objective SMBR optimization problem: PMA produced through the raffinate outlet in g/hr against the percentage conversion of ethyl acetate

Table 18 Optimal operating conditions for SMBR from the multi-objective optimization analysis for maximizing PMA production rate and ethyl acetate conversion.

Parameters	70% conversion	80% conversion	90% conversion	95% conversion
Desorbent flow rate [m/hr]	2.53	1.95	1.13	0.73
Extract flow rate [m/hr]	1.70	1.38	0.82	0.52
Feed flow rate [m/hr]	0.24	0.057	0.023	0.012
Raffinate Flow rate [m/hr]	1.09	0.63	0.34	0.22
Switch time [min]	5.93	7.62	11.82	16.90
EtAc concentration in Feed [vol%]	45.7	99	99	99

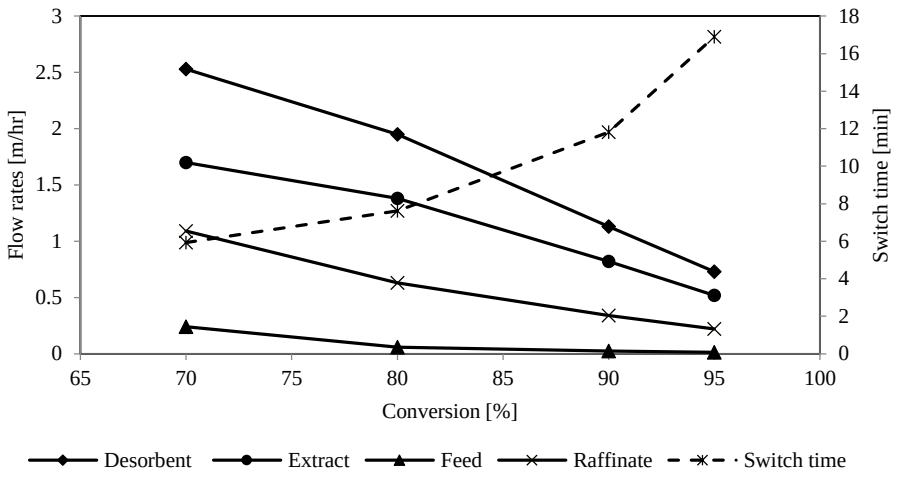

Figure 47 Plot of operating conditions against conversion

Figure 48 shows an internal concentration profile of SMBR simulation at 95% conversion of ethyl acetate. The figure plots the profile at 80 seconds after the beginning of the step (t/t_{step}=0.086) at the cyclic steady state. It can be seen that at the inlet of zone III, where feed of ethyl acetate is injected, we observe a sharp rise in the ethyl acetate concentration. The separation between the two products, PMA and ethanol, can be improved significantly compared to single column experiments. This enables us to obtain a more highly concentrated product of PMA in the raffinate stream, and a more highly concentrated ethanol in the extract stream. In addition, separation of products increased the conversion to the direction of further PMA production exceeding a thermodynamic equilibrium, reaching a significantly higher value of 95%.

The plot shows constant concentration profile of catalyst around 0.034 mol/L. The catalyst concentration fluctuates in less than 4% when there's inlet or outlet streams that dilute the catalyst. The plot also shows volume change inside the reactor that may have been caused by compositional change. The sum of the volume of all components is calculated based on the following equation.

$$\sum_{i=1}^{Ncomp} C_i u_i \quad (35)$$

where C_i is concentration of each component and u_i is molar volume of each component. As can be seen from the plot, this value stays almost constant at 1, with variation less than 3%. This justifies our assumption of constant volumetric flow rate inside a column from Equation 1.

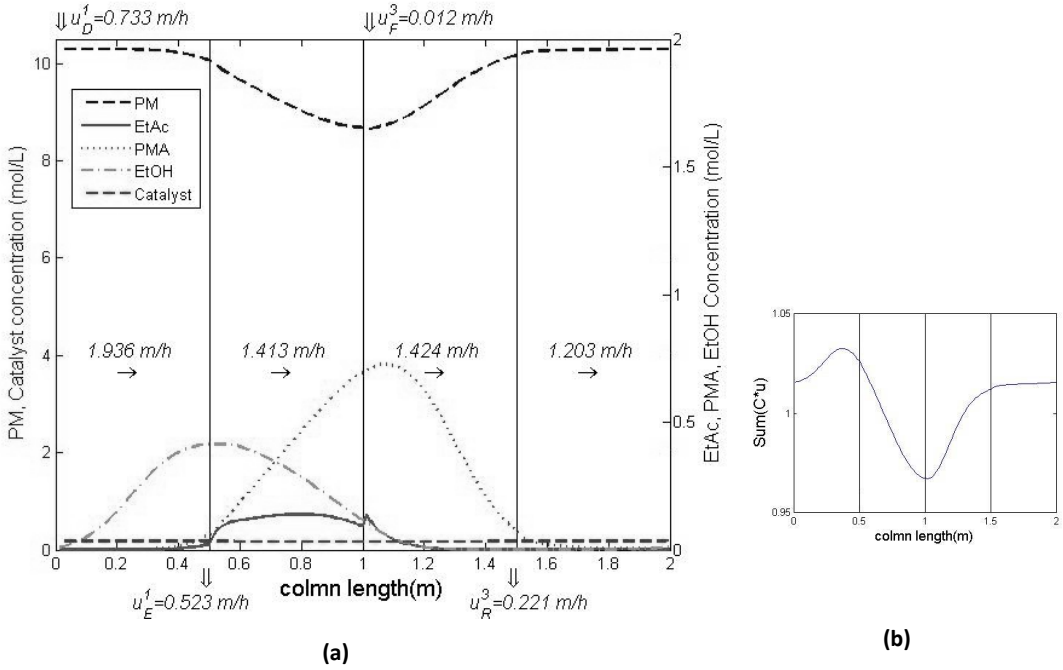

Figure 48 Internal concentration profiles inside the SMBR slightly after the beginning of the step (t/t_{step}=0.086), for 95% conversion of ethyl acetate. (a) Concentration profile of PM, EtAc, PMA, and EtOH (b) Value of Equation 19

7.5 Conclusion and future work

This chapter discussed the applicability of homogeneous catalysis of the transesterification of ethyl acetate with PM to reactive chromatography. The kinetics of transesterification was studied with a chromatographic reactor using a homogeneous catalyst. A mathematical model was developed from experimental chromatograms.

Furthermore, an SMBR process was designed using the model, which is expected to achieve a high conversion of 95%.

Batch reactor experiments were performed at different temperatures and catalyst concentrations. It was found that conversion was limited by equilibrium, and the final conversion in a batch reactor could not be improved significantly by increasing temperature. Adsorption constants were obtained by performing a pulse injection of each non-reacting component in a chromatographic column. Reactive chromatography experiments were performed using a chromatographic reactor by injecting ethyl acetate at different temperatures and residence times. The experiment demonstrated that reactive chromatography can be applied to the synthesis of PMA for the simultaneous reaction and separation of products.

A transport dispersive model with a linear driving force (LDF) for the adsorption rate was fitted to multiple pulse injection experiments and adsorption equilibrium and kinetic parameters are estimated. The LDF model with axial dispersion fitted the experimental chromatogram relatively well, and the model was validated by predicting the experiment at different conditions. To support the motivation of developing a continuous multi-column system, simulated SMBR operations were optimized using the model that was validated from single column experiments. In this analysis, a multi-objective optimization problem was formulated and the trade-off between the production rate of PMA and the conversion was analyzed. A high conversion of up to 95% was predicted through applying the SMBR system, which was not possible in batch reactors.

There are several questions which must be addressed before validating the model through SMBR experiment. There are drawbacks of using a homogeneous catalyst in

continuous systems. The solvent (PM) and catalyst (alkoxide) are very hygroscopic, and thus care must be taken when handling solvent storage at atmospheric condition. In addition, a separation unit is needed at the outlet of the reactor to separate the catalyst from the product stream. Since separation of homogeneous alkoxide catalyst is costly, an in-depth economic analysis may be required in the future.

Although the mathematical model developed described the experimental chromatograms relatively well, further improvements can be expected. In particular, isotherms of all components were assumed linear in our study, but validation of the appropriateness of linear isotherms instead of a full Langmuir isotherm at higher concentrations may be needed. Furthermore, the reaction kinetics may need to be modeled considering the non-ideal activities. Finally, the relationship between the reaction rate and catalyst concentration should be characterized through experiments at different catalyst concentrations and model fitting.

CHAPTER 8. HETEROGENEOUS TRANSESTERIFICATION WITH TYPE II RESIN FOR THE PRODUCTION OF PM

8.1 Motivation

In this chapter, Type II resin is studied for the transesterification reaction of PMA synthesis through chromatographic reactor. Figure 49 shows the chemical structure of Type II resins. Chapter 6 already discussed the advantages of transesterification over esterification. However, in Chapter 6, deactivation occurred with Type I anion exchange resin, which was used as a heterogeneous catalyst and resulted in loss of productivity. In this chapter, Type II resin is studied as a solution to the deactivation of Type I resin.

Type I anion exchange resins have trimethyl ammonium groups (Figure 49(a)) which impart higher basicity than Type II resins, thus more favorable in a variety of commercial use such as water treatment. In addition, Type I resins can be applied at higher temperatures [95]. However, the efficiency of regeneration of the resin to the hydroxide form is lower than that of Type II resins, particularly when the resin is saturated with monovalent anions, such as chloride and nitrate. This can be seen from Table **19** where selectivity coefficients of two types of resins are compared with various anions. Selectivity coefficients are a measurement of a reins' preference for an ion. Table 19 shows that Type I resins have higher selectivity to acetate ion (with selectivity coefficients of 3.2) than hydroxyl ion (selectivity coefficient 1.0). This accounts for the rapid deactivation of Type I resin in transesterification in Chapter 6, where acetate ions are formed inside the reactor as a result of ionization of acetic acid with cations.

Type II anion exchange resins have dimethylethanolamine groups (Figure 49) which impart slightly lower basicity than Type I resins. However, the resin has a higher

affinity to hydroxyl ion over acetate as can be seen from Table 19 where the selectivity coefficient for acetate vs. hydroxyl ion is 0.5. Even though the Type II resins have lower basicity than Type I, chemical stability of resin in the hydroxyl form is extremely important when acetate ion is expected to be present in the column throughout the process. Since Type II resin has higher affinity to hydroxyl ion over acetate ion, it is expected to maintain the activity for longer process time without deactivation when applied to transesterification for PMA synthesis.

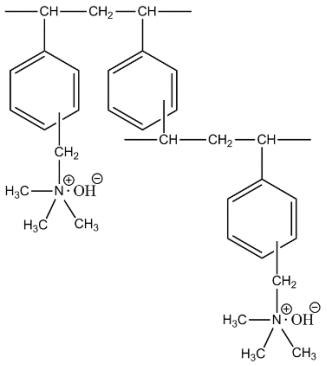

(a) Chemical structure of Type I anion exchange resin

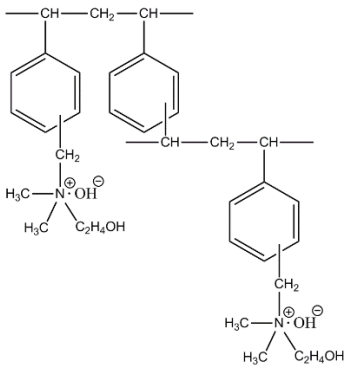

(b) Chemical structure of Type II anion exchange resin

Figure 49 Chemical structures of anion exchange resins

In this Chapter, we demonstrate the applicability of Type II resins to the reactive chromatography for the PMA production. To analyze the stability of a resin, an accelerated deactivation test was performed. In addition, reactive chromatography experiments are performed with the selected resin at similar conditions as in Chapter 6. At the end, results of reactions with Type II resins are compared to the results of Type I resin from Chapter 6.

8.2 Materials and Methods

8.2.1 Materials

PM (1-methoxy-2-propanol, > 99%), PMA (propylene glycol methyl ether acetate, > 99%) and ethyl acetate (HPLC grade, 99.5+%) were purchased from Alfa Aesar, and ethanol (anhydrous, 99.5+%) was purchased from Acros Organics. All of chemicals were used without further purification.

Properties of anion exchange resins considered in this chapter are summarized in Table 20. Diaion PA418 was purchased from Alfa Aesar in the Cl^- form. Dowex^{TM} 22 was purchased from The Dow Chemical Company in the OH^- form. Diaion PA418 in Cl^- form was converted to OH^- form by flushing the resin with 12BV of a 5wt% NaOH solution at 0.1BV/min, and then with 18BV (bed volumes) of DI water at 0.1 BV/min.

8.2.2 Experimental methods

The experimental procedures explained in Chapter 3 are followed for single chromatographic reactor experiments. For accelerated deactivation tests, procedures explained in Chapter 6.3.7 are followed.

Table 19 selectivity Coefficients of Various Anions (Compared with the Hydroxyl Ion) on Functionalized Styrene-Divinylbenzene Anion Exchange Resins of Different Base Strength [95]

Ion	Type I	Type II
OH^-	1.0	1.0
Benzene Sulphonate	500	75
Salicylate	450	65
Citrate	220	23
I^-	175	17
Phenate	110	27
HSO_4^-	85	15
ClO_3^-	74	12
NO_3^-	65	8
Br^-	50	6
CN^-	28	3
HSO_3^-	27	3
BrO_3^-	27	3
NO_2^-	24	3
Cl^-	22	2.3
HCO_3^-	6.0	1.2
IO_3^-	5.5	0.5
Formate	4.6	0.5
Acetate	3.2	0.5
Propionate	2.6	0.3
F^-	1.6	0.3
$HSiO_{3-}$	< 1.0	< 1.0
$H2PO_{4-}$	5.0	0.5

Table 20 Properties of anion exchange resins that are used in Chapter 8

	PA 418	**Dowex 22**
Type	Type II anion exchange resin	Type II anion exchange resin
Matrix	Styrene-DVB Macroporous	Styrene-DVB Macroporous
Total exchange capacity (meq/mL)	1.3	1.2
Size (um)	300-1180	300-1200
Max operating temp (°C) in OH^-	40	46
Total exchange capacity (meq/ml) in OH from	1.3 (salt splitting capacity)	1.2

8.3 Results and Discussions

8.3.1 Accelerated deactivation test

To verify the chemical stability of Type II resins in the hydroxyl form over acetate ion, two Type II resins are tested for the accelerated deactivation following the procedure explained in Chapter 6.3.7. Figure 50 shows the results of the deactivation test of two Type II resins: Dowex 22 and PA418, and a Type I resin: IRA904OH^-. The result of Type I resin is excerpted from Chapter 6. All of the experiments are performed by injecting PM and EtAc into each column at a same flow rate, so that the inlet mixture has concentration of 50/50 vol% of EtAc/PM.

In Figure 50, the PMA concentration at the outlet of the column is plotted against the amount of EtAc flown through the column. Both Type II resins show significantly better activation stability compared to the IRA 904 OH^-, Type I resin. The final data point corresponds to about 600 ml of EtAc and is equivalent to 48 column volumes. Up until this point, among the two Type II resins, Dowex 22 shows a higher conversion by approximately 1% point as can be seen from Figure 1. Thus, Dowex 22 is selected for the following reactive chromatography experiments.

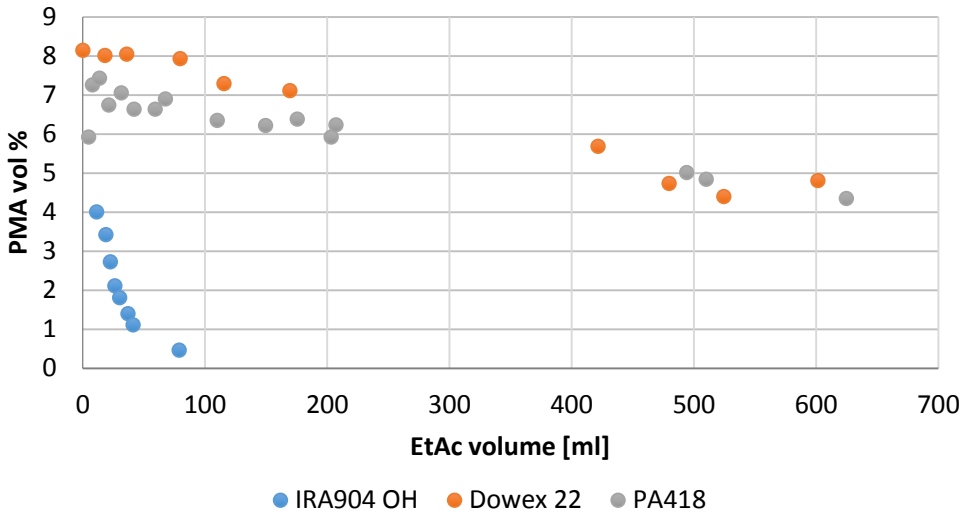

Figure 50 Deactivation test result of IRA904 OH^- (Type I), Dowex 22(Type II) and PA 418 (Type II). PM and EtAc are injected into each column at a same flow rate, and PMA concentration at the outlet of the column is plotted.

8.3.2 Adsorption experiment

To study the selectivity of the resin, an adsorption experiment is performed with a stainless steel column of internal diameter of 0.8 cm and length of 25 cm packed with Dowex 22. While PM is supplied at the flow rate of 0.5ml/min, a feed mixture of 100 µL that consists of PMA and EtOH at different concentrations are injected into the column. Samples that are below 100% concentrations are diluted with PM, the mobile phase.

Figure 51 shows resulting chromatograms. As can be seen from PMA peaks, retention time of each peaks are still constant at different concentrations. Same results are obtained from EtOH injections. However, both peaks are rather asymmetric, which indicates that the nonlinear equilibrium model should be adequate. The difference in retention times of PMA and EtOH shows good separation between the two products, which is important for reactive chromatography to achieve a high conversion.

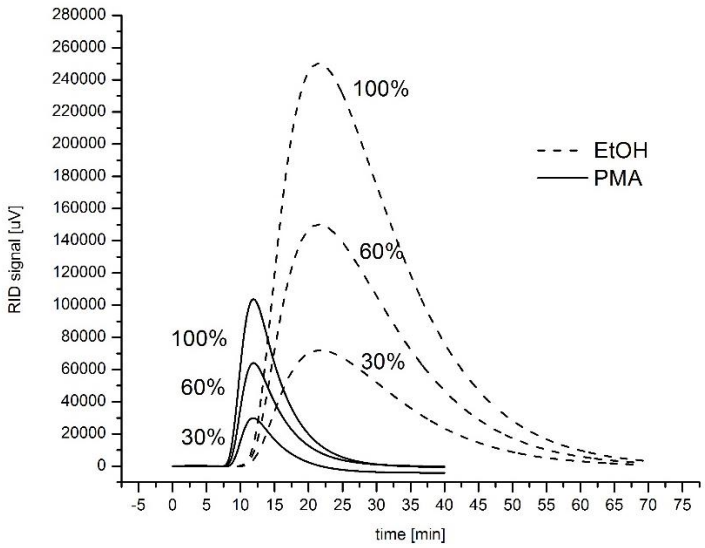

Figure 51 Elution profiles for various injection concentrations of EtOH and PMA (flow rate = 0.5ml/min, injection volume = 100μL).

8.3.3 Reactive chromatography experiments

8.3.3.1 Effect of residence time

To study the effect of residence time on reactive chromatography, experiments are performed at two different flow rates, and two different column lengths. Figure 52 shows the result of three experiments, where Figure 52(a) is the result of injecting 1 ml of 100% EtAc into the column while PM flows at 0.5 ml/min and (b) is injecting the same amount of EtAc while the flow rate is increased to 1 ml/min. Conversions are calculated based on the area under the peak of unreacted EtAc and plotted in Figure 53. The conversions are significantly increased from 48% to 62% when flow rates are decreased. This increase is due to an increased contact time of reactants with catalyst. A similar result is observed in work described in previous chapters.

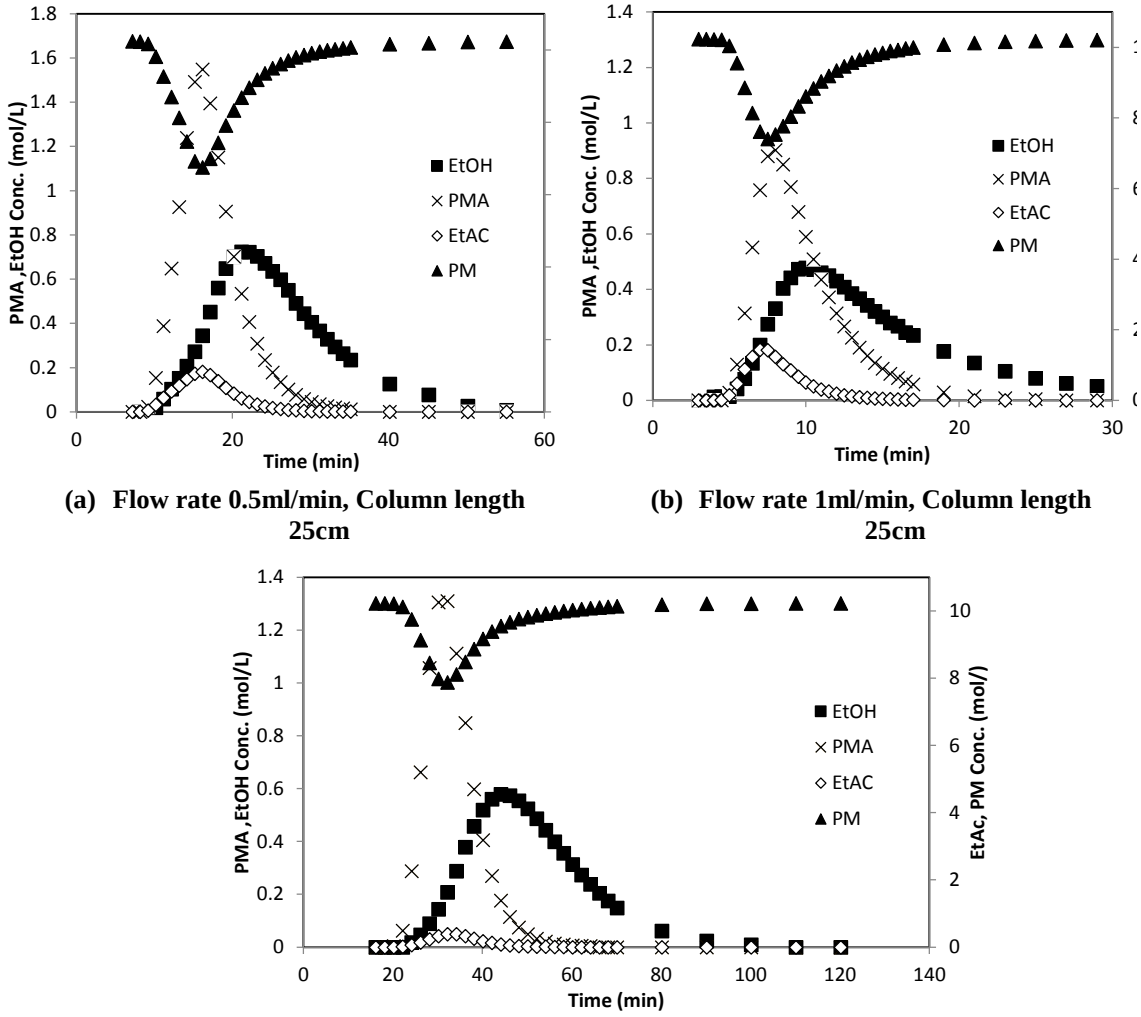

(a) Flow rate 0.5ml/min, Column length 25cm

(b) Flow rate 1ml/min, Column length 25cm

(c) Flow rate 0.5ml/min, Column length 50cm

Figure 52 Elution profiles for injection of 1ml 100% EtAc into a column packed with Dowex 22 at 40°C while varying the flow rates and column length

Figure 52(c) shows the result of injecting the same amount of EtAc while the length of the column is increased to 50 cm from 25 cm. The flow rate is set to 0.5 ml/min. Based on the amount of unreacted EtAc, the conversion is increased with the increase of column length. Again, the conversion increase is caused by the increase of the contact time. Figure 53 shows that the conversion is significantly affected by the residence time of reactants inside the column.

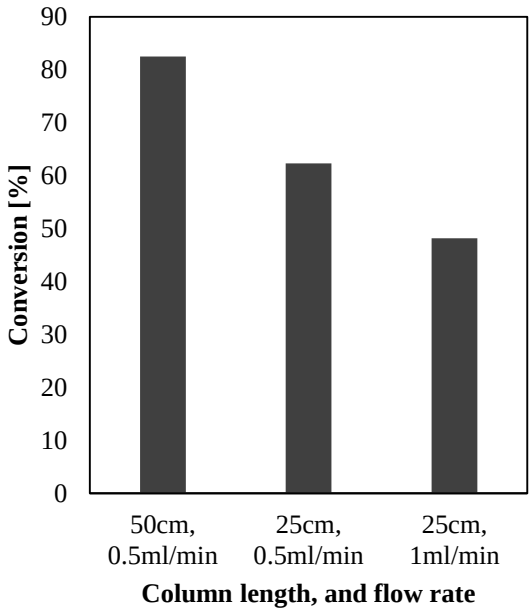

Figure 53: Conversion of EtAc from experiments performed at different column lengths (25 cm, 50 cm) and flow rates (0.5 ml/min, 1 ml/min)

8.3.3.2 Effect of feed condition

To study the effect of injection feed volume and concentration, experiments are performed at different conditions. Figure 54 (a) and (b) show experiments performed at different feed injection volume, of 500 μL and 1 ml. Conversion increases when a smaller volume of reactant is injected. This is mainly because a smaller amount of limiting reactant is present inside the reactor. Figure 54 (b) and (c) show the effect of feed concentration, where 50% and 100% EtAc are injected into the reactor. Again, when a smaller amount of limiting reactant is injected, higher conversion is achieved. All of the Figures show that the feed volume or concentration does not affect the selectivity or separation of products.

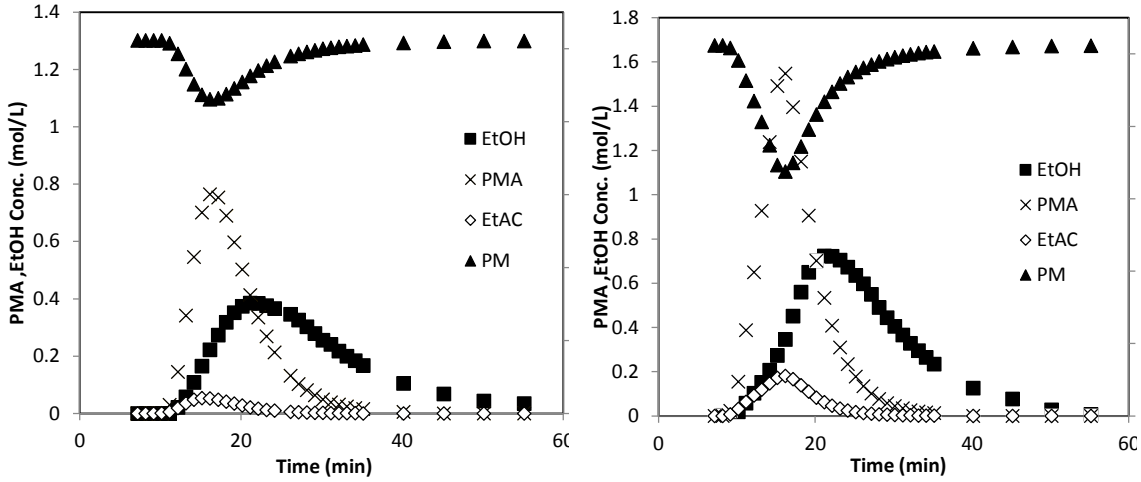

(a) 100% 0.5 ml **(b) 100% 1 ml**

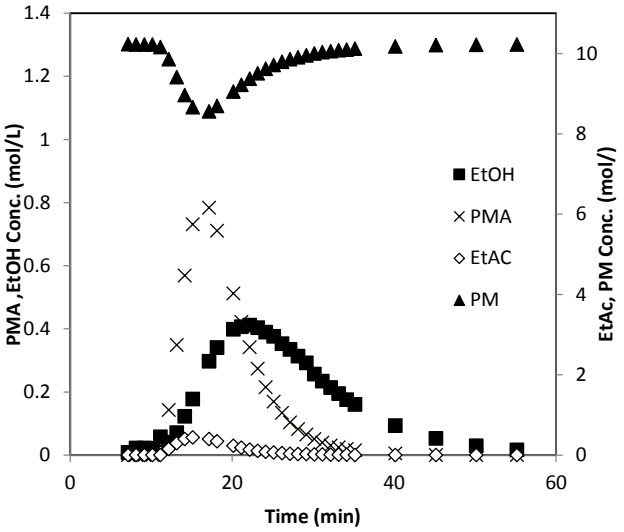

(c) 50% 1 ml

Figure 54: Elution profile of EtAc injection into a column with 25 cm length while PM flows at 0.5 ml/min at 40°C at different feed volume and concentration

8.3.4. Comparison with transesterification with different catalyst

It is important to compare the transesterification result with Type II catalyst from this Chapter with results from previous Chapters, where different types of catalysts are used. Chapter 6 used Type I anion exchange resin, IRA904 OH^- as a heterogeneous catalyst. Chapter 7 used sodium alkoxide as a homogeneous catalyst while IRA904 Cl^- was used as an adsorbent. Since all of the system produce the same product, PMA through the same

transesterification reaction, comparison of all of these results will give a valuable insight into what type of catalysts are most suitable for such a reaction.

Figure 55 shows the result of all three experiments performed at 40°C, injecting 100% 1 ml EtAc into a column of the internal diameter of 0.8 cm and length of 25 cm while PM is supplied at 0.5 ml/min. Figure 55(a) is the result of using IRA904 OH^-, a Type I resin as a heterogeneous catalyst. Two product peaks have good separation and conversion is relatively high as shown in Table 21. However, as mentioned in Chapter 6, rapid deactivation of catalyst is observed and concluded to be not suitable for continuous systems. Figure 55(b) shows the result of using sodium alkoxide as a homogeneous catalyst while IRA 904Cl^- is used as an adsorbent. Two product peaks have the least amount of separation when IRA904Cl^- is used as shown in Table 21. Conversion is also the lowest among the three systems. Figure 6(c) shows the result from this Chapter, where Dowex 22 Type II resin is used as a heterogeneous catalyst. The long tail of the EtOH peak may lower the productivity of chromatographic reactor. However, the conversion is the highest among all three systems, and separation between the two products are also very effective as can be seen from Table 21. In addition, use of heterogeneous catalyst has many advantages over homogeneous catalyst such as ease of catalyst separation. Thus, we believe Dowex 22 Type II catalyst is the most promising catalyst for the PMA production through transesterification.

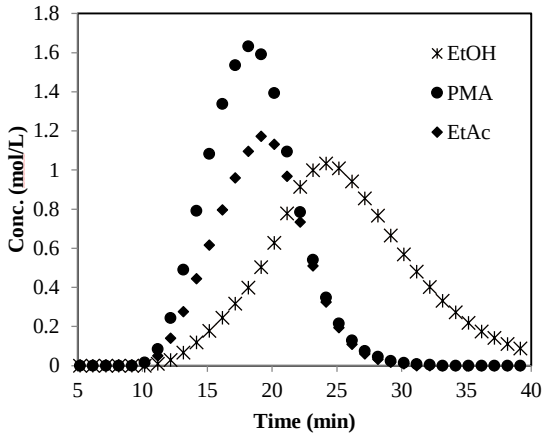

(**a) Result from Chapter 6, use of IRA904 OH^- (Type I resin) as a heterogeneous catalyst (conversion 65%)**

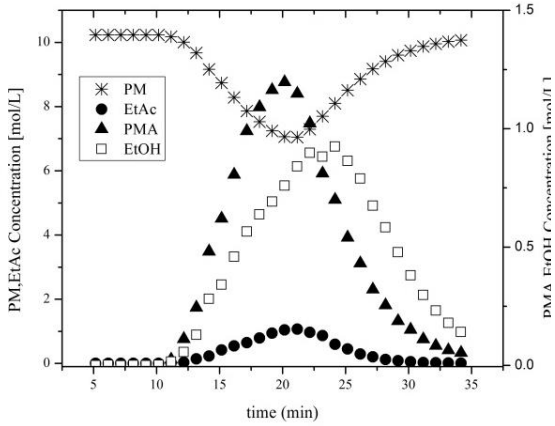

(b) Result from Chapter 7, use of sodium alkoxide as a homogeneous catalyst, 3.4g/L (conversion 52%)

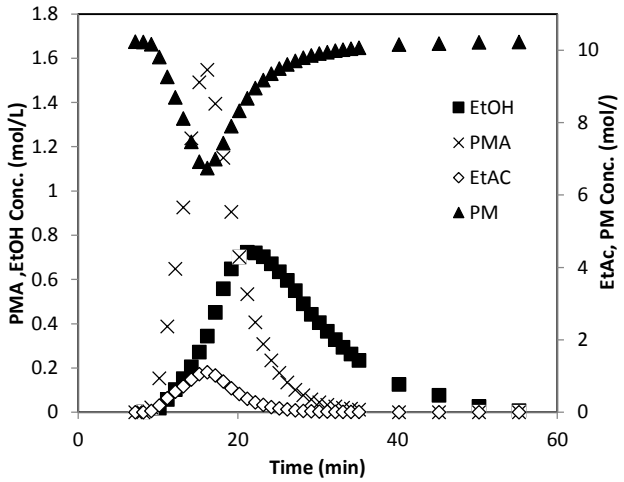

(c) Result from Chapter 8, use of Dowex 22 (Type II resin) as a heterogeneous catalyst (conversion 63%)

Figure 55 Injection of 100% 1ml EtAc at 40°C while PM flows at 0.5ml/min into columns packed with different adsorbent and catalyst (a) IRA 904OH^- (b) Sodium alkoxide (c) Dowex 22

Table 21 Conversion and retention time of PMA and EtOH of transesterification experiments with different catalysts. Injection of 100% 1ml EtAc at 40°C while PM flows at 0.5ml/min.

Catalyst	Conversion [%]	PMA retention time [min]	EtOH retention time [min]
Type I anion exchange resin (IRA 094 OH^-)	65	18.1	24.2
Homogeneous catalyst (Sodium alkoxide)	52	21.1	23.1
Type II anion exchange resin (Dowex 22)	63	16.1	21.1

8.4 Conclusion and future study

In this Chapter, a Type II resin is applied successfully to a reactive chromatography system to produce PMA through transesterification of EtAc and PM. To investigate the chemical stability of a Type II resin over a Type I resin, an accelerated deactivation test is performed. The stability test showed that the Type II resin has a higher stability compared to Type I resin while acetate ions are present in the system. This indicates that Type II resin is more suitable for a transesterification reaction that produces PMA where acetate ions are formed as a result of side reactions.

Using the Type II anion exchange resin selected in this chapter, Dowex 22, the selectivity is tested by injecting PMA and EtOH separately into the column packed with the catalyst. The result shows a good separation between the two products, while the long tail of the EtOH and PMA peak may lower the productivity of the process.

Reactive chromatographic experiments are performed at different residence times and feed conditions. Increasing the residence time by decreasing the flow rate or by increasing the column length result in higher conversion values. This is due to the increased contact time between the catalyst and reactants, and similar results are obtained also from previous chapters. Feed concentration and injection volume are varied. The data showed that when the amount of limiting reactant is decreased, the conversion is increased as expected from equilibrium.

Finally, transesterifications inside reactive chromatography with different catalysts are compared in terms of separation and conversion. The experiment with Type I catalyst shows the highest conversion, but deactivation of catalyst is considered a significant drawback if employed in a continuous system. The experiment with a homogeneous

catalyst shows a low conversion and poorer separation of two products compared to other systems with heterogeneous catalysts. Thus, we believe Type II catalyst is the most promising catalyst for transesterification in reactive chromatography, where the conversion is high and separation between the two products is efficient enough. In addition, Type II resin shows higher chemical stability than Type I resin, which will be beneficial for designing a continuous system such as SMBR.

A future study would include obtaining a model parameters of Type II resin catalyzed transesterification. Based on the asymmetry of EtOH and PMA peak, a nonlinear isotherm should be applied. Furthermore, design and optimization of SMBR using the model is desired to analyze the conversion and productivity. Finally, experimental validation of SMBR model also remains as a future work.

CHAPTER 9. CONCLUSIONS AND FUTURE WORK

9.1 Conclusions

The results presented in this thesis have met the three main objectives stated in Chapter 2:

1. Apply esterification for the development of SMBR with a cation exchange resin to produce PMA
2. Verify the potential of transesterification to be applied to SMBR for the production of PMA
3. Identify alternative solutions to improve SMBR for the production of PMA: Homogeneous catalysis system and Type II resin

The first objective is discussed in detail in Chapter 5, where esterification reaction is studied to produce PMA through a reactive chromatography system. A cation exchange resin, Amberlyst 15, is used as a catalyst that also functions as an adsorbent. Before conducting the reaction via reactive chromatography, a simple well-stirred batch reactor experiment is performed to study the significance of external and internal mass transfer resistance, effect of catalyst loading, effect of initial molar ratio, and temperature. The resulting data is fitted to a pseudo-homogeneous kinetic model and the reaction rate constant is obtained as a result. Once preliminary experiments with a well-stirred batch reactor are completed, experiments using chromatographic reactor are performed. The first step is injecting single components into the column separately and obtain adsorption parameters without the influence of reaction. The second step is to inject reaction mixture into the column at different conditions such as feed concentration, flow rate, injection volume, and temperature. The resulting chromatograms are fitted to the model, and all parameters including adsorption parameters and reaction kinetic constants are obtained.

Using the set of parameters, SMBR, the continuous reactive chromatography system, is optimized to achieve higher conversions of up to 95%.

This case study shows that PMA can be synthesized through reactive chromatography, while reaching a high conversion that exceeds equilibrium by continuous separation of products from the reaction mixture. In addition, this chapter shows that when the single column system is further improved to SMBR, such a high conversion can be achieved while continuous collection of products at a high purity is realized. This study shows a systematic procedure for applying a reaction to the reactive chromatography system where kinetics had not been well-studied. This study successfully shows that the model developed in this study is suitable for the selected system, and shows potential for application of SMBR for industrial applications.

The second objective is discussed in Chapter 6, where a transesterification reaction is studied for the application of the reactive chromatography for the production of PMA. This chapter's work represents one of the first attempts to apply transesterification to reactive chromatography outside of biodiesel production. Due to the high level of originality, thorough screening of anion exchange resins has to be performed to select a suitable resin. Based on the swelling ratio of the resin bed, IRA904 is used for the catalyst and the adsorbent. Similar experiments to the ones for esterification in Chapter 5 are performed for transesterification. Well-stirred batch reactor experiments are performed to study the reaction kinetics. Then, each component is injected into a column packed with IRA904 OH^- and adsorption is studied. Finally, a reaction mixture is injected into a column and a set of parameters is obtained for the reactive chromatography model. When the experiment results are compared to that of the esterification from Chapter 5, the

transesterification has a higher conversion of 80% at a low temperature of 60°C. In addition, the byproduct, EtOH, elutes off the column faster than the byproduct of esterification, which is water. This improves the productivity of the system since the process time can be decreased to wash out the byproduct. However, it has been found that IRA904OH^- deactivates in terms of a process running time. Even a very small amount of water (< 0.005 vol%) present in the mobile phase goes through a reaction with EtAc and the resulting acid deactivates the basic site of resin. As a result, IRA904OH^- is concluded to be not a suitable resin for the production of PMA. Thus, no further optimization of SMBR is performed, since alternative solution to the problem found in this Chapter is presented in Chapter 7 and 8.

The last objective is discussed in Chapter 7 and 8, where an alternative solution to the Type I anion exchange resin is given. Even though in Chapter 6 transesterification was found to have a higher conversion at the same temperature compared to the esterification, we conclude that the anion exchange resin is not suitable for PMA production due to the deactivation. As a solution to a such problem, Chapter 7 studies the homogeneous catalyst for the transesterification. Sodium alkoxide is studied as the homogeneous catalyst in a well-stirred batch reactor in terms of effect on temperature and on catalyst concentration. For an application to reactive chromatography, the anion exchange resin from Chapter 6, IRA904, is used as an adsorbent in a different ionic form, which is Cl^-. The catalyst is injected into the system while dissolved in the mobile phase. The reaction model is modified to include the concentration of catalyst. The chromatogram of each component is fitted to the model and a set of parameters is obtained. The parameters are used to optimize the SMBR process, where homogeneous catalyst is injected through the feed and desorbent

streams. The result of SMBR optimization shows that the process can achieve a high conversion of 95% with continuous collection of products at high purities. The work from Chapter 7 shows the first successful study of applying a homogeneous transesterification to reactive chromatography. The result shows high conversion and purity of products, which demonstrates the practicality of the process for PMA production. However, one has to account for separation of homogeneous catalyst from the product stream, which will require an in-depth economic analysis before drawing conclusions.

Chapter 8 discusses another approach to the transesterification by using Type II resin. A type II resin is an anion exchange resin that has dimethylethanolamine groups, compared to trimethyl ammonium groups of Type I resin used in Chapter 6. Type I resin is more commonly used in previous studies since it has higher basicity. However, in this application of PMA production, the chemical stability of the resin in presence of acetate ion, is a crucial factor for maintaining stability. Type II resin has higher affinity to the hydroxide ion compared to an acetate ion, and is expected to have higher stability in the current system. The stability test confirms that Dowex 22 has significantly higher stability and conversion compared to Type I resin. A column packed with Dowex 22 is used for testing adsorption, and it shows efficient separation between the two products. Reactive chromatography experiments show that Dowex 22 gives the highest conversion among all types of transesterification experiments performed in the previous Chapter 6 and 7. The peak of the byproducte EtOH has a long tail, which will affect the productivity of the system, and more detailed analysis is needed to draw a conclusion.

All contributions in this work demonstrate that reactive chromatography can be potentially applied to produce PMA. The study also shows that such application

significantly increases conversion and productivity of reversible and equilibrium- limited reactions. In addition, techniques and approaches described in this study are not confined to production of PMA but can be widely applied to designing a reactive chromatography process for any reversible reaction whose kinetics are unknown. Finally, this work also leads to some recommendations that could be followed up in future work, discussed in the next section.

9.2 Future Work

After performing the work in this thesis, there are some recommendations for future research projects.

9.2.1 Extension of Type II study

Chapter 8 discusses applicability of Type II resin to reactive chromatography and successfully shows advantages of Type II resin over other types of transesterification catalysts. This study can further be extended to obtaining model parameters through fitting the model to the current experimental results as shown in Chapter 5-7. Based on the comparison of conversion and separation performance to different systems of homogeneous and Type I resin, Type II resin shows more promising results. This provides enough motivation to develop an SMBR model and optimize the SMBR process using Type II resin. The optimization results can be compared to those of homogeneous transesterification and esterification. This comparison will provide a valuable insight of which reaction and what type of catalyst is most suitable for the production of PMA through SMBR. There are a lot of previous studies where different types of heterogeneous or homogeneous catalysts are compared for certain reactions. Nevertheless, comparison of

different reaction in addition to different types of catalyst will be a valuable data for designing a SMBR for production of esters in the future.

9.2.2 Experimental validation of SMBR optimization result

The objective of this thesis is to show the applicability of reactive chromatography to PMA production. Thus, many chapters conclude the work after the optimization of SMBR and no experimental result of SMBR is shown. Only the work from Chapter 5 has been extended to validating the model by performing SMBR experiment by another group member [63]. On the other hand, transesterification is studied in many directions with different catalysts in Chapter 6-8, and thus, the details of experimental verification have not been decided. Once Type II resin from Chapter 8 is studied more thoroughly and parameters are obtained, SMBR optimization can be performed. Then based on the SMBR optimization result of homogeneous catalyst (Chapter 7) and Type II resin, conclusion can be drawn which catalyst is most suitable for transesterification. The result can be homogeneous catalyst or Type II heterogeneous catalyst, but regardless of the result, experimental validation of model is extremely important to show the accuracy of the model that is used for optimization and simulation of SMBR. Furthermore, additional model refinement can be performed based on the result from the experiment.

9.2.3 Extension of SMBR to advance operations

The SMBR operation can be further extended to some of the advanced operating strategies that are discussed below.

9.2.3.1 ModiCon strategy

In this study, we restricted our investigations to a strategy where conditions of all inlet streams of SMBR remain constant within a step time. However, change of feed

concentration within the step time can be allowed, which is an operation called ModiCon. Such an operation is first proposed by Schramm et al. for the separation of binary mixtures [27]. Figure 56 shows the variation of acetic acid concentration in the feed which is studied by Gaurav et al. for the production of PMA through esterification [9]. Agrawal et al. shows that by varying the inlet concentration of SMBR, a higher PMA production rate is achieved with increased product recovery rate and purity [9]. Such modulation of inlet feed concentration improves the process performance by overcoming the separation limitation of the internal concentration profiles inside the SMBR [27].

In a similar way, ModiCon can be applied to transesterification where the concentration of EtAc varies within the step time. It has the potential to improve the performance further, and a similar case study of esterification has shown improved performance, which provides good motivation [63].

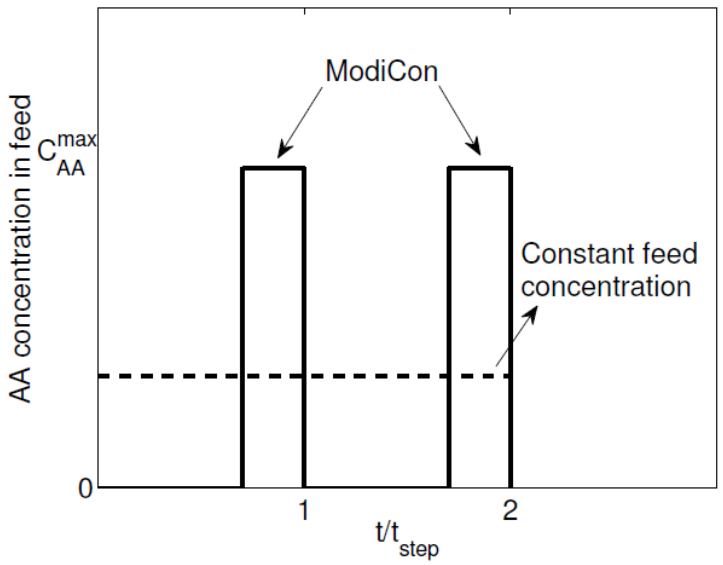

Figure 56 Variation of the inlet feed concentration [9] (1) constant feed concentration strategy (dotted) (2) ModiCon strategy (solid)

9.2.3.2 Superstructure formulation

In addition to allowing the variance of the feed stream condition, the position of the inlet and outlet streams can be varied and optimized, which operation can be explained as superstructure, proposed by Kawajiri and Biegler [96]. In the superstructure approach, numerous SMBR configurations can be incorporated into a single formulation and the optimizer extracts the best design that optimizes the SMBR process which meeting all the process and product specifications at the same time. Previous studies have already shown the advantages of superstructure over standard SMB or SMBR for binary or ternary mixture separations [39, 96]. The future study will include extending the optimization of SMBR for PMA production to superstructure which has potential for improved operation result.

9.2.4 Model refinement

Although the mathematical model developed in this study describes the experimental chromatograms relatively well, further improvements can be expected.

9.2.4.1 Kinetic model refinement

The study assumed pseudo-homogeneous reaction kinetic model for both esterification and transesterification for heterogeneously catalyzed systems. However, more thorough analysis of reaction kinetics can be performed and consider other types of reaction mechanisms such as Langmuir-Hinshelwood or Eley-Rideal mechanisms. There are numerous studies which only focus on finding the suitable mechanism for heterogeneously catalyzed reaction. Based on the rate-determining step, there can be 12 different equations that describe the reaction mechanism. Such analysis is out of scope of this study, and the assumption of pseudo-homogeneous model is made throughout the

thesis. However, to improve the model with accurate description of reaction mechanism on the model, such an analysis should be performed.

9.2.4.2 Nonlinear adsorption isotherm

Throughout the thesis, a linear isotherm model has been used to describe the equilibrium between liquid and solid phase. However, as discussed in Chapter 4, the linearity assumption holds only at the relatively low concentrations of components, which is valid in the single column experiments in this study. However, the nonlinearity in the system becomes significant when the chromatographic system is overloaded either in terms of concentration or volume compared to the exchange capacity of the resin. Such high concentrations are more likely to occur inside the SMBR compared to the single column experiments, since a continuous flow of reactant is injected into SMBR columns. In such an operation, nonlinear models are necessary such as Langmuir, bi-Langmuir, or competitive isotherms. Thus, while utilizing the parameters obtained from single column experiments as a starting point for both SMBR parameter optimization and SMBR experimental conditions, further nonlinear model parameter estimation should be performed using the SMBR experimental data.

9.2.4.3 SMBR model refinement

As explained in Chapter 4, liquid phase mass balance equation assumes constant velocity within the column. However, as discussed in Chapter 8, 3% fluctuation of volume has been observed from the simulation result. To describe the process result more accurately, the variation of velocity within the column should be accounted in the model by containing the *du/dx* term in the liquid phase mass balance equation. In addition, the injection of the feed should be performed carefully to maintain a rectangular pule, while

suppressing the viscous fingering, or the model can be modified to describe an imperfect rectangular pulse.

REFERENCES

[1] A.E. Rodrigues, C.S.M. Pereira, J.C. Santos, Chromatographic Reactors, Chem Eng Technol, 35 (2012) 1171-1183.

[2] A.A. Backhaus, Continuous process for the manufacture of esters, in, Google Patents, 1921.

[3] A. Sy, L. Smith, J. Chen, F.M. Dautzenberg, Catalytic distillation route for cumene, in: DeWitt Petrochemical Review, Houston, 1993.

[4] K. Rock, G.R. Gildert, T. McGuirk, Catalytic distillation extends its reach, Chem Eng-New York, 104 (1997) 78-&.

[5] D. Hearn, H.M. Putman, Hydrodesulfurization process utilizing a distillation column reactor, in, 1998.

[6] F.M. Dautzenberg, M. Mukherjee, Process intensification using multifunctional reactors, Chem Eng Sci, 56 (2001) 251-267.

[7] W.J. Koros, Y.H. Ma, T. Shimidzu, Terminology for membranes and membrane processes, Pure Appl Chem, 68 (1996) 1479-1489.

[8] F. Gallucci, A. Basile, F.I. Hai, Introduction- A review of membrane reactors in: Membranes for membrane reactors: preparation, optimization and selection, John Wiley & sons., United Kingdom, 2011.

[9] G. Agrawal, J. Oh, B. Sreedhar, S. Tie, M.E. Donaldson, T.C. Frank, A.K. Schultz, A.S. Bommarius, Y. Kawajiri, Optimization of reactive simulated moving bed systems with modulation of feed concentration for production of glycol ether ester, J Chromatogr A, 1360 (2014) 196-208.

[10] H. Schmidt-Traub, Preparative Chromatography of Fine Chemicals and Pharmaceutical Agents Preface, Preparative Chromatography of Fine Chemicals and Pharmaceutical Agents, (2006) Xiii-+.

[11] M.R. Altiokka, A. Citak, Kinetics study of esterification of acetic acid with isobutanol in the presence of amberlite catalyst, Appl Catal a-Gen, 239 (2003) 141-148.

[12] C.S.M. Pereira, M. Zabka, V.M.T.M. Silva, A.E. Rodrigues, A novel process for the ethyl lactate synthesis in a simulated moving bed reactor (SMBR), Chem Eng Sci, 64 (2009) 3301-3310.

[13] J.J. McKetta, Encyclopedia of Chemical Processing and Design, in, Marcel Dekker, New York, 1983.

[14] J. Oh, G. Agrawal, B. Sreedhar, M.E. Donaldson, A.K. Schultz, T.C. Frank, A.S. Bommarius, Y. Kawajiri, Conversion improvement for catalytic synthesis of propylene glycol methyl ether acetate by reactive chromatography: Experiments and parameter estimation, Chem Eng J, 259 (2015) 397-409.

[15] Propylene Glycol Ethers, in: SIDS Initial Assessment Report for SIAM 17, Arona, Italy, 2003.

[16] C.T. Hsieh, M.J. Lee, H.M. Lin, Multiphase equilibria for mixtures containing acetic acid, water, propylene glycol monomethyl ether, and propylene glycol methyl ether acetate, Ind Eng Chem Res, 45 (2006) 2123-2130.

[17] O. Chiavonefilho, P. Proust, P. Rasmussen, Vapor-Liquid-Equilibria for Glycol Ether Plus Water-Systems, J Chem Eng Data, 38 (1993) 128-131.

[18] F. Lode, G. Francesconi, M. Mazzotti, M. Morbidelli, Synthesis of methylacetate in a simulated moving-bed reactor: Experiments and modeling, Aiche J, 49 (2003) 1516-1524.

[19] M. Mazzotti, A. Kruglov, B. Neri, D. Gelosa, M. Morbidelli, A continuous chromatographic reactor: SMBR, Chem Eng Sci, 51 (1996) 1827-1836.

[20] M. Kawase, T.B. Suzuki, K. Inoue, K. Yoshimoto, K. Hashimoto, Increased esterification conversion by application of the simulated moving-bed reactor, Chem Eng Sci, 51 (1996) 2971-2976.

[21] M. Kawase, Y. Inoue, T. Araki, K. Hashimoto, The simulated moving-bed reactor for production of bisphenol A, Catal Today, 48 (1999) 199-209.

[22] M. Kawase, A. Pilgrim, T. Araki, K. Hashimoto, Lactosucrose production using a simulated moving bed reactor, Chem Eng Sci, 56 (2001) 453-458.

[23] M.T. Shieh, P.E. Barker, Combined bioreaction and separation in a simulated counter-current chromatographic bioreactor-separator for the hydrolysis of lactose, J Chem Technol Biot, 66 (1996) 265-278.

[24] K. Hashimoto, S. Adachi, H. Noujima, H. Maruyama, Models for the Separation of Glucose Fructose Mixture Using a Simulated Moving-Bed Adsorber, J Chem Eng Jpn, 16 (1983) 400-406.

[25] O. Ludemann-Hombourger, R.M. Nicoud, M. Bailly, The "VARICOL" process: A new multicolumn continuous chromatographic process, Separation Science and Technology, 35 (2000) 1829-1862.

[26] Z.Y. Zhang, M. Mazzotti, M. Morbidelli, PowerFeed operation of simulated moving bed units: changing flow-rates during the switching interval, J Chromatogr A, 1006 (2003) 87-99.

[27] H. Schramm, A. Kienle, M. Kaspereit, A. Seidel-Morgenstern, Improved operation of simulated moving bed processes through cyclic modulation of feed flow and feed concentration, Chem Eng Sci, 58 (2003) 5217-5227.

[28] A.S. Kurup, H.J. Subramani, K. Hidajat, A.K. Ray, Optimal design and operation of SMB bioreactor for sucrose inversion, Chem Eng J, 108 (2005) 19-33.

[29] W.F. Yu, K. Hidajat, A.K. Ray, Determination of adsorption and kinetic parameters for methyl acetate esterification and hydrolysis reaction catalyzed by Amberlyst 15, Appl Catal a-Gen, 260 (2004) 191-205.

[30] N. Calvar, B. Gonzalez, A. Dominguez, Esterification of acetic acid with ethanol: Reaction kinetics and operation in a packed bed reactive distillation column, Chem Eng Process, 46 (2007) 1317-1323.

[31] J.G.S. Doug Geier, SIMULTANEOUS SYNTHESIS AND PURIFICATION OF A FATTY ACID MONOESTER BIODIESEL FUEL, in, United States, 2006.

[32] D.C.S. Azevedo, A.E. Rodrigues, Design methodology and operation of a simulated moving bed reactor for the inversion of sucrose and glucose-fructose separation, Chem Eng J, 82 (2001) 95-107.

[33] C.P. Ribeiro, C.P. Borges, P.L.C. Lage, A new route combining direct-contact evaporation and vapor permeation for obtaining high-quality fruit juice concentrates. Part II: Modeling and simulation, Ind Eng Chem Res, 44 (2005) 6903-6915.

[34] M. Minceva, A.E. Rodrigues, Simulated moving-bed reactor: Reactive-separation regions, Aiche J, 51 (2005) 2737-2751.

[35] M.S. H. Schmidt-Traub, A. Seidel-Morgenstern, Preparative Chromatograpy, Wiley-VCH, 2012.

[36] G. Guiochon, A. Felinger, D.G. Shirazi, A.M. Katti, Fundamentals of Preparative and Nonlinear Chromatography, Elsevier Inc. , San Diego, USA, 2006.

[37] A.N. Tikhonov, A.S. Leonov, A.G. Yagola, Nonlinear ill-posed problems, World Congress of Nonlinear Analysis '92, Vols 1-4, (1995) 505-511.

[38] P.C. Hansen, D.P. Oleary, The Use of the L-Curve in the Regularization of Discrete Iii-Posed Problems, Siam J Sci Comput, 14 (1993) 1487-1503.

[39] G. Agrawal, Y. Kawajiri, Comparison of various ternary simulated moving bed separation schemes by multi-objective optimization, J Chromatogr A, 1238 (2012) 105-113.

[40] E. Kloppenburg, E.D. Gilles, A new concept for operating simulated moving-bed processes, Chem Eng Technol, 22 (1999) 813-+.

[41] Y. Kawajiri, L.T. Biegler, Optimization strategies for simulated moving bed and PowerFeed processes, Aiche J, 52 (2006) 1343-1350.

[42] A. Wachter, L.T. Biegler, On the implementation of an interior-point filter line-search algorithm for large-scale nonlinear programming, Math Program, 106 (2006) 25-57.

[43] R. Fourer, D.M. Gay, B.W. Kernighan, A Modeling Language for Mathematical-Programming, Manage Sci, 36 (1990) 519-554.

[44] E. Sert, A.D. Buluklu, S. Karakus, F.S. Atalay, Kinetic study of catalytic esterification of acrylic acid with butanol catalyzed by different ion exchange resins, Chem Eng Process, 73 (2013) 23-28.

[45] S.H. Ali, Kinetics of Catalytic Esterification of Propionic Acid with Different Alcohols over Amberlyst 15, Int J Chem Kinet, 41 (2009) 432-448.

[46] M.J. Lee, J.Y. Chiu, H.M. Lin, Kinetics of catalytic esterification of propionic acid and n-butanol over Amberlyst 35, Ind Eng Chem Res, 41 (2002) 2882-2887.

[47] M.T. Sanz, R. Murga, S. Beltran, J.L. Cabezas, J. Coca, Kinetic study for the reactive system of lactic acid esterification with methanol: Methyl lactate hydrolysis reaction, Ind Eng Chem Res, 43 (2004) 2049-2053.

[48] A. Orjuela, A.J. Yanez, A. Santhanakrishnan, C.T. Lira, D.J. Miller, Kinetics of mixed succinic acid/acetic acid esterification with Amberlyst 70 ion exchange resin as catalyst, Chem Eng J, 188 (2012) 98-107.

[49] Y.T. Tsai, H.M. Lin, M.J. Lee, Kinetics behavior of esterification of acetic acid with methanol over Amberlyst 36, Chem Eng J, 171 (2011) 1367-1372.

[50] S.J. Miao, B.H. Shanks, Mechanism of acetic acid esterification over sulfonic acid-functionalized mesoporous silica, J Catal, 279 (2011) 136-143.

[51] R.a. Hass, Amberlyst 15 Product Information, (2006).

[52] T.D. Vu, A. Seidel-Morgenstern, Quantifying temperature and flow rate effects on the performance of a fixed-bed chromatographic reactor, J Chromatogr A, 1218 (2011) 8097-8109.

[53] P.T. Mai, T.D. Vu, K.X. Mai, A. Seidel-Morgenstern, Analysis of heterogeneously catalyzed ester hydrolysis performed in a chromatographic reactor and in a reaction calorimeter, Ind Eng Chem Res, 43 (2004) 4691-4702.

[54] Z.Y. Zhang, K. Hidajat, A.K. Ray, Application of simulated countercurrent moving-bed chromatographic reactor for MTBE synthesis, Ind Eng Chem Res, 40 (2001) 5305-5316.

[55] D. Patel, B. Saha, Esterification of Acetic Acid with n-Hexanol in Batch and Continuous Chromatographic Reactors Using a Gelular Ion-Exchange Resin as a Catalyst, Ind Eng Chem Res, 51 (2012) 11965-11974.

[56] S.H. Ali, S.Q. Merchant, Kinetic Study of Dowex 50 Wx8-Catalyzed Esterification and Hydrolysis of Benzyl Acetate, Ind Eng Chem Res, 48 (2009) 2519-2532.

[57] S. Akyalcin, M.R. Altiokka, Kinetics of esterification of acetic acid with 1-octanol in the presence of Amberlyst 36, Appl Catal a-Gen, 429 (2012) 79-84.

[58] B. Saha, M. Streat, Transesterification of cyclohexyl acrylate with n-butanol and 2-ethylhexanol: acid-treated clay, ion exchange resins and tetrabutyl titanate as catalysts, React Funct Polym, 40 (1999) 13-27.

[59] Y. Bard, Comparison of Gradient Methods for Solution of Nonlinear Parameter Estimation Problems, Siam J Numer Anal, 7 (1970) 157-&.

[60] Y. Cheng, Y.H. Feng, Y.B. Ren, X. Liu, A.R. Gao, B.Q. He, F. Yan, J.X. Li, Comprehensive kinetic studies of acidic oil continuous esterification by cation-exchange resin in fixed bed reactors, Bioresource Technol, 113 (2012) 65-72.

[61] F. Lode, M. Houmard, C. Migliorini, M. Mazzotti, M. Morbidelli, Continuous reactive chromatography, Chem Eng Sci, 56 (2001) 269-291.

[62] P.C. Hansen, Discrete Inverse Problems: Insight and Algorithms, Fund Algorithms, (2010) 1-213.

[63] S. Tie, B. Sreedhar, G. Agrawal, J.M. Oh, M. Donaldson, T. Frank, A. Schultz, A. Bommarius, Y. Kawajiri, Model-based design and experimental validation of simulated moving bed reactor for production of glycol ether ester, Chem Eng J, 301 (2016) 188-199.

[64] J. Otera, Transesterification, Chem Rev, 93 (1993) 1449-1470.

[65] Y. Xiao, L.J. Gao, G.M. Xiao, J.H. Lv, Kinetics of the Transesterification Reaction Catalyzed by Solid Base in a Fixed-Bed Reactor, Energ Fuel, 24 (2010) 5829-5833.

[66] N. Shibasaki-Kitakawa, H. Honda, H. Kuribayashi, T. Toda, T. Fukumura, T. Yonemoto, Biodiesel production using anionic ion-exchange resin as heterogeneous catalyst, Bioresource Technol, 98 (2007) 416-421.

[67] G. Paterson, T. Issariyakul, C. Baroi, A. Bassi, A. Dalai, Ion-exchange resins as catalysts in transesterification of triolein, Catal Today, 212 (2013) 157-163.

[68] B.Y. Xu, W.J. Zhang, X.M. Zhang, C.F. Zhou, Kinetic Study of Transesterification of Methyl Acetate with n-Butanol Catalyzed by NKC-9, Int J Chem Kinet, 41 (2009) 101-106.

[69] E. Bozek-Winkler, J. Gmehling, Transesterification of methyl acetate and n-butanol catalyzed by Amberlyst 15, Ind Eng Chem Res, 45 (2006) 6648-6654.

[70] E. Sert, F.S. Atalay, Determination of Adsorption and Kinetic Parameters for Transesterification of Methyl Acetate with Hexanol Catalyzed by Ion Exchange Resin, Ind Eng Chem Res, 51 (2012) 6350-6355.

[71] J.L. Cai, X.B. Cui, Z.C. Yang, Simulation for Transesterification of Methyl Acetate and n-Butanol in a Reactive and Extractive Distillation Column Using Ionic Liquids as Entrainer and Catalyst, Chinese J Chem Eng, 19 (2011) 754-762.

[72] J. He, B.Y. Xu, W.J. Zhang, C.F. Zhou, X.J. Chen, Experimental study and process simulation of n-butyl acetate produced by transesterification in a catalytic distillation column, Chem Eng Process, 49 (2010) 132-137.

[73] T. Keller, J. Holtbruegge, A. Gorak, Transesterification of dimethyl carbonate with ethanol in a pilot-scale reactive distillation column, Chem Eng J, 180 (2012) 309-322.

[74] K. Prasertsit, C. Mueanmas, C. Tongurai, Transesterification of palm oil with methanol in a reactive distillation column, Chem Eng Process, 70 (2013) 21-26.

[75] S. Steinigeweg, J. Gmehling, Transesterification processes by combination of reactive distillation and pervaporation, Chem Eng Process, 43 (2004) 447-456.

[76] Joelianingsih, H. Nabetani, Y. Sagara, A.H. Tambunan, K. Abdullah, A continuous-flow bubble column reactor for biodiesel production by non-catalytic transesterification, Fuel, 96 (2012) 595-599.

[77] J. Lianingsih, H. Maeda, S. Hagiwara, H. Nabetani, Y. Sagara, T.H. Soerawidjaya, A.H. Tambunan, K. Abdullah, Biodiesel fuels from palm oil via the non-catalytic transesterification in a bubble column reactor at atmospheric pressure: A kinetic study, Renew Energ, 33 (2008) 1629-1636.

[78] H. Hattori, Solid base catalysts: Generation, characterization, and catalytic behavior of basic sites, J Jpn Petrol Inst, 47 (2004) 67-81.

[79] Y. Xie, C.Y. Chin, D.S.C. Phelps, C.H. Lee, K.B. Lee, S. Mun, N.H.L. Wang, A five-zone simulated moving bed for the isolation of six sugars from biomass hydrolyzate, Ind Eng Chem Res, 44 (2005) 9904-9920.

[80] G. Paredes, M. Mazzotti, J. Stadler, S. Makart, M. Morbidelli, SMB operation for three-fraction separations: Purification of plasmid DNA, Adsorption, 11 (2005) 841-845.

[81] M. Kim, S.O. Salley, K.Y.S. Ng, Transesterification of Glycerides Using a Heterogeneous Resin Catalyst Combined with a Homogeneous Catalyst, Energ Fuel, 22 (2008) 3594-3599.

[82] M.M.R. Talukder, K.L.M. Beatrice, O.P. Song, S. Puah, J.C. Wu, C.J. Won, Y. Chow, Improved method for efficient production of biodiesel from palm oil, Energ Fuel, 22 (2008) 141-144.

[83] F.N. Tapur, M.I. Bhanger, A.U. Rahman, G.Z. Memon, Application of factorial design in optimization of anion exchange resin based methylation of vegetable oil and fats, Innov Food Sci Emerg, 9 (2008) 608-613.

[84] N. Jaya, B.K. Selvan, S.J. Vennison, Synthesis of biodiesel from pongamia oil using heterogeneous ion-exchange resin catalyst, Ecotox. Environ. Safe., 121 (2015) 3-9.

[85] D. Geier, J. Soper, Simultaneous synthesis and purification of a fatty acid monoester biodiesel fuel, in, United States, 2007.

[86] N. Kitagawa, T. Yonemoto, Regeneration of anion exchange resin used for continuous manufacture of fatty acid ester, involves supplying methanol to anion exchange resin, eluting glycerol adsorbed to resin and supplying methanol solution of acetic acid to resin, in, Univ Tohoku (Toho-C), pp. 22.

[87] B. He, Y. Ren, Y. Cheng, J. Li, Deactivation and in Situ Regeneration of Anion Exchange Resin in the Continuous Transesterification for Biodiesel Production, Energ Fuel, 26 (2012) 3897-3902.

[88] J.P. Yonemoto T, J.P. Kitagawa N, J.P. Nakagawa Y, J.P. Nakayama M, Manufacture of fatty acid ester involves supplying oil and fats and alcohol to reactor filled with anion exchanger, transesterifying, separating fatty acid ester from by-product, and regenerating anion exchanger, in, NAKAYAMA M (NAKA-Individual) UNIV TOHOKU (TOHO-C) NIPPON WATER TREATMENT CO LTD (NREN-C), pp. 13.

[89] T. Yonemoto, N. Kitagawa, T. Toda, Manufacture of fatty acid ester used as bio-diesel fuel, involves transesterifying preset amount of alcohol and oil-and-fat, using anion exchanger as catalyst, in, TOHOKU TECHNOARCH KK (TOHO-Non-standard) MITSUBISHI CHEM CORP (MITU-C) TOHOKU TECHNOARCH KK (TOHO-Non-standard) MITSUBISHI CHEM CORP (MITU-C), pp. 12.

[90] L.C. Meher, D.V. Sagar, S.N. Naik, Technical aspects of biodiesel production by transesterification - a review, Renew Sust Energ Rev, 10 (2006) 248-268.

[91] U. Schuchardt, R. Sercheli, R.M. Vargas, Transesterification of vegetable oils: a review, J Brazil Chem Soc, 9 (1998) 199-210.

[92] A. Demirbas, Comparison of transesterification methods for production of biodiesel from vegetable oils and fats, Energy Conversion and Management, 49 (2008) 125-130.

[93] D.W. Lee, Y.M. Park, K.Y. Lee, Heterogeneous Base Catalysts for Transesterification in Biodiesel Synthesis, Catal Surv Asia, 13 (2009) 63-77.

[94] J. Oh, B. Sreedhar, M.E. Donaldson, T.C. Frank, A.K. Schultz, A.S. Bommarius, Y. Kawajiri, Transesterification of propylene glycol methyl ether in chromatographic reactors using anion exchange resin as a catalyst, J Chromatogr A, 1466 (2016) 84-95.

[95] Dow, Dowex Ion Exchange Resins Fundamentals of Ion Exchange, in, Dow, 2000.

[96] Y. Kawajiri, L.T. Biegler, Nonlinear programming superstructure for optimal dynamic operations of simulated moving bed processes, Ind Eng Chem Res, 45 (2006) 8503-8513.